Tumors of the Liver

13

Jorge Albores-Saavedra, Donald E. Henson, and David S. Klimstra

Tumors of the Liver

Histology of the Liver

The anatomic and functional unit of the liver is the hepatic lobule or the hepatic acinus as defined by Rappaport [1, 2]. The latter is a regular three-dimensional structure in which blood flows from the central axis, formed by the terminal portal venule and terminal hepatic arteriole in the portal tract into the acinar sinusoids, and empties into several terminal hepatic venules at the periphery of the acinus. In contrast the hepatic lobule consists of an afferent central venule with cords of hepatocytes radiating to several peripheral portal tracts. Therefore, in a two-dimensional view, the acinus occupies parts of several adjacent lobules. The division of the hepatic lobules into three zones, centrolobular, midzonal, and periportal, is still used as a convenient landmark. The acinus is subdivided into zones 1, 2, and 3 with decreasing oxygenation and increasing susceptibility to ischemia and toxic or drug-induced injury. The hepatocytes in zone 1 are nearest to portal tracts and correspond to the periportal areas of the lobule. Zone 2 corresponds to the midzonal area of a lobule, and zone 3 corresponds to parts of several centrolobular areas.

The hepatocytes are arranged in plates that in adults are one-cell-layer thick and are separated by sinusoids along which blood flows from portal tracts to terminal hepatic venules. Surrounding the terminal hepatic venules, the hepatocytes exhibit a more regular radial pattern. The hepatocytes bordering the portal tracts are joined together and form a distinct row called the limiting plate.

In children 5–6 years of age, the liver cells are uniform and arranged in two-cell-thick plates. The individual hepatocyte is a polygonal epithelial cell with a well-defined plasma membrane that is differentiated into three specialized regions or domains: basolateral (70% of total surface area) which faces the sinusoid, bile canalicular (15%) bounding part of the intercellular space that constitutes the bile canaliculi, and lateral (15%) facing the rest of the intercellular spaces. Each domain has different molecular, chemical, and antigenic compositions and functions. The nucleus is centrally located and round and contains one or two nucleoli. The cytoplasm of the hepatocytes is eosinophilic due to numerous mitochondria. Abundant glycogen is also present in the cytoplasm. Glycogen accumulation in hepatocyte nuclei around portal tracts produces a vacuolated appearance and is common in adolescents and young adults. In adults such an appearance may be conspicuous in diabetes, glucose intolerance, Wilson's disease, and carcinoma of the pancreas.

Sinusoidal lining cells include endothelial and Kupffer cells. The Kupffer cells have a bean-shaped nucleus and plump cytoplasm with star-shaped extensions. Stellate cells are difficult to differentiate from sinusoidal lining cells. They are modified resting fibroblasts that can store fat and vitamin A and produce hepatocyte growth factor and collagen. Hepatic stellate cells are the main fibrogenic cell type in injured liver.

For many years pit cells were misinterpreted by light microscopy. Under the electron microscope, they have neurosecretory-like electron dense granules and vesicles suggesting endocrine differentiation. However, recent studies indicate that pit cells contain numerous lysosomes and therefore are not endocrine cells but correspond to the large granular lymphocytes and have natural killer cells activity [3]. Pit cells are attached to the endothelium, and sometimes they are in contact with Kupffer cells.

J. Albores-Saavedra (✉)
Department of Pathology, Medica Sur Clinic and Foundation, National University of Mexico, School of Medicine, Mexico City, Mexico

D. E. Henson
Department of Preventative Medicine and Biostatistics, Uniformed Services University of the Health Sciences, Bethesda, MD, USA

D. S. Klimstra
Department of Pathology, Memorial Sloan Kettering Cancer Center, Weill Medical College of Cornel University, New York, NY, USA

C. A. Moran et al. (eds.), *Oncological Surgical Pathology*, https://doi.org/10.1007/978-3-319-96681-6_13

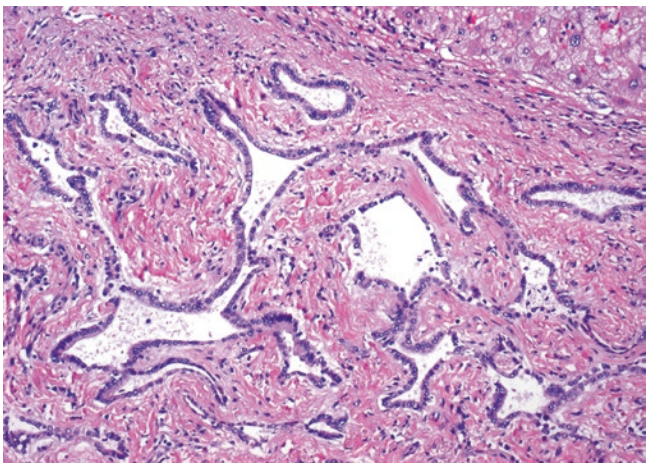

Fig. 13.1 Von Meyenburg complex consists of irregular bile ducts, some dilated and embedded in a fibrous stroma

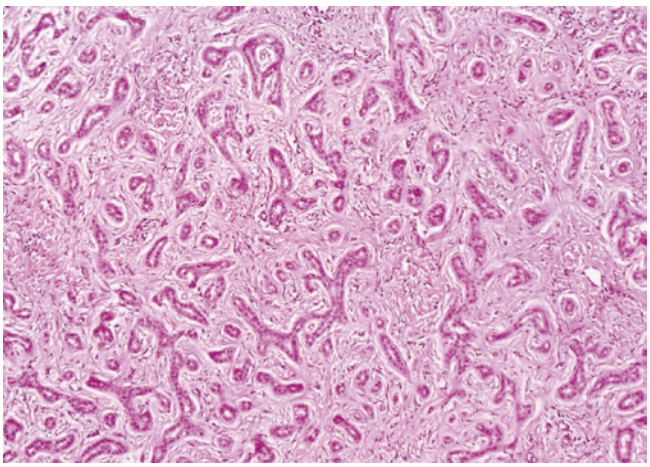

Fig. 13.2 Bile duct adenoma. The tumor is composed of numerous structures similar to intrahepatic bile ducts that tend to branch and are separated by fibrous stroma

Portal Tracts

Each portal tract contains a bile duct, several bile ductules, a hepatic artery branch, a portal vein branch, and lymphatic channels embedded in connective tissue. The portal tracts normally contain a few lymphocytes, macrophages, and mast cells but no polymorphonuclear leukocytes and plasma cells.

Benign Biliary Neoplasms and Tumor-Like Lesions

Von Meyenburg Complex

Von Meyenburg complex is a congenital anomaly that is usually an incidental finding. It consists of multiple small nodules (less than 5 mm) that are found in a paraportal location and consist of a variable number of ductal structures embedded in a hyalinized stroma [4]. The ductal elements are usually dilated or cystic, and their lumen may contain bile (Fig. 13.1). Von Meyenburg complex can be associated with adult polycystic renal disease and Caroli's disease [5]. Preoperative diagnosis can be suspected with magnetic resonance imaging studies, but definitive diagnosis requires histologic examination [6]. Based on molecular abnormalities, it has recently been reported that Von Meyenburg complex has a malignant potential [7], an opinion we do not share.

Solitary Bile Duct Cyst

In contrast to the multilocular cystadenomas, solitary bile duct cysts (SBDCs) lack the ovarian-like stroma, but both lesions share a similar epithelial lining. SBDCs occur at all ages but are rare in children [8]. Most patients are asymptomatic. Jaundice is an infrequent symptom. Acute abdominal pain may result from torsion, rupture, or hemorrhage into the cyst. Diagnosis is established or highly suspected by ultrasonography or computed tomography.

Gross Features

SBDCs are more common in the right lobe than in the left lobe. Rarely, they arise in the falciform ligament. The inner lining is pink and smooth. The larger cysts may contain abundant clear fluid, which may be focally mucoid. The fluid may be hemorrhagic or bile stained if the cyst communicates with a bile duct.

Microscopic Features

The cyst wall is fibrotic and is lined by a single layer of nondysplastic flat, cuboidal or columnar biliary cells, which rest on a basement membrane. Malignant neoplasms especially adenocarcinomas, squamous cell carcinoma, or carcinoid tumor may arise from the cyst.

Bile Duct Adenoma (Peribiliary Gland Hamartoma)

Definition

Bile duct adenoma, also known as peribiliary gland hamartoma, is a small well-circumscribed lesion composed of tubular structures similar to the intrahepatic bile ducts that express CK7 and CK19 (Figs. 13.2 and 13.3) [9, 10]. They are usually incidental findings during abdominal surgery for adenocarcinoma of the colon, pancreas, or any other pathologic condition. Because of this, they may be confused with metastatic adenocarcinoma [10]. In our experience, when bile duct adenomas arise in cirrhotic livers, they appear more cellular and therefore closely resemble well-differentiated cholangiocar-

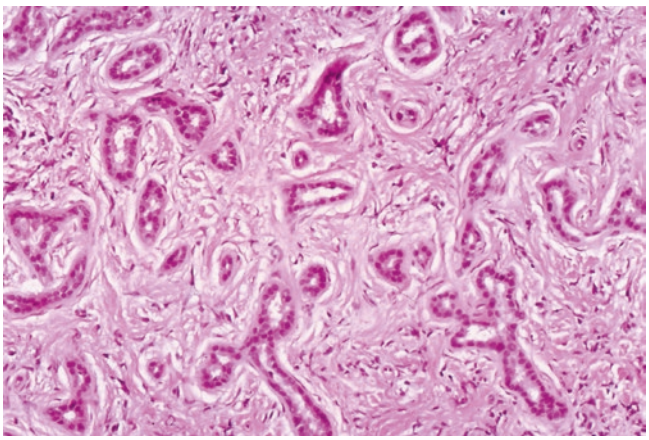

Fig. 13.3 Bile duct adenoma. Higher magnification of tumor shown in Fig. 13.2. The tubules are lined by a single layer of cuboidal cells. The poorly cellular fibrous stroma is also seen

cinoma (Fig. 13.4a, b). Most patients are adult males. Rarely, however, bile duct adenomas occur in children [9].

Gross Features

Over 80% of bile duct adenomas are solitary nodular lesions, and close to 16% are multiple. They measure 10 mm or less and are well demarcated but non-encapsulated. The nodules are gray or tan and of firm consistency.

Microscopic Features

Bile duct adenomas consist of tubular structures that usually branch and are similar to intrahepatic bile ducts (Fig. 13.2). The lumen does not show bile but may contain a small amount of acid mucin (Fig. 13.3). The tubules are lined by a single layer of cuboidal or columnar cells resting on a basement membrane. The nuclei are basally placed and lack atypia or mitotic figures. Stromal fibrosis is often present in the central portion of the adenoma [9]. Malignant transformation does occur but is exceptional [10].

Immunohistochemistry

Bile duct adenoma labels with CK7, CK19, and CEA [11]. They also express MUC6 (94%), MUC5AC (90%), TFF2 (80%), antigen D10 (67%), IF6 (61%), and varying degrees of acid mucins (100%) [12]. It has recently been postulated that bile adenomas develop as a localized healing response equivalent to the function of pyloric gland metaplasia in the foregut [12].

Atypical Bile Duct Adenoma, Clear Cell Type

The atypical bile duct adenoma, clear cell type, is an extremely rare benign neoplasm of the liver. Since its description by Albores-Saavedra et al. in 2001, only an additional case has been reported [13, 14] in a liver with diffuse steatosis. Similar to bile duct adenomas of conventional type, those composed of clear cells are small subcapsular nodules measuring 10 mm or less in adult patients. Following wedge biopsies, no patient has developed recurrence or metastases.

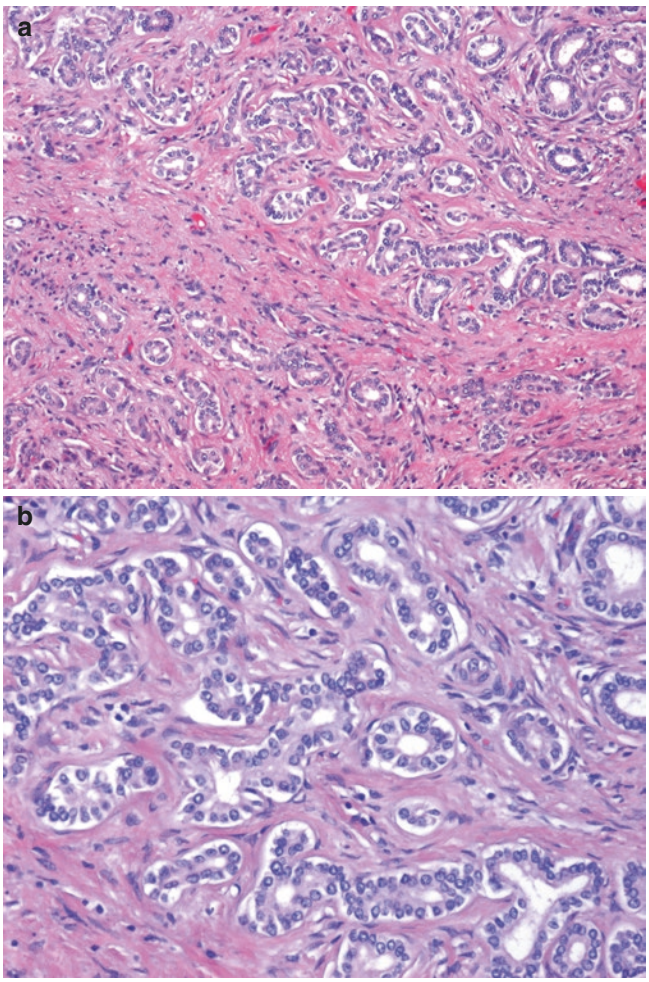

Fig. 13.4 (**a**) Bile duct adenoma that arose in a cirrhotic liver. It is more cellular and contains less fibrous stroma than the conventional bile duct adenoma. (**b**) Higher magnification of the adenoma shown in Fig. 13.4a. This area is more cellular and the lining epithelial cells show slight cytologic atypia. Because of these features, it can be confused with well-differentiated cholangiocarcinoma. Compare to Fig. 13.37

Microscopic Features

This exceedingly rare variant of bile duct adenoma is composed exclusively of clear cells with ample cytoplasm and well-defined cytoplasmic borders. The neoplastic cells line small tubules or form small nests, which most likely represent tubular structures whose lumen is obliterated by the ample cytoplasm of the clear cells (Fig. 13.5a, b). The small nests rest on a PAS-positive basement membrane and occasionally had a small central lumen. Entrapped bile ducts are partially lined by clear cells. The nuclei of the clear cells are

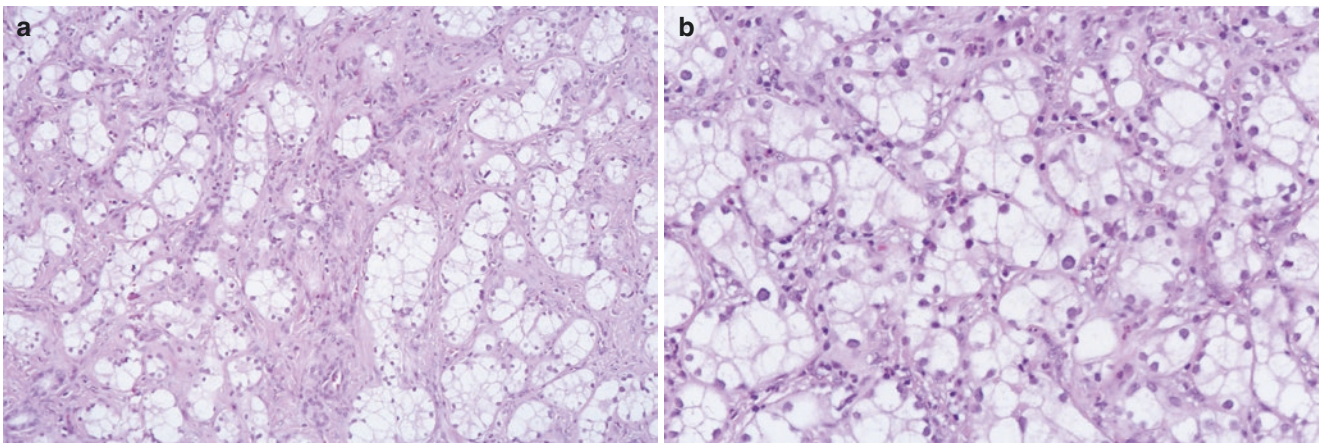

Fig. 13.5 (**a**) Atypical clear cell bile duct adenoma. The tubules are poorly defined and are lined by clear cells having abundant clear cytoplasms. Nests of clear cells are also present. A fibrous stroma separates the tubules. (**b**) Atypical clear cell bile duct adenoma. Higher magnification of atypical clear cell bile duct adenoma. The nuclei are hyperchromatic and show some variation in size and shape

round or ovoid and hyperchromatic with inconspicuous nucleoli. There are no mitotic features. Although the tumors are well demarcated, focal extension into adjacent liver parenchyma is occasionally seen. Mild stromal sclerosis may be present. Low proliferative activity as measured by the Ki-67 antibody is estimated at 0–2%. The neoplastic cells express cytokeratin (CK) 7, p53 protein, epithelial membrane antigen (EMA), and polyclonal carcinoembryonic antigen (CEA) [13, 14].

Atypical bile duct adenoma, clear cell type, should be distinguished from intrahepatic cholangiocarcinoma clear cell type and metastatic clear cell carcinoma that arise in various anatomic sites, especially the kidney.

The clear cell variant of cholangiocarcinoma is larger and shows greater cytologic atypia, increased mitotic activity, and elevated proliferative index as measured by the Ki-67 antibody than the clear cell variant of bile duct adenoma. Moreover, with limited resection, cholangiocarcinoma may recur and metastasize.

Metastases of renal cell carcinoma clear cell type are larger and exhibit greater cytologic atypia and mitotic activity than clear cell bile duct adenomas. Moreover, renal cell carcinoma clear cell type shows an immunoprofile different from that of clear cell type bile duct adenoma [13].

Benign Hepatocellular Neoplasms and Tumor-Like Lesions

Hepatocellular Adenoma (HCA)

Definition

HCA is a benign uncommon neoplasm that arises in noncirrhotic liver and is composed of cells closely resembling normal hepatocytes. When multiple adenomas (more than 10) are present in a patient, the term liver adenomatosis is employed [15].

HCA usually develops in young women with oral contraceptive steroid use. Epidemiological case-control studies found an annual incidence of 3–4/100,000 in long-term oral contraceptive users but only 1 per million in nonusers or women with <2 years exposure [15–17]. The introduction of lower-dose oral contraceptive drugs has resulted in a decrease in the incidence of HCA [18]. Other steroid hormones including non-contraceptive estrogen and anabolic/androgenic steroids have been associated with HCA. Cases of HCA have been reported in men, children, and women not taking oral contraceptives.

Other conditions associated with HCA include glycogen storage diseases especially type 1a, III, and IV [19]. Patients with these inherited disorders may have multiple adenomas. Patients with a form of autosomal dominant familial diabetes mellitus termed maturity-onset diabetes of the young type 3 or MODY3 also develop multiple adenomas. These patients have been found to have a germline mutation of the TCF1 gene, which codes hepatocyte nuclear factor 1a (HNF1a), a transcription factor that controls numerous genes. Somatic mutations with HNF1a inactivation are also found in 35–50% of sporadic or contraceptive steroid-associated HCA. Adenomas that lack HNF1a mutations may have mutations in genes leading to b-catenin activation.

Clinical Features

Most HCAs occur in young adult women between 20 and 39 years of age usually long-term contraceptive users. Occasionally, these tumors occur in children, men, and women outside the reproductive age group. A small number of HCAs are found incidentally. Symptomatic patients have symptoms, which include abdominal mass, mild episodic abdominal pain, and acute abdominal pain (30–40% of

cases) due to hemorrhage into the tumor or into the peritoneal cavity due to rupture of the tumor [20–22]. Pregnancy is a recognized risk factor for rupture [23, 24].

Intraperitoneal hemorrhage, the most serious complication of HCA, often requires emergency surgery and may cause circulatory collapse and death in 20% of patients [20]. Surgical treatment is recommended for all HCA. However, steroid-associated adenomas may regress if the patient stops taking the hormones, while those associated with glycogen storage disease may regress with dietary therapy. Patients with unresectable tumors or multiple tumors in liver adenomatosis have been successfully treated with liver transplantation [25]. Malignant transformation occurs rarely and may be difficult or impossible to prove histologically, especially in needle core biopsies [26, 27].

Gross Features

HCA is usually a solitary nodule of yellow to brown color. Adenomas related to anabolic androgen therapy and the glycogenosis are often multiple. Most HCAs are well-demarcated but non-encapsulated and measure between 5 and 15 cm. Rarely, adenomas may replace an entire hepatic lobe and measure up to 25 cm. Some may appear red because of hemorrhage or infarction, while those that produce bile may show green color (Fig. 13.6a) [20, 21].

Microscopic Features

HCAs are composed of normal-appearing hepatocytes arranged in cords and sheets with a preserved reticulin network, without acinar structures and portal spaces (Fig. 13.6b–d). Adenomas associated to anabolic steroid use often show pseudoglandular formation with bile plugging of centrally located canaliculi. Multiple foci of peliosis may be seen in oral contraceptive-related adenomas. Glycogen storage disease-related adenomas usually show less glycogen than the adjacent liver parenchyma. In some adenomas, steatosis, bile pigment, and a focal inflammatory infiltrate may be seen (Fig. 13.6e).

Molecular Classification

The molecular abnormalities detected in HCA revealed the heterogeneity of the neoplasm. These studies led to a molecular classification of HCA with strong translational impact in terms of diagnostic immunocytochemical markers worldwide validated [28–33]. According to this classification, HCAs are divided into four major subgroups:

Hepatocyte Nuclear Factor 1 A (HNF1A)-Inactivated HCC (H-HCA)

The first group of HCA is defined by somatic inactivation of HNF1A gene by a mutational mechanism in tumor cells and accounts for 30% of HCAs. HNF1a is a transcription factor controlling hepatocyte metabolism. Most H-HCA show macrovesicular steatosis of variable extent, and no atypical hepatocytes are associated to metabolic syndrome. A few tumors arise in patients carrying a germline HNF1 mutation in one allele, which is associated with maturity-onset type 3 diabetes (MODY3). In this setting adenomas undergo a second somatic mutation inactivating the second allele in the neoplastic hepatocytes. Patients with germline mutation of HNF1A are predisposed to develop liver adenomatosis. Expression of liver fatty acid-binding protein (LFABP) involved in lipid trafficking usually expressed in the normal liver is specifically downregulated in H-HCA (100% accuracy) as a consequence of HNF1A mutation and serves as a translational marker to identify H-HCA.

Inflammatory HCA (I-HCA)

The second group of HCA corresponds to inflammatory adenomas and accounts 40–50% of all HCAs. Inflammatory syndrome, obesity, and alcohol assumption are reported in these patients. These HCAs show the greater morphologic pleomorphism. They may show pseudoportal tracts, ductular proliferation, sinusoidal dilatation, dystrophic arteries, and inflammatory infiltrates. Steatosis occasionally occurs. The cardinal feature of these tumors is the activation of the JAK/stat pathway. They also show overexpression of serum amyloid alpha (SAA) and C-reactive protein (CRP), two proteins of the acute inflammation driven by inflammatory cytokines and chemokines induced by STAT3. Five different molecules drives, namely, IL6 traducer (coding for gp130, mutated in 60% of I-HCA), FRK (10%), STAT3 (5%), GNAS (5%), and JAK1 (1%), have been reported. Each mutation is exclusive from the others, and the five mutated genes are involved in more than 80% of the overall I-HCAs. CRP and SAA are the translational markers used to identify this particular type of adenoma.

B-catenin Mutated HCA (B-HCA)

The third group is the B-catenin-mutated HCA (B-HCA), which constitutes approximately 10–15% of all HCAs. Females and males are equally affected some with associated congenital metabolic diseases. Morphologically these adenomas have atypical architectural and cytologic features that are insufficient for a diagnosis of HCC. Mutations in the CTNNB1 gene coding for B-catenin are localized at hot spots in exon 3. B-catenin mutations are exclusive of HNF1A mutations, but half of B-HCAs are also inflammatory and mostly characterize by concomitant gp130 or GNAS mutations. B-catenin mutations are associated with a high risk of malignant transformation with HCC developing from this type of adenoma or elsewhere in the liver. B-HCAs show strong overexpression of GLUL (coding for GS), a target gene as revealed by quantitative reverse-transcription polymerase chain reaction analysis. The diagnosis of B-HCA is made using B-catenin and GS immunostaining as transla-

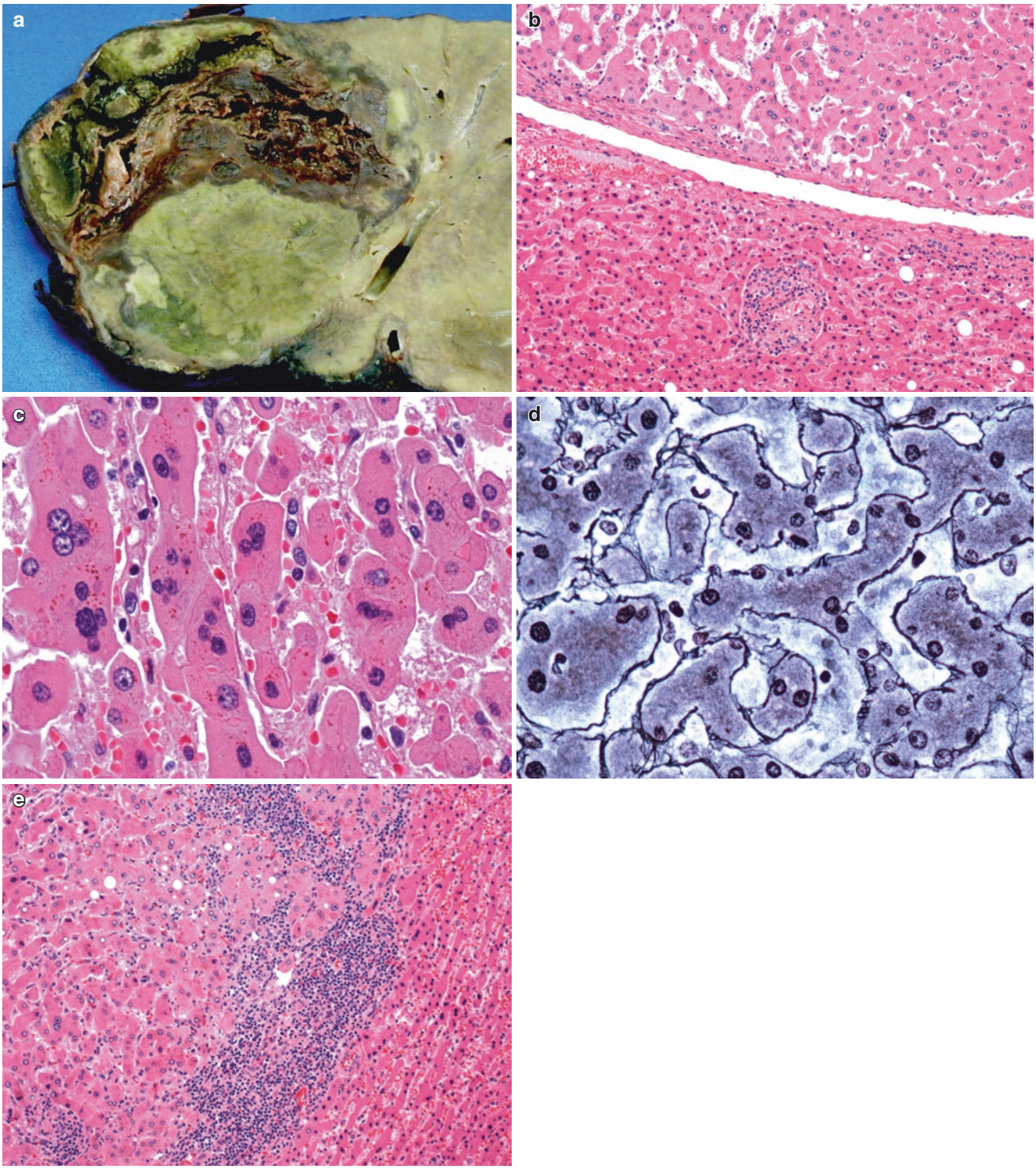

Fig. 13.6 (**a**) Hepatocellular adenoma. The tumor is well-demarcated and shows extensive hemorrhage and a green appearance. The hemorrhage was due to bleeding of the tumor. (**b**) Hepatocellular adenoma. The adenoma (top) contains dilated sinusoids and is separated by the normal liver (bottom). (**c**) Hepatocellular adenoma. Higher magnification of the tumor. The hepatocytes grow in cords and some contain two or three nuclei and bile pigment. (**d**) Hepatocellular adenoma. The reticulin pattern is preserved. (**e**) Hepatocellular adenoma. Between adenoma and normal liver, there are collections of lymphocytes

tional markers. B-HCAs are characterized by a strong homogeneous non-map-like cytoplasmic expression of GS and nuclear and cytoplasmic immunostaining of B-catenin. Other hot spot B-catenin mutations at exons of 7–8 have also been reported. Immunohistochemistry of such cases revealed a faint and patchy GS expression without nuclear expression of B-catenin. As translational markers of B-catenin mutations, B-catenin nuclear staining and GS overexpression have absolute specificity but suboptimal sensitivity (75–85%).

Unclassified HCA (U-HCA)

Unclassified adenomas represent approximately 10% of all HCAs. Their identification is made by exclusion of criteria featuring the other subtypes. Their underlying pathogenesis remains unclear.

The molecular identification is used by pathologists in resected specimens or in needle biopsies. The translational markers such as LAFBP, B-catenin, GS, SAA, and CRP have been adopted as a panel to support a diagnosis of adenoma subtype and distinction from FNH.

Differential Diagnosis

The main differential diagnosis is with well-differentiated hepatocellular carcinoma. In fact distinction of HCA from well-differentiated hepatocellular carcinoma is sometimes difficult or impossible especially in needle core biopsies. A well-defined trabecular pattern, cytologic atypia, and occasional mitotic figures favor carcinoma. Tumors measuring 5 cm or larger with minimal cytologic atypia arising in cirrhotic liver should be considered well-differentiated hepatocellular carcinoma. However, adenomas may occasionally show large cell dysplasia, which should not be regarded as evidence of malignancy. Adenomas may show macro- and microvesicular steatosis as well as cells containing hyaline Mallory bodies.

Liver Adenomatosis

Most patients with hepatocellular adenomatosis have four to more than ten adenomas. This lesion occurs in both men and women and appears unrelated to oral contraceptives. Most cases of liver adenomatosis are asymptomatic, and bleeding is a common complication [34, 35].

Focal Nodular Hyperplasia (FNH)

Definition

A tumor-like lesion composed of hyperplastic hepatocytes arranged in nodules separated by fibrous septae, which form a central or eccentric stellate scar [36]. Abnormal thick-walled vessels especially arteries are present in the fibrous septae, and bile ductules are located between the scar and at the periphery of the nodules of hepatocytes. FNH accounts for up to 8% of all liver neoplasms [15, 25].

Clinical Features

FNH occurs most commonly in adult females, although rarely it has been reported in children. Most examples of FNH are incidental findings during abdominal surgery. Only 20% are symptomatic especially the large ones, which may be palpated. In contrast to hepatocellular adenoma, FNH is not associated with the use of contraceptive steroids [37]. Most authors believe that abnormal blood flow is an important pathogenic mechanism [38].

If single, FNH may be associated with hemangioma or adenoma of the liver. When multiple, FNH may coexist with hemangioma of the liver, meningioma, astrocytoma, telangiectasia of the brain, berry aneurysm, and portal vein ectasia. Some authors have proposed that this represent a new syndrome caused by underlying systemic abnormality of blood vessel development [39]. FNH and FNH-like lesions also occur in association with other vascular abnormalities, such as hereditary hemorrhagic telangiectasia (Rendu-Osler-Weber disease) and congenital absence of the portal vein [40]. In Budd-Chiari syndrome and in rarer vascular disorders, FNH and large regenerative nodules/FNH-like have also been reported [41].

Rarely portal hypertension has been reported in patients with FNH. However, liver function tests are normal. The preoperative diagnosis of FNH is usually made by CT, ultrasonography, or magnetic resonance imaging. Occasionally, cases of FNH are discovered during cholecystectomy.

Gross Features

FNH is usually a single nodular lesion (80%) but may be multiple. It is most commonly found in the right lobe than in the left lobe. Most examples of FNH measure 5 cm or less in greatest dimension. Approximately, 15% of patients have lesions measuring between 5 and 12 cm.

On gross examination FNH is a well-demarcated non-encapsulated multinodular lesion with prominent vessels coursing over the surface (Fig. 13.7). However, around 8% of FNH have a pseudocapsule [15]. The nodules are of different sizes and show brown to yellow-tan color different from the adjacent liver parenchyma.

The most characteristic gross feature of FNH is the presence of a stellate central or eccentric scar, which divides the liver parenchyma into small nodules.

Microscopic Features

Microscopically FNH invariably shows fibrous septae of variable thickness that often run into a stellate scar. This contains numerous vessels, both arteries and veins, the former with irregular thickness walls due to intimal proliferation

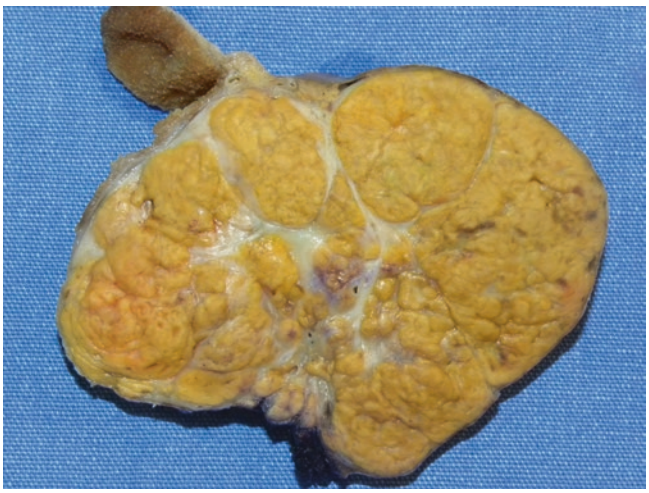

Fig. 13.7 Focal nodular hyperplasia. The lesion is well circumscribed and displays the characteristic central scar and the nodular appearance of the liver

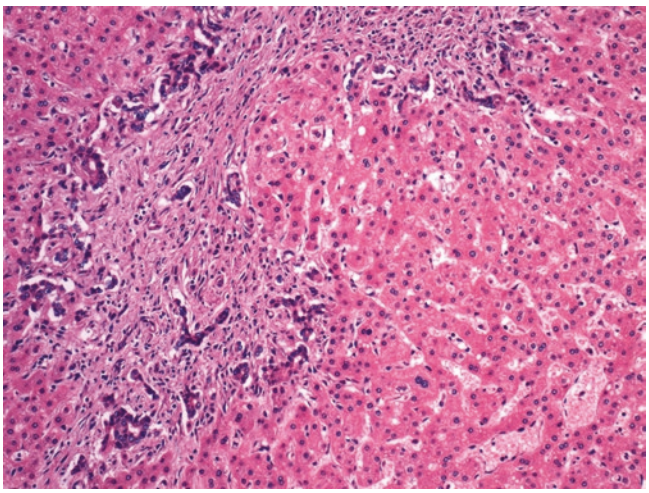

Fig. 13.9 Focal nodular hyperplasia. Small bile duct proliferation attached to the nodules and within the fibrous bands

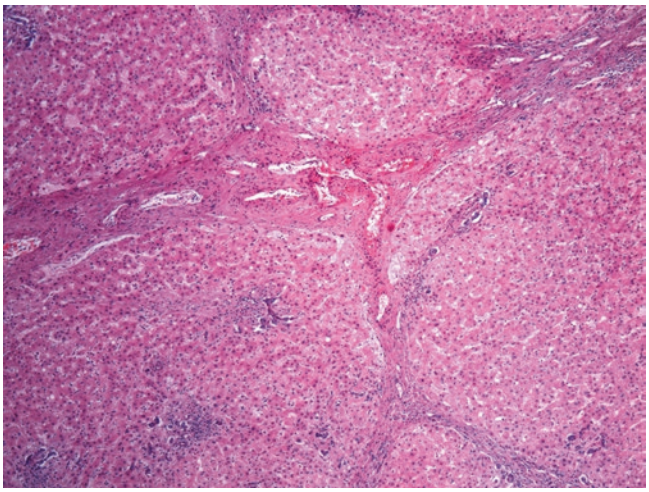

Fig. 13.8 Focal nodular hyperplasia. The lesion is subdivided into nodules by fibrous septa, which contain abnormal vessels

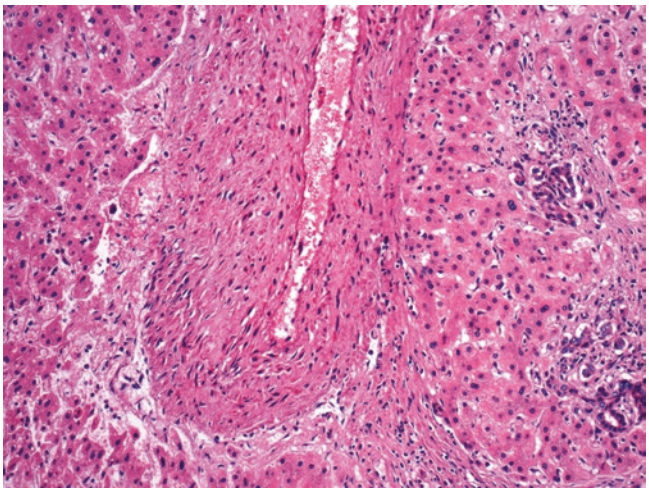

Fig. 13.10 Focal nodular hyperplasia. A medium-sized vessel with a thickened wall is seen

and muscular hyperplasia with disruption of the elastic lamina. The veins often show no histologic abnormalities. Ductules but not bile ducts are seen at the periphery of the hyperplastic nodules of hepatocytes (Figs. 13.8, 13.9, 13.10, and 13.11). Chronic cholestasis is often present in the liver cells adjacent to the fibrous septae.

Molecular Features

FNH is a nodular polyclonal tumor-like lesion that does not undergo hemorrhage or malignant transformation. Clonal analysis using the HUMARA test demonstrated the reactive polyclonal nature of liver cells in FNH in 50–100% of the cases [42]. Messenger RNA (mRNA) expression levels of the angiopoietin genes (ANGPT1 and ANGPT2) involved in vessel maturation are altered, with the ANGPT1/ANGPT2 ratio increased as compared with normal liver, cirrhosis, and other liver tumors [38]. These data support the importance of vascular alterations in the pathogenesis of FNH [43]. Nonclonal β-catenin activation, without mutations, has been shown to occur in FNH, contributing to hepatocellular hyperplasia and regeneration [44, 45]. β-Catenin appears to be activated due to perivascular hypoxic conditions, modulating cellular regeneration and hyperplasia.

Dysplastic Nodules (DNs)

In contrast to large cell dysplasia, dysplastic nodules are considered to be the precursors of a significant number of hepatocellular carcinomas. DNs occur in cirrhotic livers, are

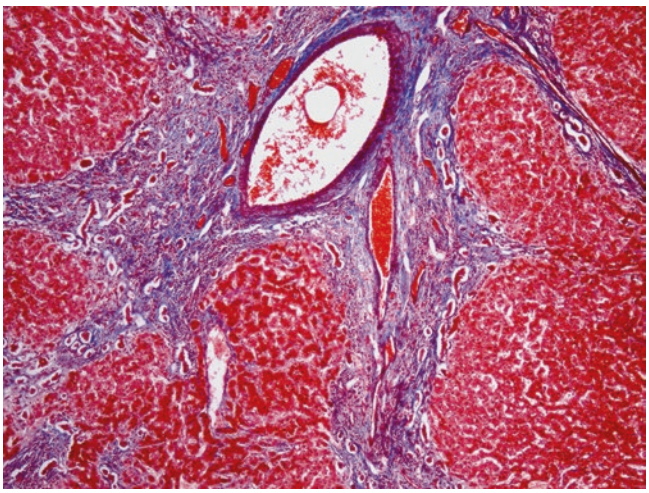

Fig. 13.11 Focal nodular hyperplasia. A trichrome stain displays the fibrous scar, the abnormal vessels, and the hyperplastic nodules of hepatocytes

microscopically distinct and larger than adjacent cirrhotic nodules, and may be detected by imaging studies.

Dysplastic nodules can be single or multiple measuring less than 15 mm in greatest dimension. Histologically, they should be distinguished from non-dysplastic large regenerative nodules and early hepatocellular carcinoma. In fact, distinction of high-grade dysplastic nodules from early hepatocellular carcinoma may be impossible. High-grade dysplastic nodules are composed of small cells with hyperchromatic nuclei having irregular nuclear contours. The cells are arranged in plates no more than four cells thick. Portal tracts are usually present within the nodules, and Mallory bodies are often identified.

Malignant Hepatocellular Tumors

Hepatocellular Carcinoma

General Features

Hepatocellular carcinoma (HCC) is the sixth most common cancer and the second leading cause of cancer-related death in the world [46]. It is also the most common primary malignancy of the liver in adults. However, HCC can rarely occur in adolescents and children [47]. In all age groups, it is most frequent in men than in women and increases in incidence with advancing age. In the USA, the incidence of HCC has progressively increased from 1973 through 2013 in men and women attributed to the rising incidence of hepatitis C and fatty liver disease-related cirrhosis (Fig. 13.12) [46]. There is striking geographic variation in the incidence of HCC and its association with viral infection and exposure to chemical agents. HCC is usually associated with chronic liver viral disease especially cirrhosis and rarely with chronic exposure to chemical carcinogens and metabolic disorders. Therefore cirrhosis is considered a major risk factor for the development of HCC. The rate of developing HCC in cases of cirrhosis stands at 2–4% per year [48]. In its early stages, it is usually an incidental finding. For instance, in explanted livers for cirrhosis, HCC usually measures 1–5 cm or less. Likewise surveillance of patients with chronic viral hepatitis or cirrhosis has led to early detection of many hepatocellular carcinomas. However, most patients with HCC still come to clinical attention when the tumor is far advanced and difficult to treat.

Clinical Features

Since HCC is often asymptomatic in its early stages, its clinical presentation is often delayed beyond the time for successful intervention. Often presentation reflects the signs and symptoms of underlying cirrhosis. A distinct mass in the liver may not be palpable. Signs and symptoms include hepatomegaly with or without a palpable mass, abdominal pain, weight loss, fatigue, jaundice, and ascites.

Gross Features

The smallest hepatocellular carcinomas we have examined were incidental findings in explanted livers for hepatic cirrhosis or resected tumors that were detected through surveillance of patients with chronic liver disease (Figs. 13.13 and 13.14a, b). In this setting HCC appears as a well-demarcated nodule measuring from 1.5 to 5 cm. Frequently small satellite nodules are present. Over time multiple nodules may involve the entire liver mimicking metastatic carcinoma (Fig. 13.15). HCC may also appear as a single large mass, gray-white to yellow color; when the tumor produces bile, it has a green color (Fig. 13.16). The portal vein, vena cava, and hepatic veins may contain tumor thrombi. Invasion of intrahepatic bile ducts is uncommon but may lead to biliary obstruction. Encapsulated HCCs grow slowing and appear to have better prognosis than the non-encapsulated forms of HCC.

Microscopic Features

Well-differentiated hepatocellular carcinomas are composed of cells similar to hepatocytes with minimal cytologic atypia and mitotic activity. Therefore they are difficult to separate from hepatocellular adenomas. A well-defined trabecular pattern is one which the trabeculae are several cells thick and are lined by endothelial cells strongly favor HCC (Figs. 13.17 and 13.18). Other HCC are moderately differentiated and show a pseudoglandular pattern (Fig. 13.19). The gland-like structures are small to medium sized, contained eosinophilic material, and are lined by a single layer of cuboidal or low columnar cells. In the sarcomatoid variant of HCC, poorly differentiated spindle cells predominate (Figs. 13.20 and 13.21). When heterologous

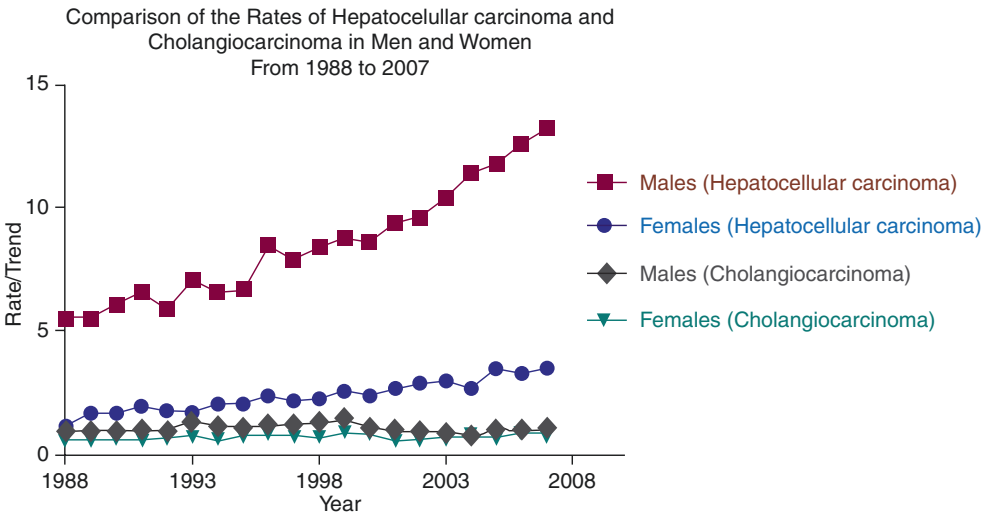

Fig. 13.12 Trends of hepatocellular carcinoma and cholangiocarcinoma in men and women for 20 years from 1988 through 2007 according to the SEER program. The trends are expressed as the number of cases per 100,000 population. In both men and women, hepatocellular carcinomas are more common than cholangiocarcinomas. Furthermore, the rates of hepatocellular carcinomas have increased in men faster than in women, while the rates of cholangiocarcinomas have not increased in either men or women

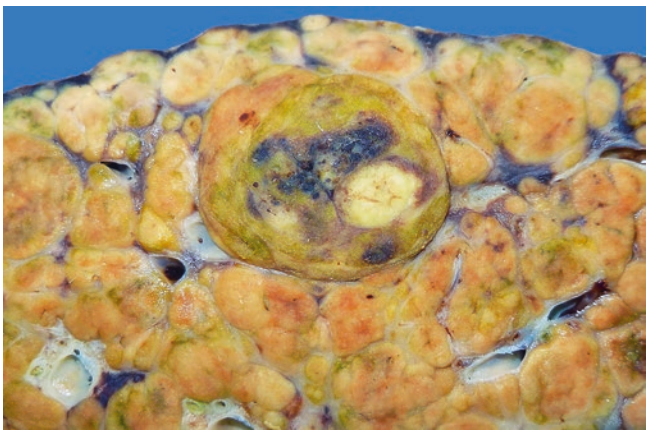

Fig. 13.13 Hepatocellular carcinoma. The tumor arose in a macronodular cirrhosis. It is larger than the cirrhotic nodules, well-demarcated, and of greenish and whitish color with focal hemorrhage

elements such as cartilage, bone, and skeletal muscle are present, we recommend the use of the term carcinosarcoma (Figs. 13.22, 13.23, 13.24, and 13.25). Other histologic variant of HCC include the giant cell type in which anaplastic giant cells predominate. This tumor should be separated from those containing osteoclast giant cells, the clear cell type, that consists of neoplastic cells with clear cytoplasm due to fat or glycogen deposition (Figs. 13.26 and 13.27). Small and large fat and glycogen cytoplasmic droplets are present in these tumors. Other cytoplasmic structures that may be present in HCCs include bile, Mallory bodies, globules of alpha-1-antitrypsin, fibrinogen bodies, and Dubin-Johnson pigments.

HCCs that contain abundant sclerotic stroma have been designated the scirrhous type. HCCs with a mixed pattern are common. Vascular invasion is common. The fibrolamellar carcinoma is a special type of hepatocellular carcinoma described below.

Liver Biopsy

The most accurate diagnostic procedure is percutaneous liver biopsy, which detects HCC in nearly 90% of cases assuming a mass is present [49]. The success of biopsy obviously depends on location of the tumor. Biopsy is usually recommended for patients with cirrhosis and for patients with solid masses without cirrhosis [50].

Immunohistochemistry

Immunohistochemical stains such as Hep-Par 1 and alpha-fetoprotein cannot distinguish hepatocellular adenoma or dysplastic nodules from HCC. Hep-Par 1 is a monoclonal antibody that reacts with the urea cycle enzyme carbamoyl phosphate synthetase of liver mitochondria with a typical granular pattern in most liver specimens. It also reacts with mitochondria of renal tubules and intestinal epithelium. Therefore, it is not specific for hepatocyte. It stains approximately 90% of well to moderately differentiated hepatocellular carcinomas and 40% of cholangiocarcinomas and metastatic adenocarcinomas. Primary hepatoid gastric and gallbladder adenocarcinomas also express Hep-Par 1. Serum alpha-fetoprotein is elevated in the majority of patients with HCC but is not a sensitive immunohistochemical marker; moreover, germ cell tumors also express alpha-fetoprotein and therefore it lacks specificity.

Genetic Abnormalities

The vast majority of HCCs are aneuploid and show different genetic abnormalities ranging from gains and losses of entire chromosomal arms to point mutations [51]. It is interesting to note that while alterations in chronic hepatitis or cirrhosis are different from those observed in HCC, dysplastic nodules show a profile that is quite similar to well-differentiated HCC. New abnormalities develop as the tumor progress to large poorly differentiated [51]. Most frequent losses have been observed at 1p, 4q, 6q, 8p, 9p, 13q, 16p, 16q, and 17p and gains at 1q, 6p, 8q, and 17q [51–63]. This genetic hetero-

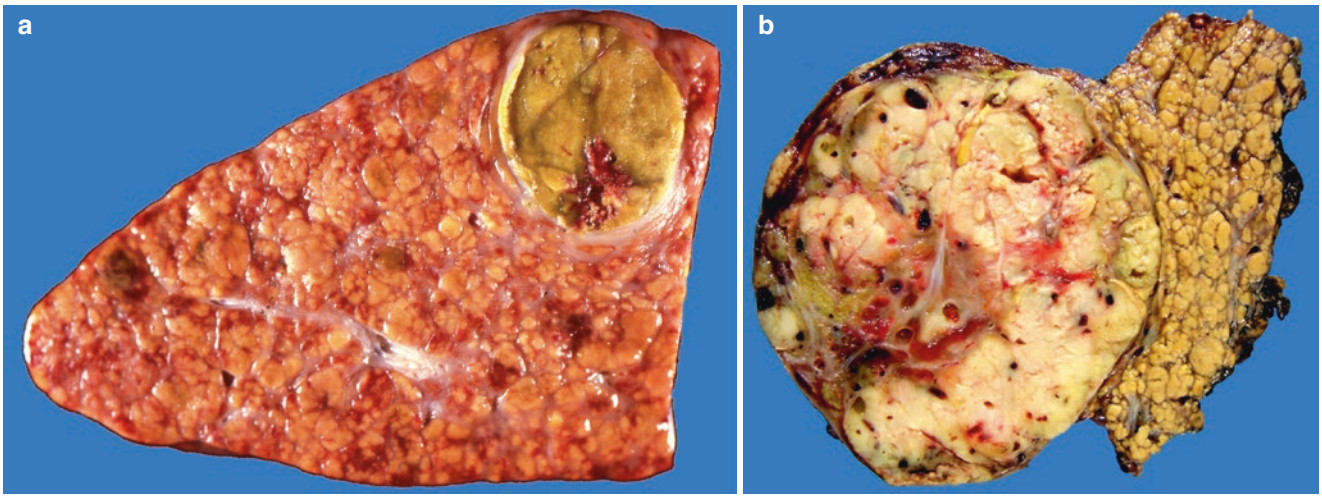

Fig. 13.14 (**a**) Hepatocellular carcinoma. The tumor arose in a macro- and micronodular cirrhosis. It is encapsulated, of greenish color, and larger than the cirrhotic nodules. (**b**) Hepatocellular carcinoma. The carcinoma is well-demarcated, multinodular, and of light-yellow color with focal hemorrhage. The tumor nodules have a different color from those of the macro- and micronodular cirrhosis

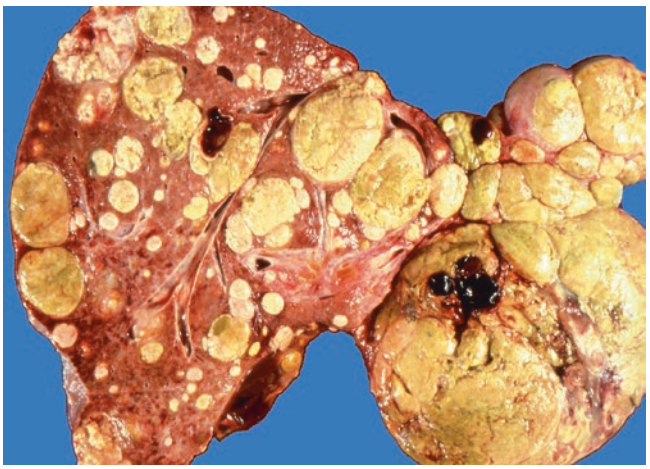

Fig. 13.15 Hepatocellular carcinoma. The tumor is multinodular and involves both hepatic lobes. The nodules are of different sizes and some are of greenish color

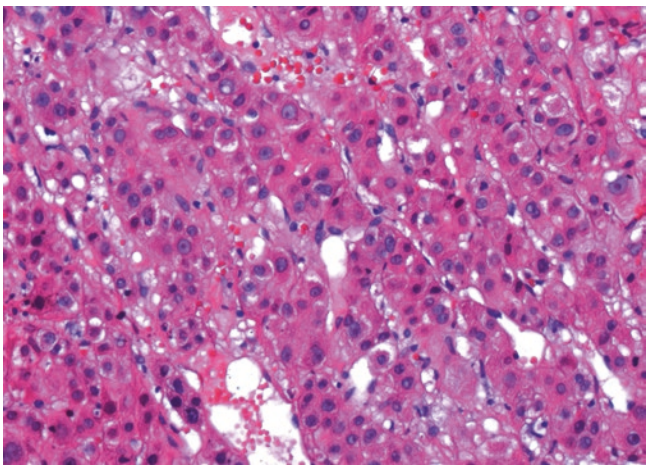

Fig. 13.17 Well-differentiated hepatocellular carcinoma. The tumor grows in cords and trabeculae and is composed of hepatocytes with mild nuclear atypia

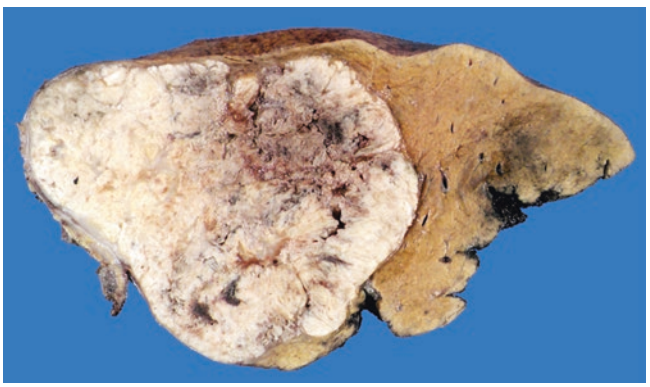

Fig. 13.16 Hepatocellular carcinoma. The carcinoma is well demarcated and whitish and arose in a non-cirrhotic liver

geneity could reflect the actions of different causative agents. For example, in some studies, it has been shown that 10q is preferentially associated with HCV-positive cases, while loss of 4q and 16q and gain of 11q are observed in most cases of HBV isolated HCC. However, most chromosomal abnormalities are observed in HCC regardless of etiology [51]. Recently it has been shown that the RB1, p53, and Wnt pathways are commonly affected in HCCs from different etiologies [51]. In fully developed HCC, a frequent deletion is observed at 13q12–14 locus that contains RB1, LEU1, and BRCA1, these well-known oncogenes [51]. In conclusion hepatocarcinogenesis is a multistep process involving different molecular pathways. The differences are partly due to the etiologic factors and to the genetic constitution of the host.

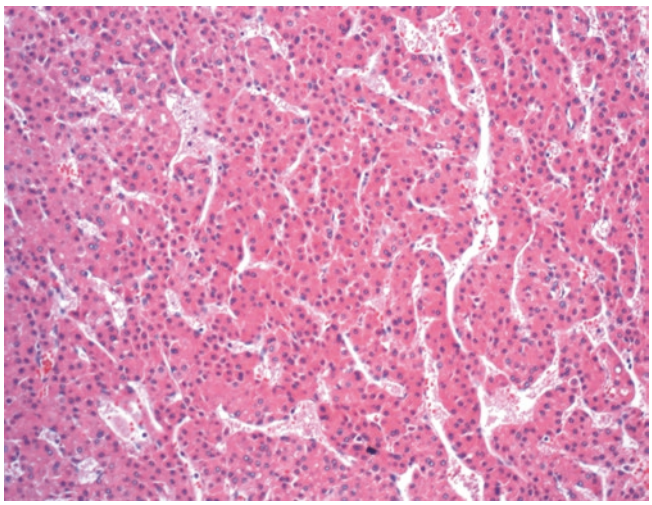

Fig. 13.18 Well-differentiated hepatocellular carcinoma. The tumor has a trabecular and sinusoidal pattern but shows minimal nuclear atypia

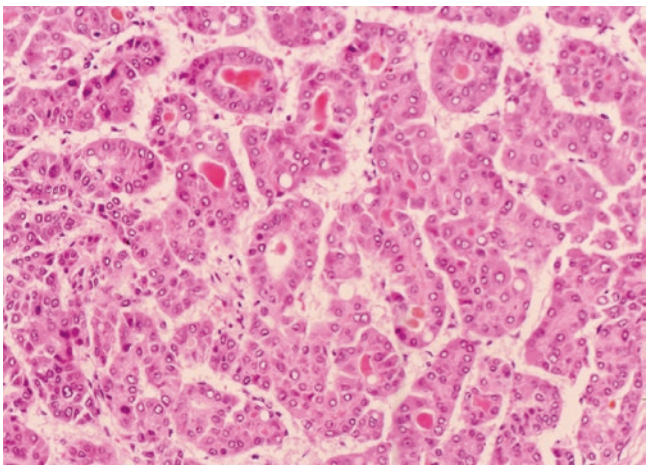

Fig. 13.19 Hepatocellular carcinoma, pseudoglandular pattern. Gland-like structures containing bile pigment are seen in this tumor

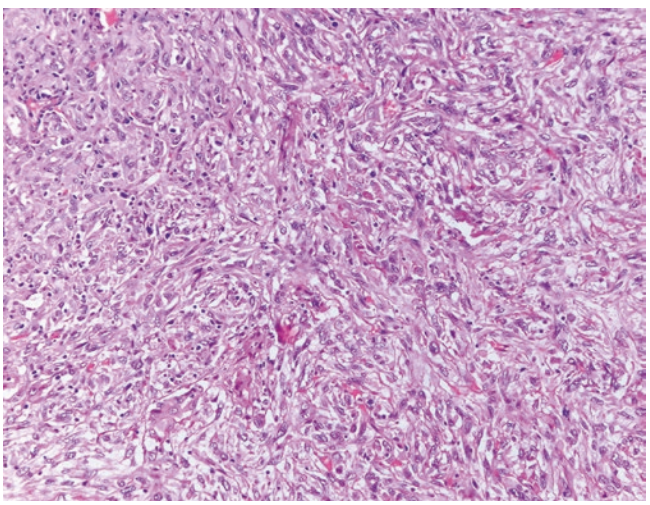

Fig. 13.20 Sarcomatoid hepatocellular carcinoma. The tumor cells are spindle shaped and grow in fascicles

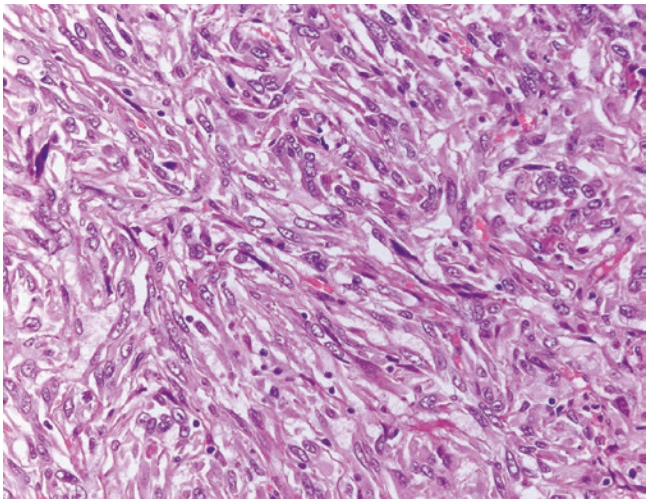

Fig. 13.21 Sarcomatoid hepatocellular carcinoma. Higher magnification of tumor shown in Fig. 13.20 with focal storiform pattern

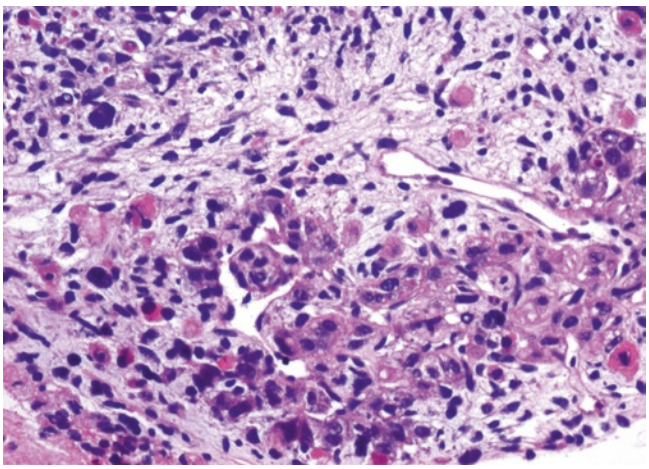

Fig. 13.22 Carcinosarcoma of liver. Both the hepatocellular and the sarcomatoid components of the tumor are clearly seen

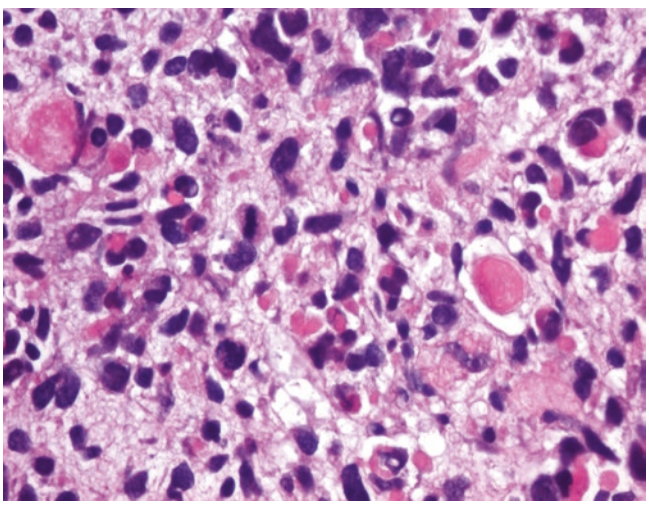

Fig. 13.23 Carcinosarcoma of liver. The rhabdomyosarcomatous component is depicted

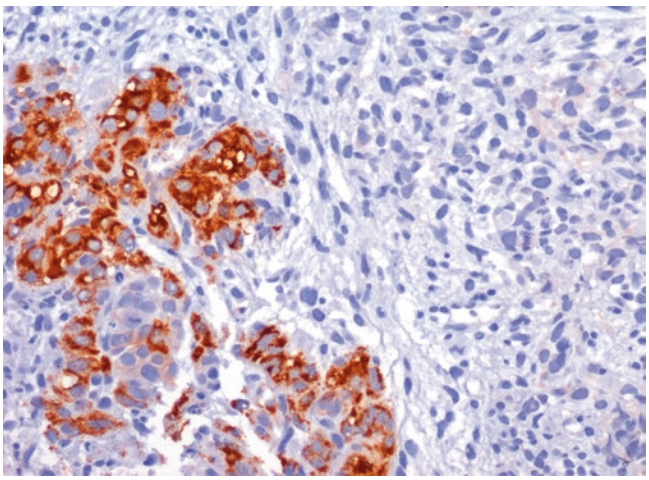

Fig. 13.24 Carcinosarcoma of liver. Hep-par 1 stains only the hepatocellular component of the tumor

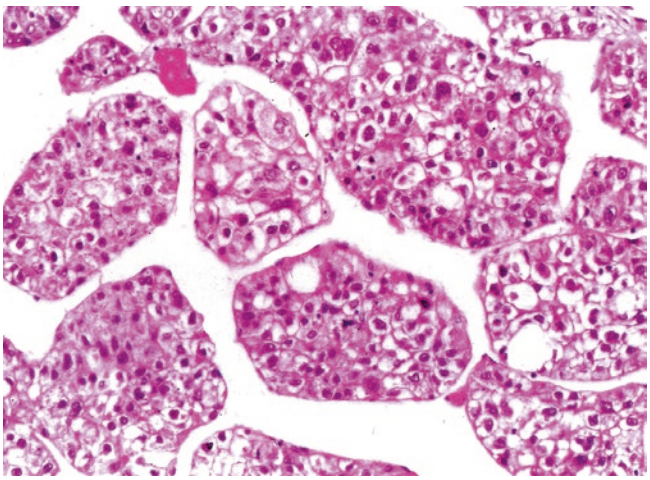

Fig. 13.26 Clear cell type hepatocellular carcinoma. The trabecular and sinusoidal patterns are clearly seen. Many of the neoplastic cells contain cytoplasmic vacuoles

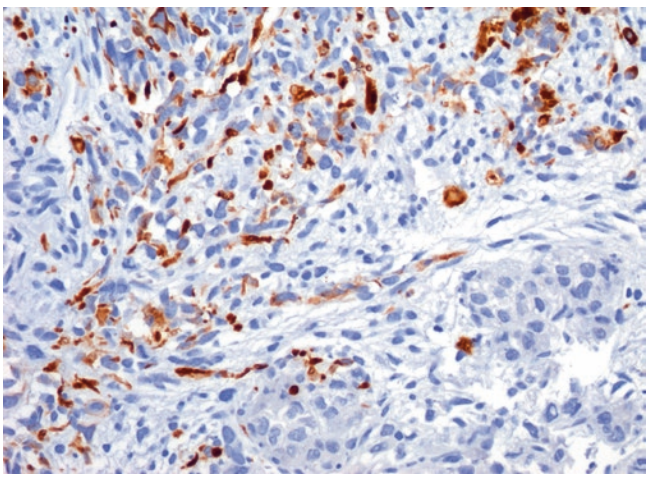

Fig. 13.25 Carcinosarcoma of liver. The rhabdomyosarcomatous component is immunoreactive for desmin

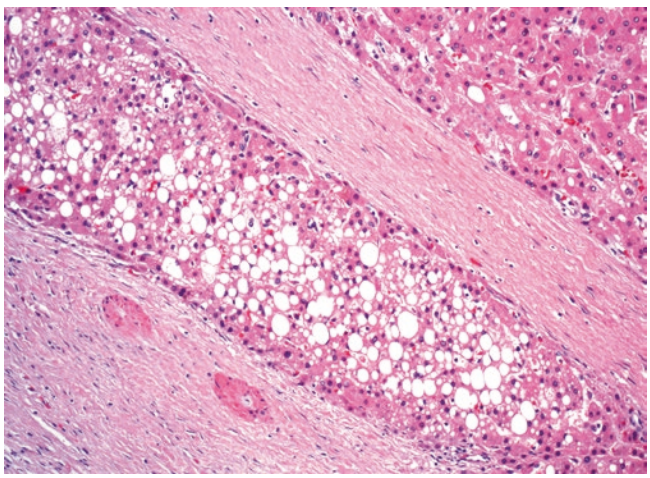

Fig. 13.27 Hepatocellular carcinoma. The clear cell hepatocellular carcinoma shows blood vessel invasion

Prevention

HCC was the first human cancer controlled by vaccination against HBV infection. A safe and effective vaccine became available in 1982 and is now standard worldwide health policy. Immunizations began in 1984, and universal coverage was achieved by 1986 [64, 65]. The incidence of HCC has been declining in some high-incidence areas such as China and Hong Kong partly related to vaccination of HBV in children.

Prognosis and Treatment

The prognosis of HCC is not favorable and depends on stage of the tumor and coexisting liver disease. Patients with small tumors measuring 5 cm or less usually detected by surveillance of patients with chronic viral hepatitis or cirrhosis have a high cure rates (60–75%). Large tumors associated with cirrhosis have a very poor prognosis. For small tumors, segmental liver resection or hepatic lobectomy may be a curative procedure. Chemotherapy and radiotherapy have not improved prognosis. Percutaneous ablation of the tumor has become the treatment of choice for early but unresectable tumors.

Fibrolamellar Carcinoma (FLC)

FLC is a variant of hepatocellular carcinoma characterized by an abundant desmoplastic stroma and tumor cells with an oncocytic appearance. It has distinctive clinical features and natural history, which justify its separation from the conventional hepatocellular carcinoma [66, 67].

Clinical Features

The mean age of the patients is 23 years, which is considerably younger than that of ordinary hepatocellular carcinoma. Children and adolescents are also affected [67, 68]. Only a small proportion of patients are older than 50 years. The tumor is more common in males with no history of preexisting liver disease. The clinical course is indolent. Symptoms include nausea, vomiting, abdominal pain, and weight loss. Jaundice is uncommon, and presentation with the Budd-Chiari syndrome due to invasion of the inferior vena cava is exceedingly rare.

Gross Features

The tumor is well-demarcated but non-encapsulated and more common in the left than the right hepatic lobe. FLC is usually larger than the conventional hepatocellular carcinoma. A central fibrous scar with focal calcifications gives the tumor a lobulated or nodular appearance similar to focal nodular hyperplasia (Fig. 13.28a). The cut surface is light brown or gray white but may be green if bile production is abundant. The non-neoplastic liver parenchyma is normal. Cirrhosis has been reported in less than 5% of the cases.

Microscopic Features

The distinctive microscopic features of FLC are the fibrous-rich stroma and the polyhedral oncocytic-appearing cells (Fig. 13.28b). The fibrous stroma consists of lamellae of varied thickness that contain hyalinized bundles of collagen as well as thinner collagen and reticulin fibers that support small groups and individual tumor cells. Neoplastic cells may also show a trabecular or sheet-like pattern.

The abundant eosinophilic granular cytoplasm of the tumor cells is due to the presence of numerous mitochondria. The tumor canaliculi may contain bile. Mallory bodies may rarely be present. Ground glass inclusions are immunoreactive for fibrinogen. The cell nuclei are often large hyperchromatic or vesicular with prominent eosinophilic cytoplasm. Multinucleated cells and mitotic figures are uncommon.

The immunostain for Hep-Par 1 is positive, while the immunostain for alpha-fetoprotein is usually negative. FLC express CK 7, 8, 18, and 19.

Molecular Pathology

In contrast to typical HCC, the fibrolamellar type does not show mutations of the TP53, Wnt/β-catenin, or survivin [67, 68]. Recently, next-generation whole transcriptome sequencing and whole genome sequencing (WGS) lead to major breakthroughs in our understanding of the pathogenesis of FL-HCC. Honeyman and colleagues reported that 15 of 15 FL-HCC samples had a single copy 400 kB deletion on chromosome 19, resulting in an in-frame fusion of exon 1 of the gene for heat shock protein 40 (DNAJB1) fused to the majority of the gene encoding the catalytic subunit of protein kinase A (PKA, PRKACA). This mutation has been confirmed in several additional FL-HCC cohorts [69].

Ultrastructure

The most striking ultrastructural feature is the presence of a large number of "back-to-back" mitochondria in the cytoplasm of tumor cells. The mitochondria show changes resembling those of Reye's syndrome.

Prognosis and Treatment

The prognosis of FLC is better than that of ordinary HCC [70, 71]. The 5-year relative survival rate is 56%. Tumor stage is the most significant factor for survival. Good results have been obtained in selected patients transplanted for FLC [70].

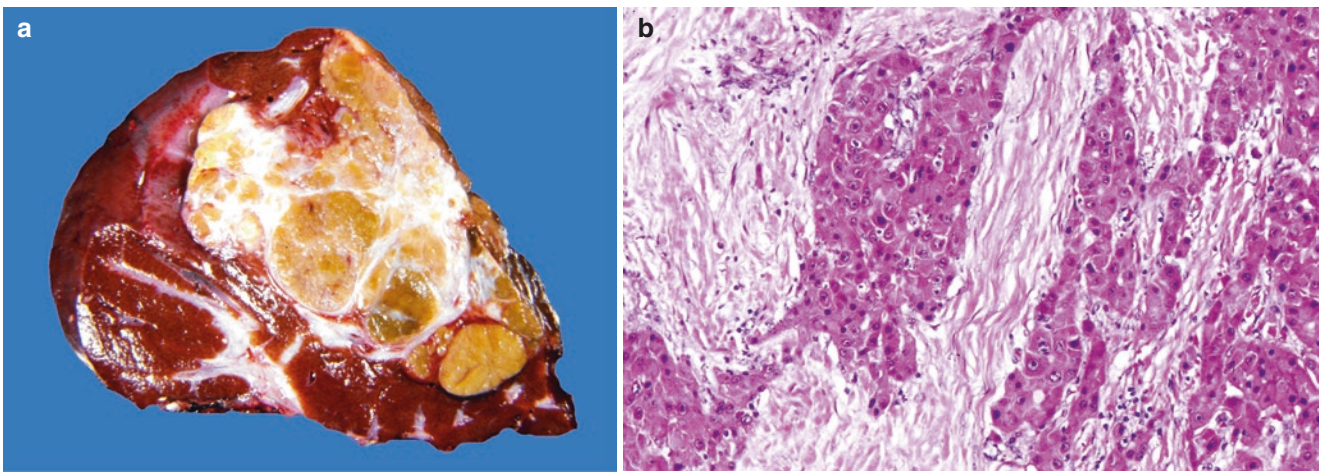

Fig. 13.28 (**a**) Fibrolamellar hepatocellular carcinoma. The tumor is large multinodular, displays extensive fibrous bands, and arose in a non-cirrhotic liver. (**b**) Fibrolamellar hepatocellular carcinoma. The tumor grows in anastomosing trabeculae, which are separated by abundant fibrous stroma. The cells have an oncocytic appearance

Hepatoblastoma

Hepatoblastoma in the most common liver tumor in children and mimics the developing fetal or embryonal liver and may contain heterologous elements such as cartilage, osteoid, and squamous epithelium [72].

Clinical Features

The vast majority of hepatoblastomas (90%) are seen in the first 5 years of life. The tumor accounts for over 40 percent of all hepatic tumors in children under 2 years of age. An increasing incidence of hepatoblastoma has been noted in very low birth weight infants [72]. There is a male predominance 2:1. Children with hepatoblastoma usually present with an enlarging abdomen, weight loss, anorexia, nausea, vomiting, and abdominal pain. A right upper quadrant abdominal mass is often palpated. Serum alpha-fetoprotein is elevated in most patients. Approximately 5% of hepatoblastomas have been associated with a great variety of congenital anomalies including cleft palate, horseshoe kidney, heterotopic lung tissue, umbilical hernia, Beckwith-Wiedemann syndrome, hemihypertrophy, gonadoblastoma, Wilm's tumor, familial adenomatosis coli, Gardner's syndrome, etc. [73–77]. Cytogenetic studies and comparative genomic hybridization have shown that tumor cells usually harbor some chromosomal abnormalities [78]. The most common genetic alterations involve chromosome 2, 20, 1, 8, and X [79]. Recent studies have shown that b-catenin genes are mutated in a large proportion of hepatoblastomas. Likewise sporadic hepatoblastomas show mismatch repair defects and p53 mutations [80].

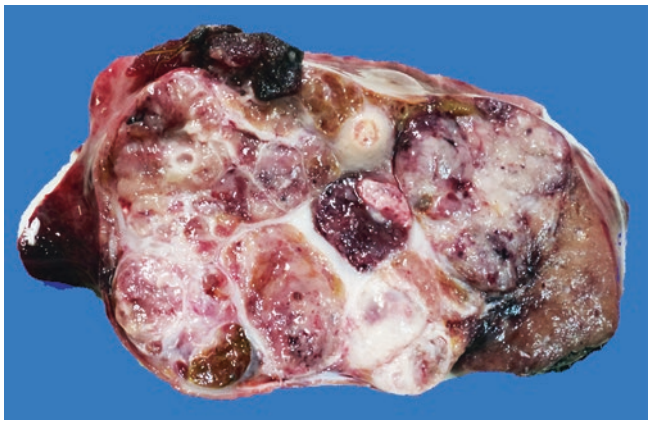

Fig. 13.29 Hepatoblastoma. The tumor is well-demarcated and is composed of nodules separated by fibrous bands. The nodules are whitish and some show focal hemorrhage. (Courtesy of Dr. E. Sadowinsky, Mexico City, Mexico)

Gross Features

Hepatoblastomas usually appear as large nodular masses that may replace an entire hepatic lobe (Fig. 13.29). On cut surface they may be yellow, brown, green, or variegated.

Histologic Features

Microscopically, hepatoblastoma has been subdivided into six types, four pure epithelial and two mixed epithelial and mesenchymal. More than half of the tumors are pure epithelial, and 44% are mixed epithelial and mesenchymal. The pure epithelial type displays four patterns: fetal, embryonal and fetal, macrotrabecular, and small cell undifferentiated pattern. The fetal pattern consists of uniform round or cuboidal cells resembling fetal hepatocytes (Figs. 13.30, 13.31, and 13.32). The cells contain clear to finely granular cytoplasm with distinct membranes, a small round nucleus with fine nuclear chromatin and small nucleolus. Variable amounts of cytoplasmic glycogen and lipid within clusters of fetal epithelial cells impart a

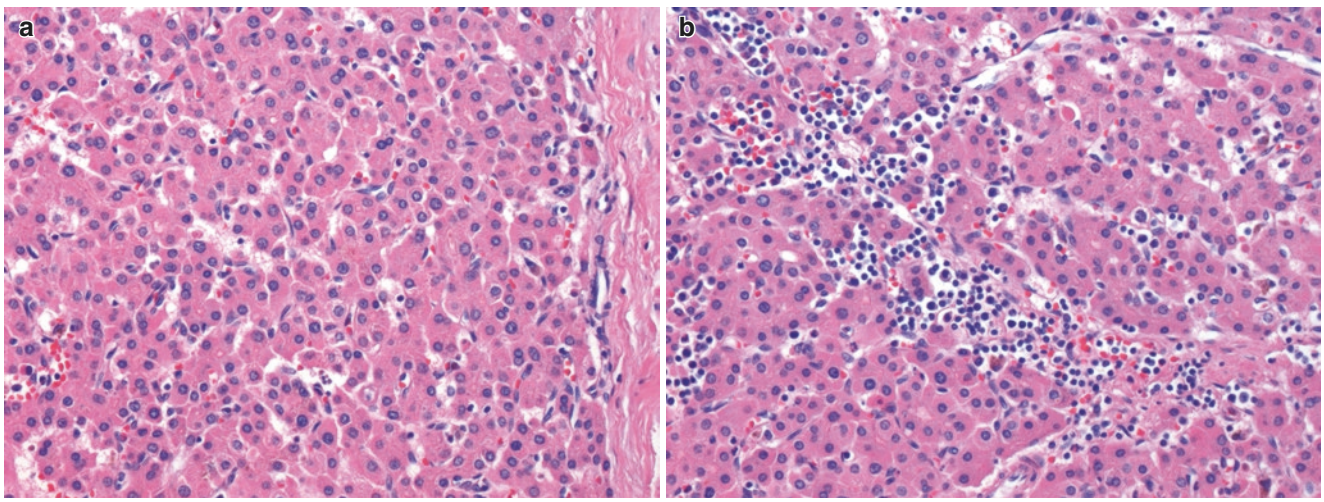

Fig. 13.30 (**a**) Fetal and embryonal epithelial hepatoblastoma. The neoplastic cells are cuboidal displaying a trabecular pattern. (**b**) Fetal epithelial hepatoblastoma. Foci of extramedullary hematopoiesis are seen in this hepatoblastoma

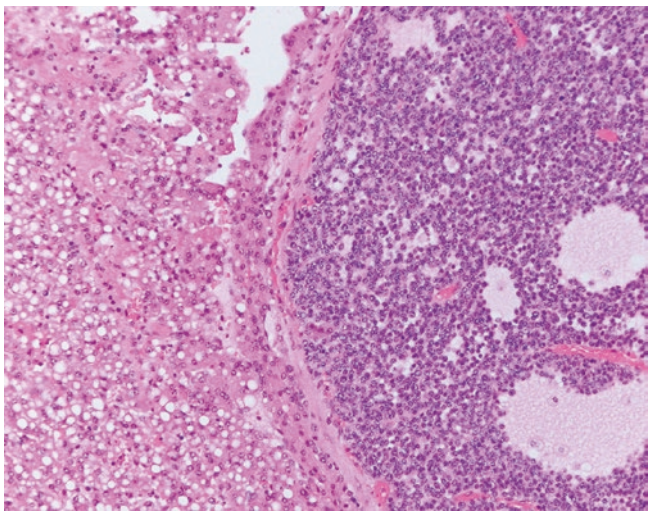

Fig. 13.31 Fetal and embryonal epithelial hepatoblastoma. The neoplastic nodule is composed of small round cells and show structures with a colloid-like material

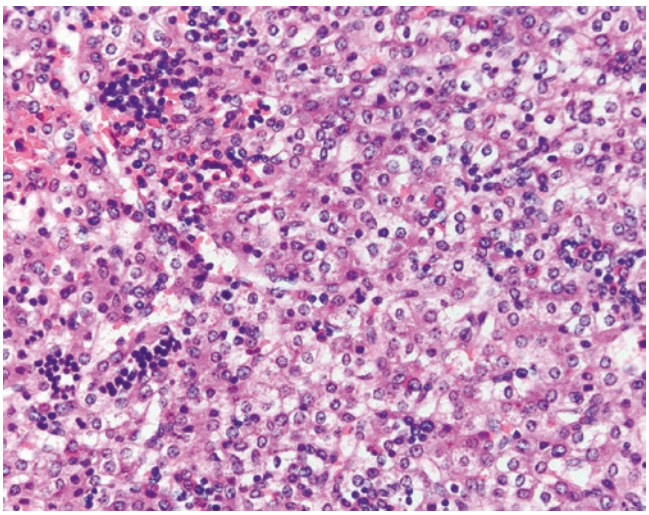

Fig. 13.32 Fetal epithelial clear cell hepatoblastoma. Most of the cells contain clear cytoplasms. Foci of extramedullary hematopoiesis are seen

"light and dark" pattern to the tumor. The cells are arranged in thin trabeculae one to three cells in thickness. Hematopoietic cells are nearly always present.

The embryonal pattern consists of a mixture of fetal epithelioid cells and small angulated cells which form acinar, glandular, or pseudorosettes. The small cell undifferentiated pattern is composed of non-cohesive sheets of small cells similar to those of other small blue cell pediatric neoplasms. The macrotrabecular pattern refers to cases of fetal or fetal/embryonal epithelial hepatoblastoma that contain numerous trabeculae more than ten cells in thickness.

The mixed epithelial and mesenchymal pattern of hepatoblastoma contains areas of epithelial cells along with areas of mesenchymal components such as cartilage and osteoid that express epithelial markers indicating that they are metaplastic rather than true mesenchymal tissues (Fig. 13.33). Other mixed hepatoblastomas are considered teratoid and contain skeletal muscle, squamous, and mucinous epithelium. Tumors treated with chemotherapy usually show extensive fibrosis, old hemorrhage, and cells with nuclear enlargement (Fig. 13.34).

Immunohistochemistry

Most hepatoblastomas express Hep-par 1and alpha-fetoprotein.

Treatment and Prognosis

Surgery is the treatment of choice and complete resection is the only chance for cure. Preoperative chemotherapy improves resectability and improves the overall 5-year survival rate to 75%. Stage of the tumor appears to be the key prognostic factor in determining survival [81].

Malignant Biliary Tumors

Cholangiocarcinoma

Cholangiocarcinoma is the second most common primary hepatic malignant tumor. It accounts for 10–15% of all malignant tumors of the liver [82, 83]. The tumor is significantly less common than hepatocellular carcinoma (HCC); although surveys indicate that cholangiocarcinoma has been increasing in incidence, the SEER data does not support this (Fig. 13.12). There seems to be a worldwide increase in the incidence of cholangiocarcinoma, especially after 1985 [84, 85]. Cholangiocarcinoma is the malignant epithelial neoplasm that arises from the intrahepatic bile ducts. In contrast to HCC, only 5% of cholangiocarcinomas originate in cirrhotic livers and less frequently in hepatitis C [82, 86]. Clinically, cholangiocarcinomas resemble HCC and metastatic adenocarcinoma. For a number of reasons, we do not recommend the use of the term cholangiocarcinoma for malignant epithelial tumors arising in the gallbladder or extrahepatic bile ducts [87]. Both cholangiocarcinoma and hepatocellular carcinoma are associated with a poor prognosis.

Clinical Features

Cholangiocarcinomas affect males and females equally (SEER Program of the National Cancer Institute, USA) (Surveillance, Epidemiology, and End Results). The mean age at presentation is in the seventh decade [83, 86]. The age range of the patients varies from 30 to 81 years. Cholangiocarcinomas are extremely rare in children [88].

Cholangiocarcinomas are sporadic and present late with an insidious onset. Symptoms include upper abdominal pain,

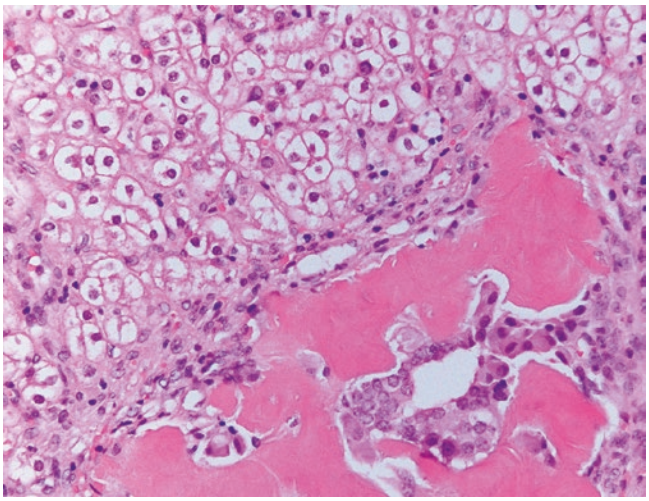

Fig. 13.33 Mixed epithelial and mesenchymal hepatoblastoma. The epithelial component consists of clear cells, while the mesenchymal component, characterized by osteoid material, is surrounded by cuboidal epithelial cells

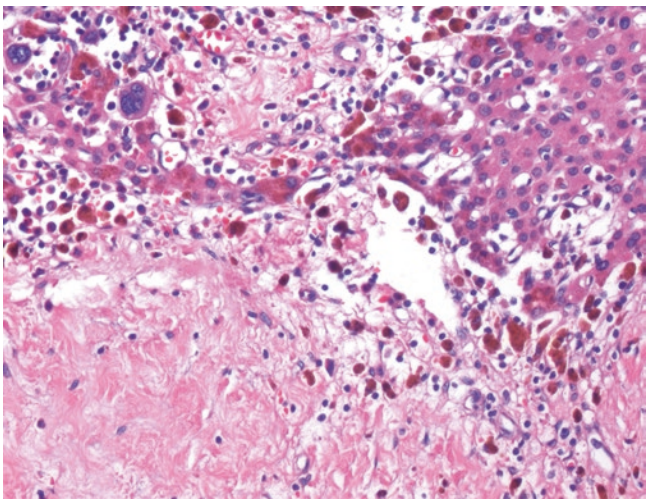

Fig. 13.34 Fetal epithelial hepatoblastoma post-chemotherapy. There is extensive fibrosis, old hemorrhage, and pronounced nuclear atypia

weight loss, ascites, fatigue, anorexia, and vomiting. Unusual presentations include a palpable mass and rupture.

A number of risk factors have been reported including Caroli's disease, solitary biliary cyst, adult polycystic renal disease, genetic hemochromatosis, extrahepatic biliary atresia, primary sclerosing cholangitis, inflammatory bowel disease, hepatolithiasis, primary biliary cirrhosis, gallstones, *Clonorchis sinensis*, *Opisthorchis viverrini*, and hepatitis B and C.

Gross Features

Cholangiocarcinoma may be nodular or diffuse and firm (Figs. 13.35a, b and 13.36a, b). When the tumor is multinodular, it closely resembles metastatic carcinoma. Cholangiocarcinoma growing around the bile ducts has been designated as periductal (Fig. 13.35b). When it grows beneath the capsule of the liver, cholangiocarcinoma tends to be umbilicated. Necrosis and hemorrhage are uncommon.

Microscopic Features

Because most carcinomas are composed of tubular or glandular structures similar to those that occur in extrahepatic adenocarcinomas and they lack specific immunohistochemical markers, they are often confused with metastatic adenocarcinomas, and the diagnosis of cholangiocarcinoma depends upon exclusion of other primary sites (Figs. 13.37, 13.38, 13.39, 13.40, 13.41, 13.42, 13.43, and 13.44).

Many unusual morphological variants of cholangiocarcinomas have been described including the papillary type, clear cell type, mucinous, squamous, mucoepidermoid, spindle cell type, the lymphoepithelioma-like carcinoma (Fig. 13.45), and the thyroid-like cholangiocarcinoma (Figs. 13.46, 13.47, 13.48, and 13.49) [82]. Well to moderately differentiated conventional cholangiocarcinomas may coexist with globular amyloidosis (Figs. 13.50a, b).

Immunohistochemical Features

The immunohistochemical profile of cholangiocarcinoma lacks specificity. The neoplastic cells express CK7, CK19 (Fig. 13.51), EMA, CEA, and CA19-9.

Prognostic Factors

Prognostic factors include tumor size, vascular invasion, lymph node metastasis, extension to extrahepatic bile ducts, and status of resection margins [89]. Additional factors likely to preclude surgery are ascitic carcinomatosis, extensive vascular invasion, and/or multiple intrahepatic metastases [89]. The superficial spreading and intraductal subtypes seem to have the most favorable outcome.

Prognosis

The prognosis is poor because most patients present with unresectable tumors. In two larger series, the median survival was 7 months. If the cholangiocarcinoma consists of a single nodule without metastases, the prognosis is better. Chemotherapy and radiotherapy do not improve prognosis.

Survival

The 5-year survival rate is poor. It is generally less than 10% (Fig. 13.52) [90]. Postsurgical outcomes for patients with recurrent intrahepatic cholangiocarcinomas have been reported. A prognostic nomogram that integrates ten clinicopathological variables for estimating survival of patients after hepatectomy for intrahepatic cholangiocarcinoma has been published [91].

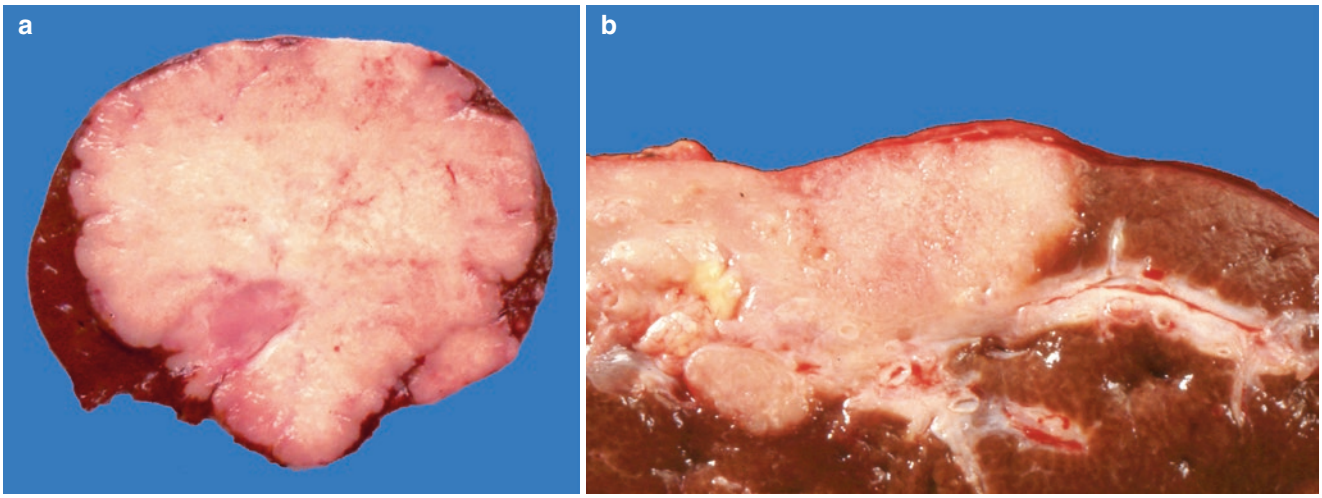

Fig. 13.35 (**a**) Cholangiocarcinoma. The tumor appears as a well-demarcated white nodule. (**b**) Cholangiocarcinoma, periductal type. The tumor appears to arise in intrahepatic bile ducts

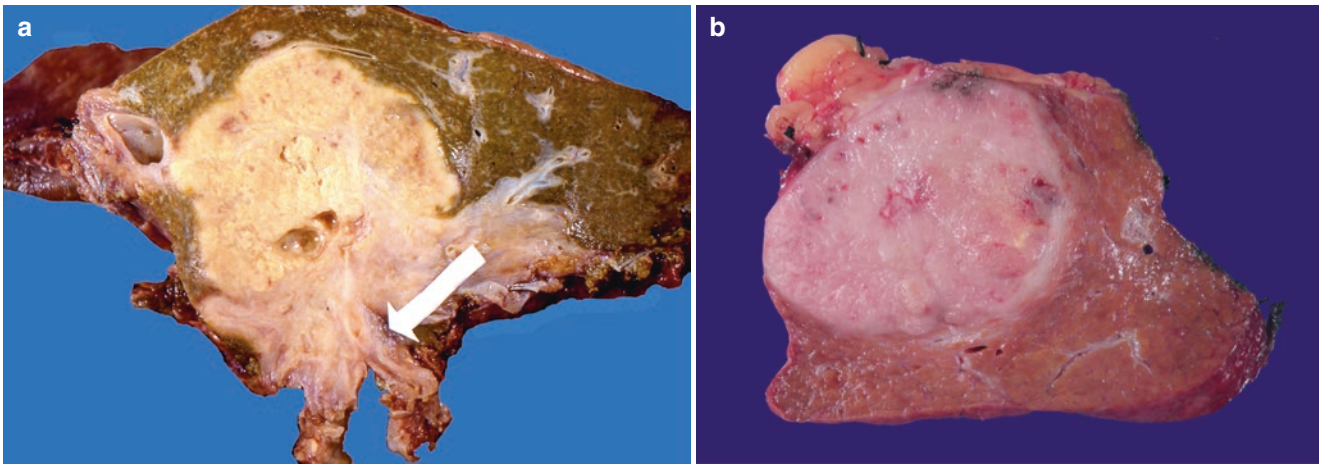

Fig. 13.36 (**a**) Cholangiocarcinoma. The tumor consists of a large gray-white to yellow nodule, which extends into the right and left hepatic ducts (arrow). (**b**) Cholangiocarcinoma. Lymphoepithelioma-like. The tumor is composed of a well-demarcated white nodule

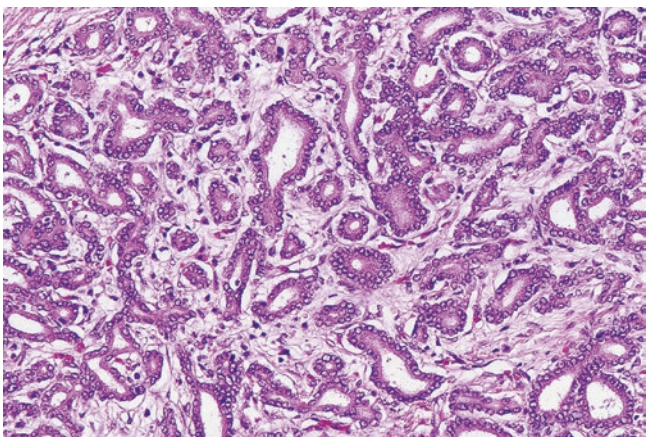

Fig. 13.37 Well-differentiated cholangiocarcinoma. The tumor is composed of varying sized tubular structures closely resembling intrahepatic bile ducts and separated by scant fibrous stroma

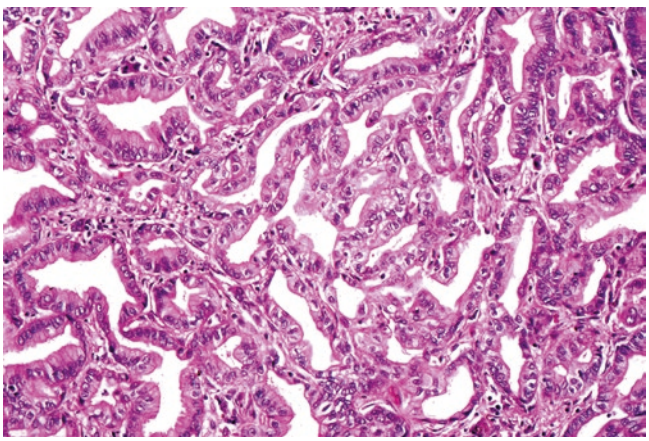

Fig. 13.38 Well-differentiated cholangiocarcinoma. The compact neoplastic tubules are separated by scant stroma and are lined by cuboidal and columnar cells

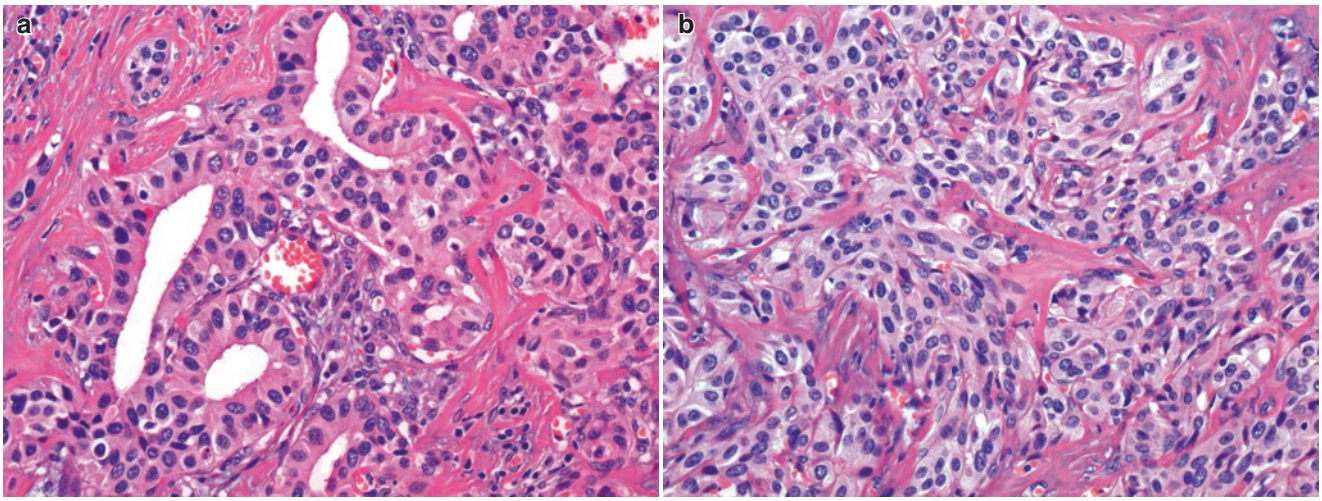

Fig. 13.39 (**a**) Moderately differentiated cholangiocarcinoma. Group of well-defined tubules are lined by cuboidal cells with moderate atypia. (**b**) Moderately differentiated cholangiocarcinoma. Here the tumor grows in nests and solid cords. Same tumor shown in Fig. 13.39a

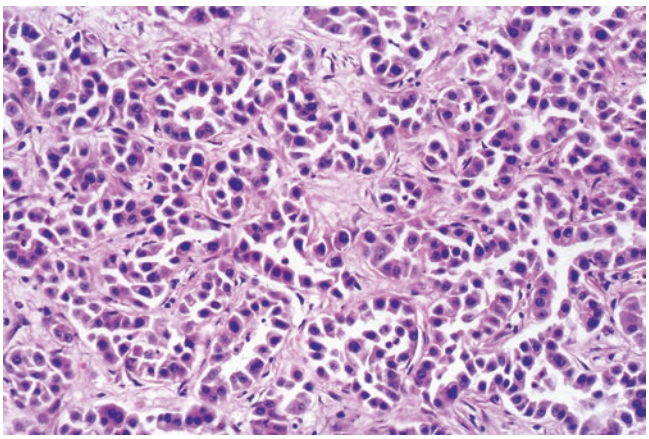

Fig. 13.40 Moderately differentiated cholangiocarcinoma. The neoplastic tubules are poorly defined and are lined by cuboidal or columnar cells with marked cytologic atypia

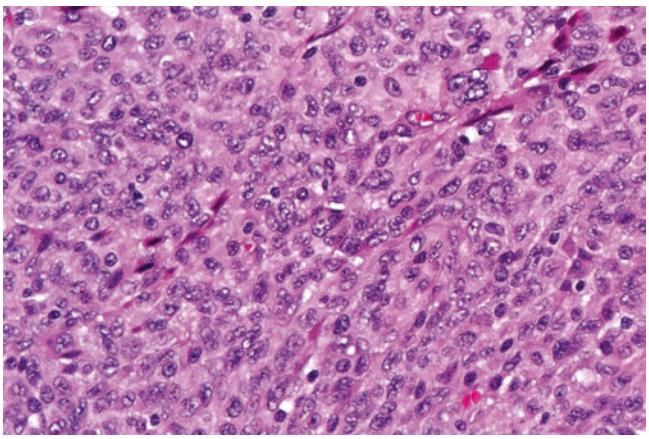

Fig. 13.42 Poorly differentiated cholangiocarcinoma. A solid area is composed of small epithelial cells with marked atypia

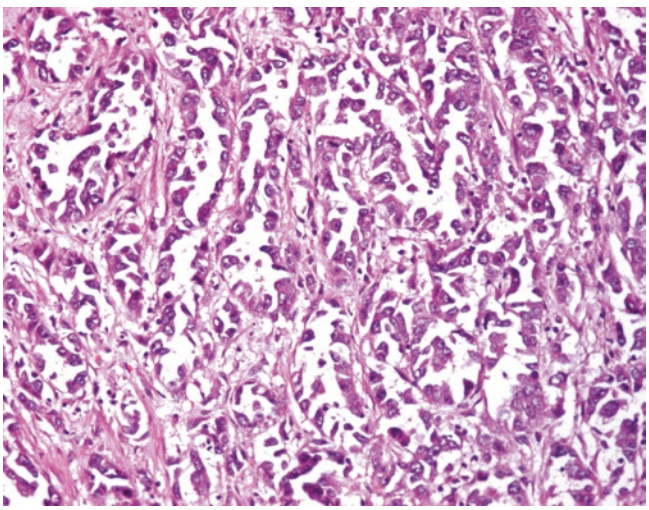

Fig. 13.41 Moderately differentiated cholangiocarcinoma. The neoplastic tubules are elongated, tend to branch, and are lined by cuboidal or columnar cells with marked cytologic atypia

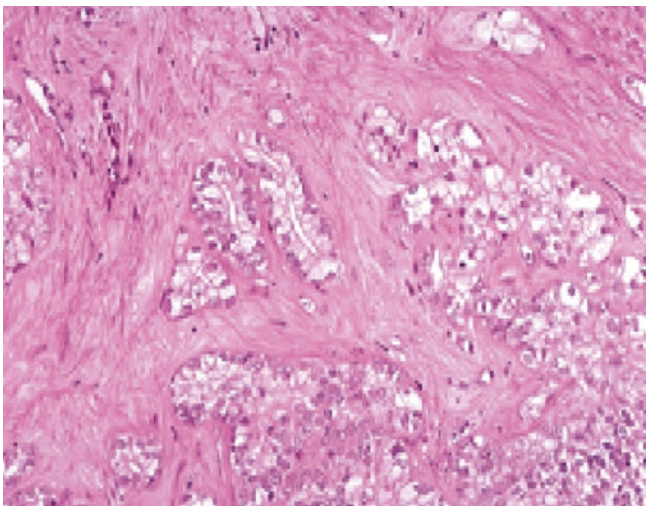

Fig. 13.43 Cholangiocarcinoma, clear cell type. The tubules and nests which are separated by abundant fibrous stroma are lined by atypical cuboidal or columnar cells with ample clear cytoplasm. Compare with atypical clear cell adenoma shown in Fig. 13.5b

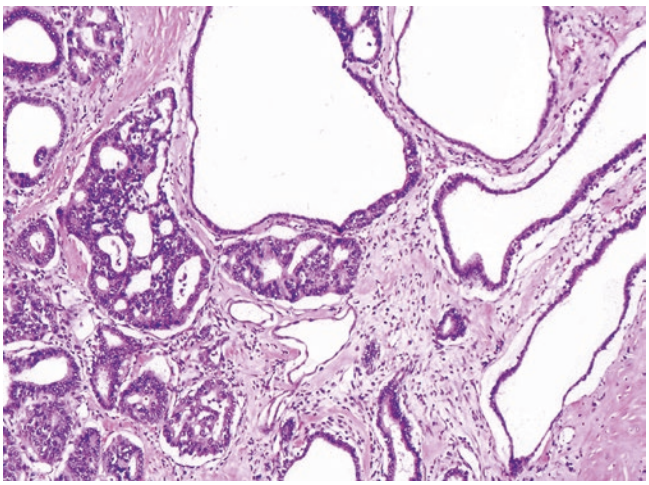

Fig. 13.44 Cholangiocarcinoma arising in Caroli's disease. The tumor shows a cribriform pattern and grows beneath dilated glands lined by benign cuboidal or columnar epithelium

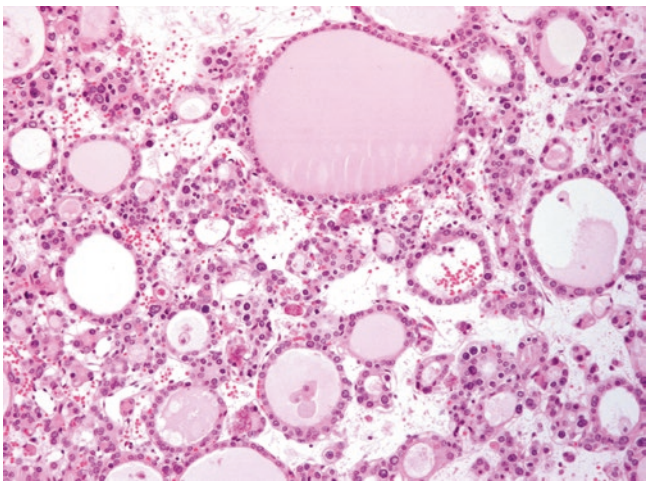

Fig. 13.46 Cholangiocarcinoma, thyroid-like variant. The varying sized neoplastic follicles contained abundant colloid-like material, some of which showed a few foamy macrophages. (With permission © 2012 Ann Hepatol [82])

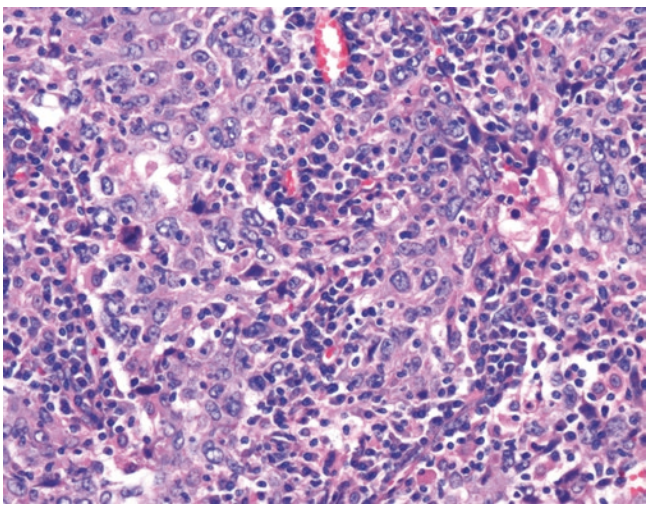

Fig. 13.45 Cholangiocarcinoma, lymphoepithelioma-like. The tumor is composed of nests of poorly differentiated epithelial cells surrounded by abundant lymphoid stroma

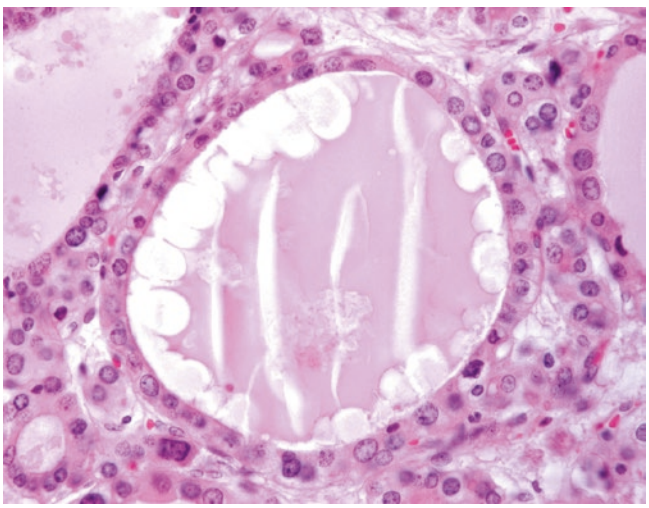

Fig. 13.47 Cholangiocarcinoma, thyroid-like variant. The follicles are lined by low cuboidal cells, some with clear nuclei. The intrafollicular colloid-like material showed peripheral vacuolation mimicking a follicle of goiter. (With permission © 2012 Ann Hepatol [82])

Intraductal Papillary Neoplasm and Cystadenoma

Intraductal Papillary Neoplasms

Papillary neoplasms of the intrahepatic bile ducts are seen in two different settings: (a) coexisting with multiple papillary tumors of the extrahepatic bile ducts, gallbladder, and occasionally pancreatic duct. This rare clinicopathological entity is designated as biliary papillomatosis and is discussed in detail under adenomas of the extrahepatic bile ducts. (b) Sporadic and usually single. The sporadic intraductal papillary neoplasms of the liver appear to be more common in men than in women. The age of the patients ranges from 35 to 80 years with a mean of 64 years [92]. The intraductal location of the tumors can be achieved by magnetic resonance imaging and magnetic resonance cholangiopancreatography [93].

Gross Features

Grossly, 57.5% of the tumors are located in the left lobe, and 29.5% are located in the right lobe. The sporadic intraductal papillary tumors appear as well-defined cystic and nodular masses ranging in size from 7 to 21 cm. Demonstrating the intratubular location of the tumors is not an easy task, and

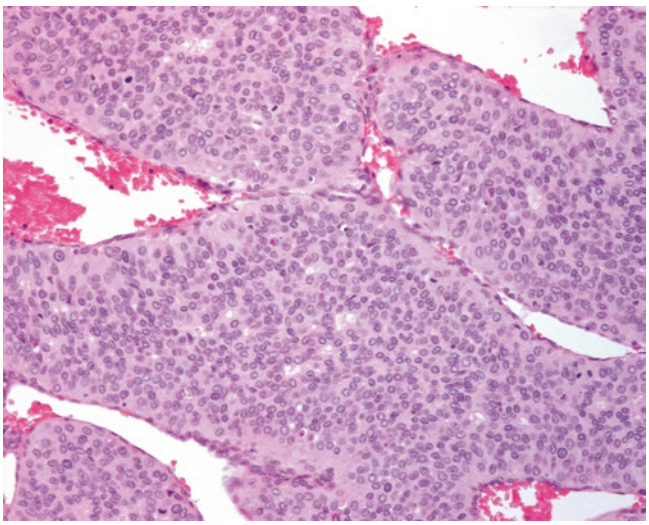

Fig. 13.48 Cholangiocarcinoma, thyroid-like variant. Insular areas similar to those seen in papillary and follicular thyroid carcinomas. (With permission © 2012 Ann Hepatol [82])

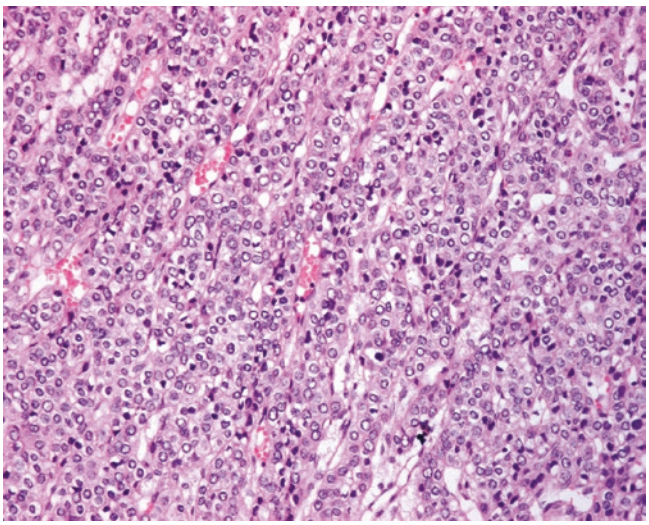

Fig. 13.49 Cholangiocarcinoma, thyroid-like variant. The trabecular areas showed cells with clear nuclei, some with grooves similar to those seen in papillary thyroid carcinoma. (With permission © 2012 Ann Hepatol [82])

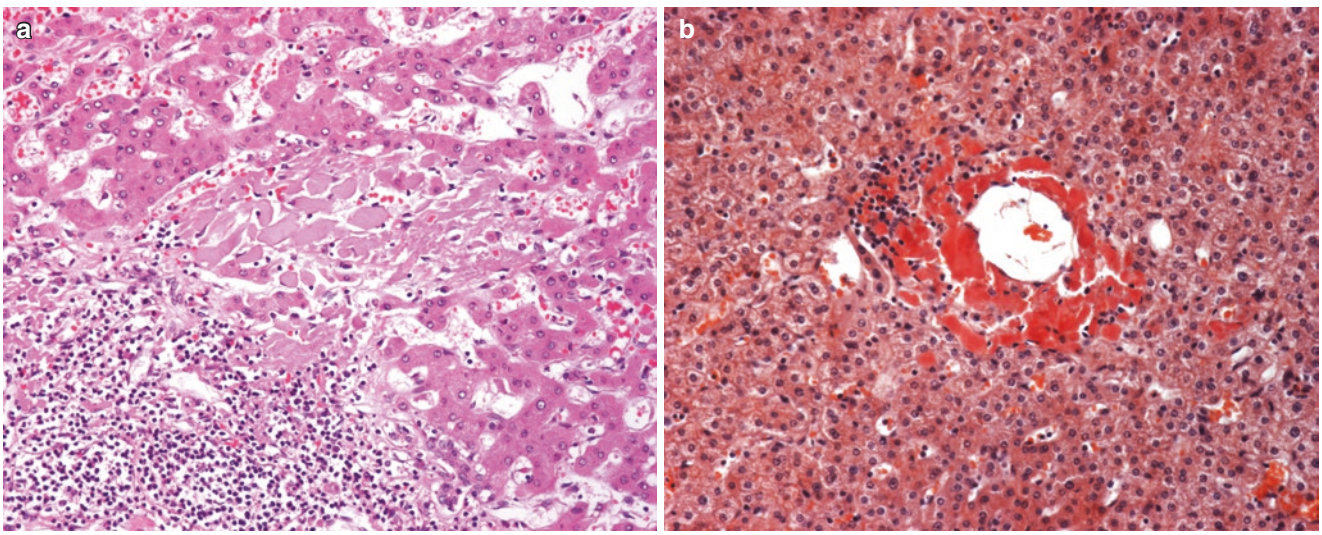

Fig. 13.50 (**a**) Globular amyloidosis associated to cholangiocarcinoma (not seen here). (**b**) Congo red amyloid deposits adjacent to a cholangiocarcinoma (not seen here)

sometimes multiple microscopic sections are needed to show the wall of the bile ducts and the intratubular location of the mass.

Microscopic Features

When the tumors are confined to the lumen of the bile duct with no evidence of invasion into the liver parenchyma, they should be regarded as intraductal papillary carcinomas. When the tumors project into the bile duct lumen but extend beyond the ductal wall into the adjacent liver parenchyma, they should be classified invasive intraductal papillary carcinomas. The tumors are predominantly exophytic into the cyst lumina and show variable degree of architectural complexity. Filiform and broad papillae are identified (Fig. 13.53a). Gland-like structures and poorly defined cribriform areas are also present. Some tumors may show solid areas of variable extent. The phenotype of the neoplastic cells may be biliary, intestinal, or oncocytic (Fig. 13.53b). The biliary type cells are cuboidal or columnar, the cells with intestinal phenotype are absorptive columnar cells mixed with goblet cells, and the cells with oncocytic features are columnar and have abundant eosinophilic and granular cytoplasm. The nuclei are centrally located and contain prominent nucleoli. The number of mitotic figures is quite variable. The biliary and oncocytic intraductal papillary carcinomas express cytokeratin 7 and 19 and are negative for CK20. The

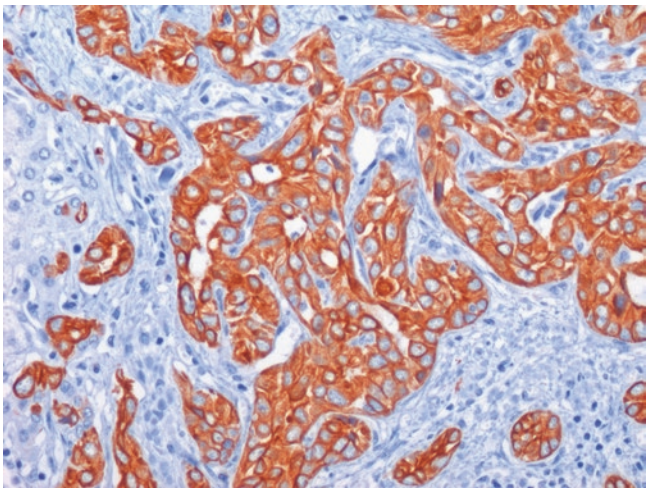

Fig. 13.51 Diffuse immunoreactivity for CK19 in a moderately differentiated cholangiocarcinoma

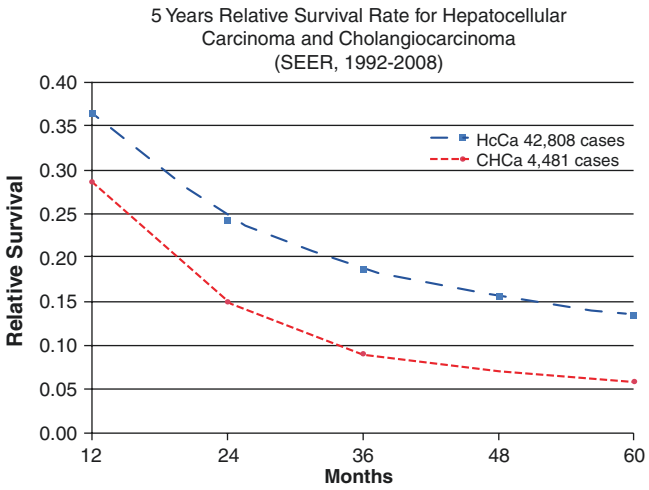

Fig. 13.52 The 5-year relative survival rate of patients with hepatocellular carcinoma and cholangiocarcinoma was 13% and 6%, respectively

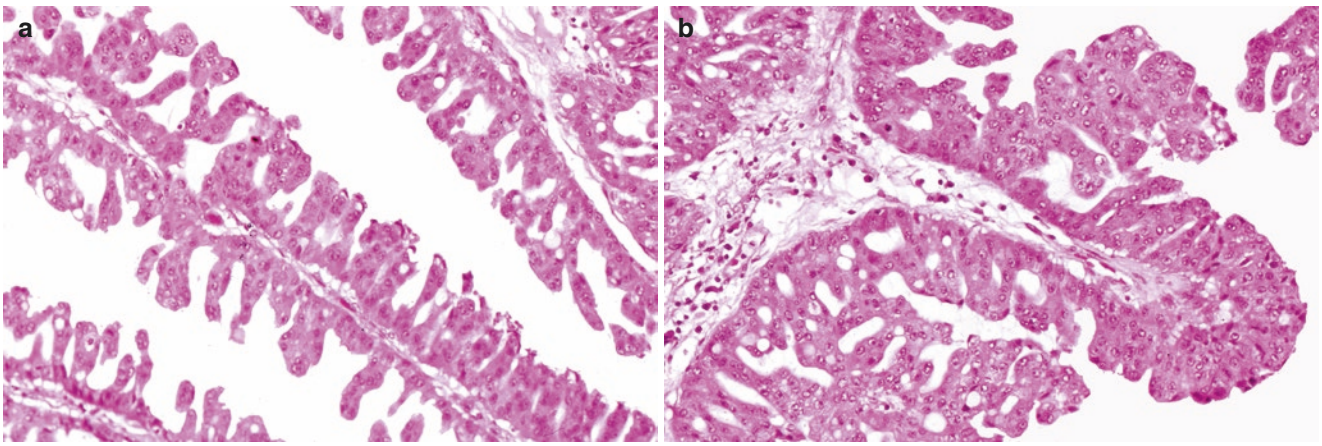

Fig. 13.53 (**a**) Intraductal papillary carcinoma, oncocytic type. Thin fibrovascular stalks are lined by cuboidal and columnar cells with abundant eosinophilic cytoplasm. (**b**) Intraductal papillary carcinoma, oncocytic type. This papillary structure is lined by pseudostratified oncocytic cells that show a focal cribriform pattern

intestinal type of intraductal papillary carcinoma expresses MUC2 and CDX2 [92–96].

Genetic tests show a stepwise progression from low-grade intraductal papillary dysplasia at its beginning to invasive adenocarcinoma at its end. Mutated KRAS, overexpression of TP53, and loss of p16 are most commonly involved in this process [92].

Prognosis

The noninvasive papillary carcinomas that are completely resected have long-term survival. In contrast, the prognosis of invasive papillary carcinomas is poor and is similar to conventional cholangiocarcinomas.

Cystadenoma

More common in the liver than in the extrahepatic bile ducts, cystadenomas are uncommon neoplasms whose terminology has been controversial. In our opinion, cystadenomas of the EHBD and liver display a predominant biliary or intestinal phenotype.

Cystadenoma of the liver and extrahepatic bile ducts is usually a benign, multiloculated neoplasm. According to their cell phenotype, cystadenomas can be divided into those with a predominant biliary phenotype (90%) and those with a predominant intestinal phenotype (10%). We believe that the term "mucinous cystic tumor" recommended by the WHO for all cystadenomas of the liver and EHBD is a mis-

nomer [97, 98]. The subepithelial stroma is densely cellular and resembles ovarian stroma. This rare but distinctive neoplasm belongs to a family of mucinous cystic tumors that can arise in the liver, in the extrahepatic biliary tree, in the pancreas, or even in the retroperitoneum unattached to any organ [98]. Although mucinous cystic tumors of the pancreas and cystic tumors of the biliary tree share some similarities, major differences exist. Of 52 biliary cystadenomas, 43 were located in the liver, 8 in the extrahepatic bile ducts, and 1 in the gallbladder [98]. Cystadenomas of the liver and pancreas may coexist in the same patient. Likewise, cystadenomas of the liver may extend into the extrahepatic bile ducts, and cystadenomas of the extrahepatic bile ducts may extend into the liver [98].

Clinical Features

Cystadenomas are seen almost exclusively among middle-aged women (mean age, 36.5 years). They are much more frequent in the liver than in the extrahepatic bile ducts. Often larger than non-cystic adenomas, cystadenomas are usually symptomatic. Many are palpable on physical examination and may be painful. Others especially those arising in the EHBDs cause obstructive jaundice and even resemble a choledochal cyst [98]. Elevated serum levels of CA19-9 have been reported in patients with these tumors [98]. Rarely, cystadenomas are incidental findings at autopsy.

Gross Features

Cystadenomas are multilocular or unilocular, well-demarcated cystic masses that when lined by intestinal epithelium contain mucin and are rich in CEA, while those lined predominantly or exclusively by biliary epithelium contain serous, clear, or hemorrhagic fluid and lack CEA (Fig. 13.54a). Their size ranges from 1.5 to 29 cm (average 11 cm) [97]. The fibrous wall is smooth and of variable thickness. The inner surface can be smooth, finely granular, or trabeculated. In some cystadenomas, small polypoid structures project into the lumen of the locules. We have seen a biliary cystadenoma that appeared as a polypoid, microcystic, yellow mass that seemed to have arisen within the liver and extended into the common hepatic duct. Another biliary cystadenoma from our collection of four cases arose in the left and right hepatic ducts and consisted of small cystic structures some containing mucin (Fig. 13.54b–d).

Microscopic Features

The locules of most cystadenomas have a characteristic three-layer structure (Fig. 13.55a), an epithelial lining, a cellular ovarian-like stroma, and an outer layer of hyalinized fibrous tissue (Fig. 13.55b–d). The lining epithelium of these cystic neoplasms is heterogeneous and may show biliary phenotype, an intestinal phenotype or both. The biliary phenotype usually predominates (90%) [97]. Focal oncocytic differentiation is seen in some cystadenomas with biliary phenotype. Cystic neoplasms with a predominant intestinal lining also show a focal biliary phenotype (Fig. 13.55e–h). Some cystadenomas display, in addition, a focal epithelial lining with a foveolar phenotype. The biliary component consists of a single layer of non-dysplastic cuboidal biliary cells; the intestinal cell component consists of absorptive columnar cells with low-grade or high-grade dysplasia and mixed with goblet, Paneth, and endocrine cells. Underlying the epithelial lining, there is a cellular band composed of spindle cells reminiscent of ovarian stroma, which is supported by an outer layer of hyalinized fibrous tissue. Inflammatory changes occur in some cases. Foamy histiocytes, multinucleated giant cells, hemosiderin-laden macrophages, areas of hemorrhage, and cholesterol clefts efface the ovarian-like stroma and the characteristic three-layer structure. Two of our cases with an intestinal phenotype contained foci of high-grade dysplasia that progressed to invasive adenocarcinoma. One of these tumors arose in the liver, while the other originated in the extrahepatic bile ducts.

Immunohistochemical Features

Given the cytologic heterogeneity of the cystadenomas, different immunohistochemical reactions are expected in different parts of the same tumor. The biliary component is immunoreactive for cytokeratin 7, cytokeratin 19, and focally to MUC1, as well as CAM5.2, epithelial membrane antigen, and the tumor-associated antigen CA19-9 [97, 98]. The intestinal component is immunoreactive for MUC2, CDX2, CEA, and cytokeratin 20 (Fig. 13.56a, b). Focal or diffuse reactivity to lysozyme is seen in the epithelium of approximately 50% of the tumors. About 33% of cystadenomas, especially those with intestinal phenotype, contain chromogranin and/or synaptophysin positive cells, some of which are also immunoreactive for serotonin (Fig. 13.56c). The spindle cells of the ovarian-like stroma label with vimentin and smooth muscle actin. Focal desmin positivity is seen in 33% of tumors, while focal inhibin reactivity is present in the spindle cells of most cystadenomas. This immunohistochemical profile is consistent with fibroblastic and myofibroblastic differentiation. The spindle cells of the ovarian-like stroma express alpha-inhibin, estrogen, and progesterone receptors (Fig. 13.56d) [97].

We have examined two cystadenomas by electron microscopy. Three cell types were identified in the stroma: undifferentiated mesenchymal cells, fibroblasts, and myofibroblasts. The lining epithelial cells were columnar and joined by desmosomes. Short apical microvilli and mucin droplets of different sizes were present in many epithelial cells.

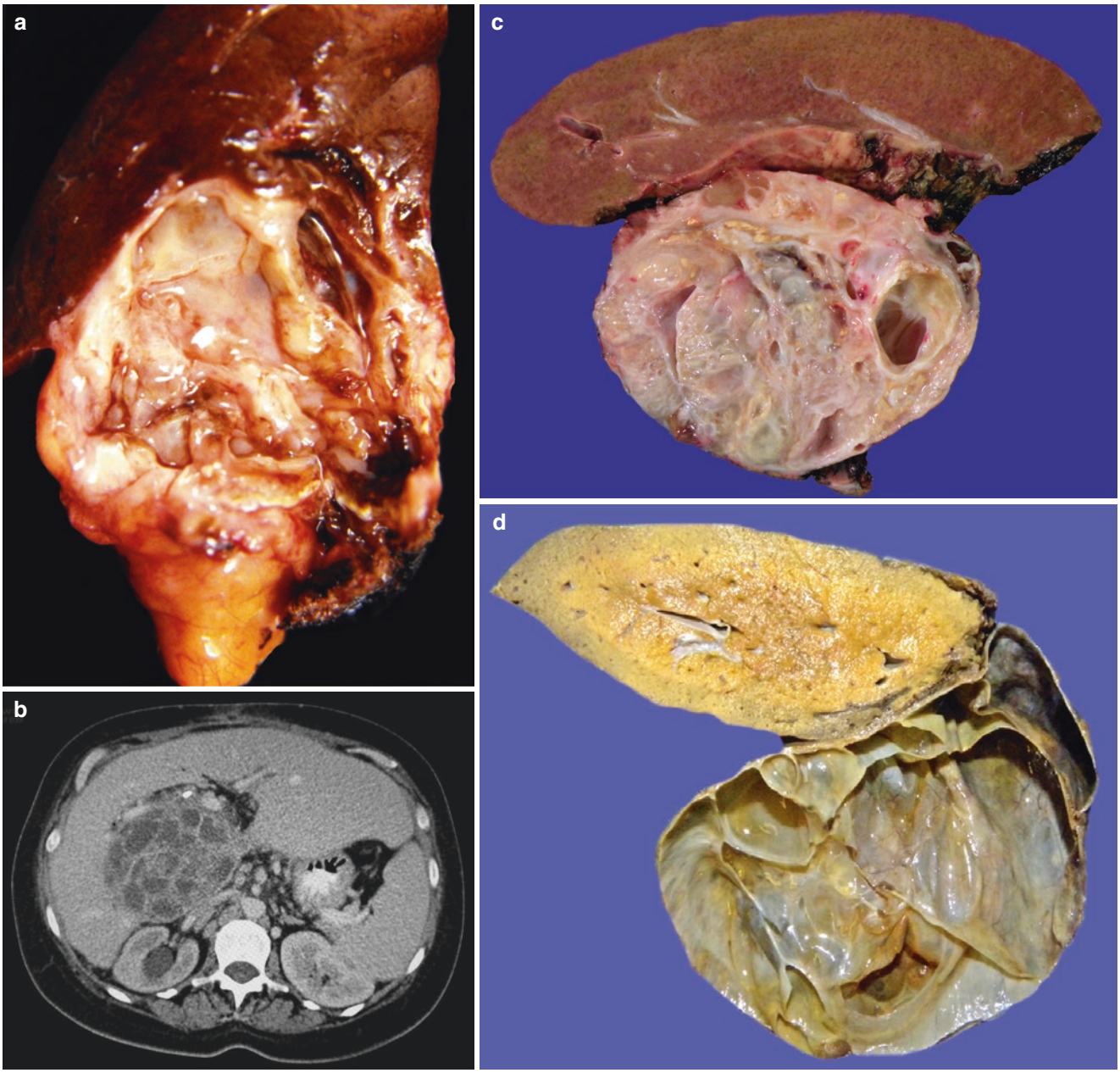

Fig. 13.54 (**a**) Cystadenoma of the right hepatic duct with extension into the common hepatic duct. A large locule has a mostly smooth inner surface with a few mucinous nodules. (**b**) Cystadenoma of extrahepatic bile ducts. Computed tomography of a cystadenoma with intestinal and biliary phenotypes that appears multiloculated. (**c**) Cut surface of the cystadenoma, intestinal type. Most of the locules are small some of which contain mucin. (**d**) Cystadenoma of the liver. The tumor is large and multiloculated, and the inner surface of the locules is smooth and glistening

Fig. 13.55 (**a**) Cystadenoma. Low-power view of a cystadenoma of the extrahepatic bile ducts showing multiple locules of different sizes. (**b**) Cystadenoma of the common hepatic duct. The epithelial lining is non-dysplastic biliary type and contains no mucin. The cellular ovarian-like stroma is seen beneath the biliary epithelium. (**c**) Cystadenoma of the left and right hepatic ducts. The tumor shows a broad papillary structure lined by non-dysplastic low cuboidal biliary epithelium. (**d**) Cystadenoma of the left and right hepatic ducts. Here the surface epithelium is columnar and mucin-producing. (**e**) Cystadenoma of common hepatic duct. A connective tissue septum is lined on one side by intestinal-type columnar epithelium and on the other by non-dysplastic low cuboidal biliary epithelium

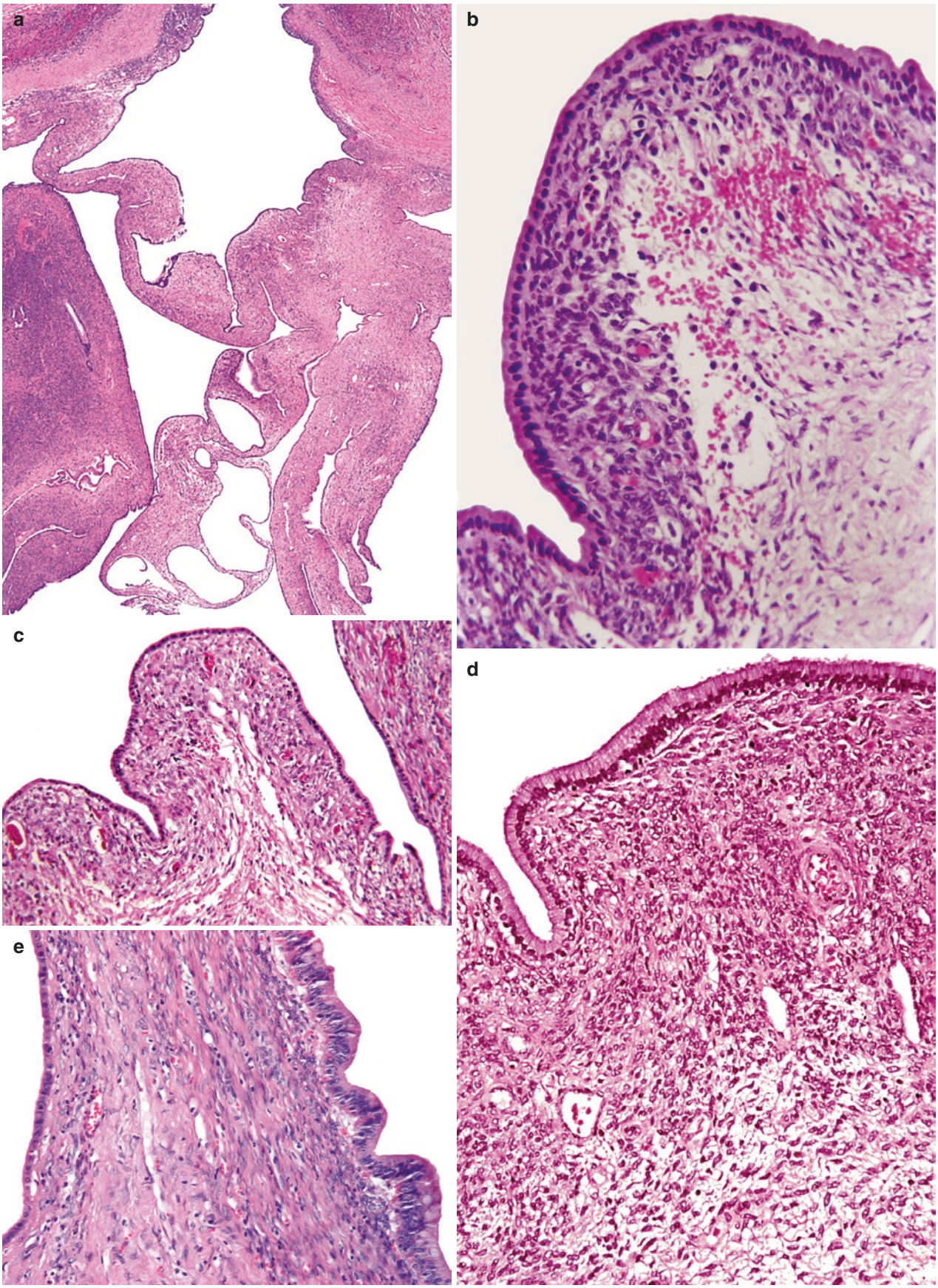
a
b
c
d
e

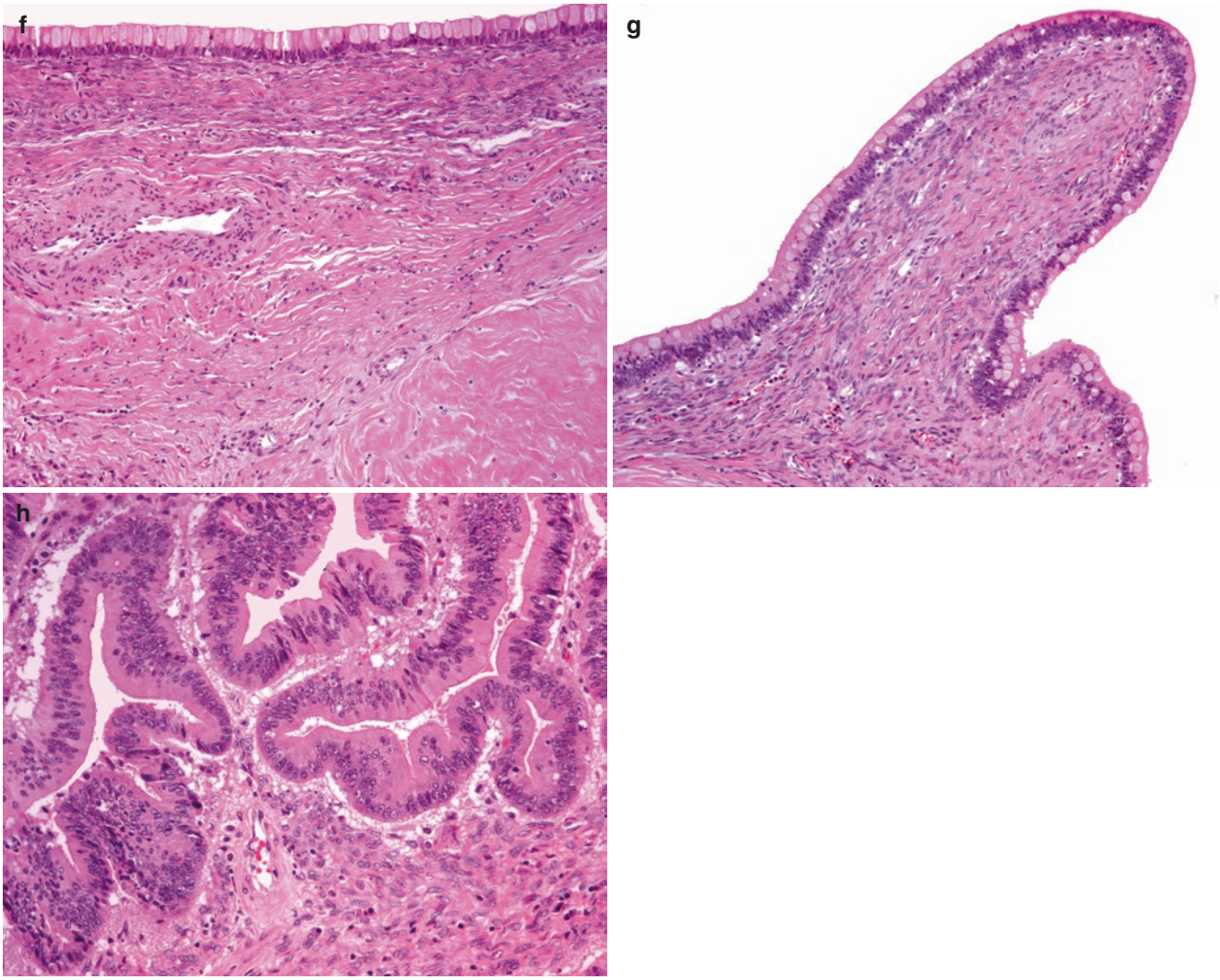

Fig. 13.55 (continued) (**f**) Cystadenoma of the left and right hepatic ducts. The epithelial lining is composed predominantly of goblet cells. A subepithelial ovarian-like stroma and dense hyalinized connective tissue are also seen. (**g**) Cystadenoma of common hepatic duct. A papillary structure is lined predominantly by goblet cells. (**h**) Dysplasia in cystadenoma. Focus of intestinal differentiation with high-grade dysplasia in biliary cystadenoma

Differential Diagnosis

Cystadenomas should be distinguished from choledochal cysts, the most common congenital anomaly of the extrahepatic biliary tree. Choledochal cysts, however, are not multiloculated. Their wall consists of dense fibrous tissue, which may be lined by normal biliary epithelium or may be devoid of an epithelial lining. The ovarian-like stroma characteristic of cystadenoma is lacking in choledochal cysts, serous cystadenomas, and intraductal papillary mucinous neoplasms. Retention cysts of periductal gland origin can be confused with cystadenomas. These retention cysts are usually multiple, asymptomatic, and smaller than cystadenomas. Their wall lacks the ovarian-like stroma and may contain inflammatory cells [98].

Treatment and Prognosis

Cystadenomas of the liver or extrahepatic bile ducts usually recur following incomplete excision [98]. Despite the focal areas of dysplasia present in 16 percent of cystadenomas, malignant transformation can occur in a few of these tumors (10%) especially those with intestinal differentiation. In our experience, two patients with adenocarcinoma with intestinal phenotype and lack of extension into the cyst capsule were asymptomatic from 3 to 11 years after surgery. Therefore, if completely excised, the prognosis of these tumors is excellent [97]. Biliary cystadenocarcinomas have been documented in the gallbladder and in the liver [98].

Vascular Tumors

Lymphangioma

Lymphangiomas are benign neoplasms composed of lymphatic vessels of varied sized and lined by endothelial cells. They are usually multiple and less frequently single. Hepatic

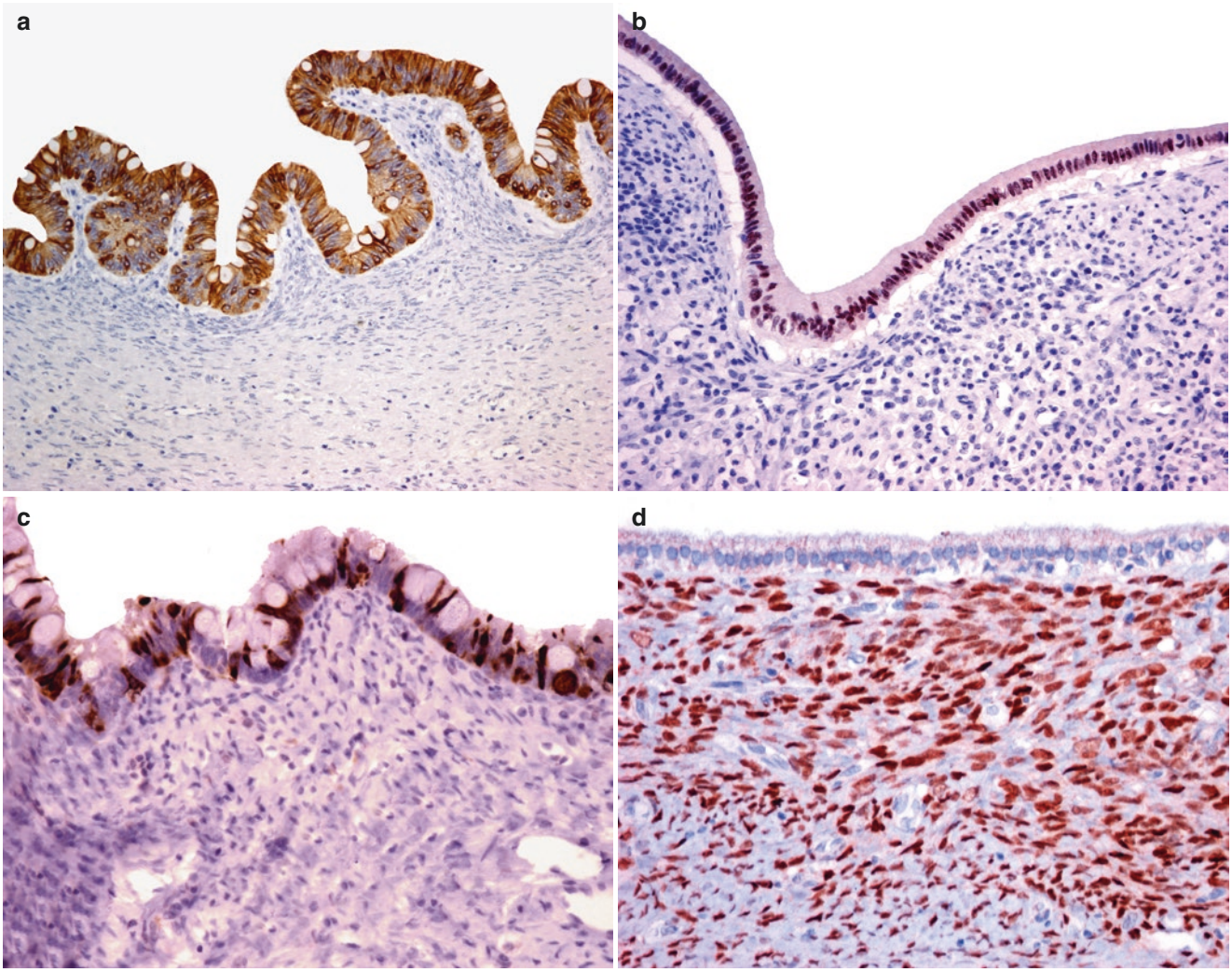

Fig. 13.56 Immunohistochemistry in cystadenoma. (**a**) The lining epithelium with intestinal phenotype is positive for MUC2 and (**b**) for CDX2 and (**c**) Chromogranin-positive cells are admixed with the goblet cells. (**d**) Progesterone receptors in cystadenoma. Nearly all nuclei of the spindle cells from the ovarian-like stroma are positive for progesterone receptors. The biliary epithelium is unreactive

lymphangiomas may coexist with lymphangiomatosis of the spleen, skeleton, and other organs [99–101].

Clinical Features

Most cases of diffuse lymphangiomatosis involving the liver, spleen, other visceral organs, and the skeleton occur in children and young adults [99]. The female to male ratio is 2 to 1. Signs and symptoms include hepatosplenomegaly, pleural effusion, abdominal swelling, multiple fractures, ascites, and liver failure. The prognosis of diffuse lymphangiomatosis is poor [100].

Gross Features

The liver is enlarged and diffusely involved by multiple cystic lesions of variable size. Most are small; some are cystically dilated and contain a chylous or milky fluid. Rarely, the liver shows a single cystic mass.

Microscopic Features

The lymphatic vessels are lined by a single layer of endothelial cells, which focally may form small papillary projections. Vessels usually contain lymph. The endothelial cells show immunoreactivity for CD31, CD34, and factor VIII. Between the lymphatic vessels, there are bands of fibrous connective tissue. Collections of lymphocytes may be present in some cases.

Hemangioma

Clinical Features

Hemangiomas are the most common benign mesenchymal neoplasms of the liver. They occur at all ages although they are most often diagnosed in adults. Women are more commonly affected than men. The pathogenesis of these tumors

however appear unrelated to steroid hormones. Small hemangiomas measuring less than 5 cm are usually asymptomatic and often represent incidental findings at laparotomy or autopsy. About half of hepatic hemangiomas >5 cm are symptomatic and produce pain or abdominal discomfort, hepatomegaly, or mass. Rarely hemangiomas can rupture leading to intraabdominal hemorrhage. Two other rare complications of hepatic hemangiomas are: (a) the association with the Kasabach-Merritt syndrome (consumptive coagulopathy) [102] and (b) erythrocytosis due to secretion of erythropoietin by the tumor [103]. Hepatic hemangiomas have been reported in association with cysts of the liver and pancreas, von Meyenburg complex, tuberous sclerosis, and focal nodular hyperplasia [104]. The preoperative diagnosis of hemangioma can be accomplished by CT, sonography, or arteriography. The most sensitive method appears to be magnetic resonance imaging. The use of needle core biopsy in the diagnosis of hepatic hemangioma is contraindicated because it may lead to severe hemorrhage [105].

Gross Features

Hepatic hemangiomas are often solitary, 10% are multiple, and less than 1% involves diffusely the liver (hepatic hemangiomatosis). They are usually small measuring less than 5 cm in greatest dimension. Some, however, are quite large measuring 20–30 cm and replacing an entire hepatic lobe. They are well-demarcated but not encapsulated, spongy, and dark.

Microscopic Features

Cavernous hemangioma, the most common histologic type, consists of blood-filled or empty vascular channels of varied size lined by flat or low cuboidal endothelial cells (Fig. 13.57a). The hemangiomas can undergo thrombosis, sclerosis, or calcification. Extensive fibrosis with hyalinization is seen in some areas of the tumor (Fig. 13.57b). Capillary hemangiomas are exceedingly rare and similar to those that occurs in the skin and mucous membranes.

Epithelioid Hemangioendothelioma

First described in the lungs by Liebow, this uncommon malignant vascular neoplasm has now been recognized in many other organs including the liver [106, 107]. The epithelioid appearance of neoplastic cells, the presence of small tubular structures, and the focal expression of cytokeratins by some tumors are responsible for its confusion with cholangiocarcinoma or metastatic carcinoma. However, the demonstration of endothelial markers by immunohistochemistry and ultrastructure in neoplastic cells has established the vascular nature of the neoplasm.

Clinical Features

The vast majority of patients with epithelioid hemangioendothelioma are adults although rarely it has been reported in children. In the largest series published the age of patients ranged from 12 to 86 years with a mean of 60 years [108]. Two thirds of the patients are females. Signs and symptoms include hepatosplenomegaly, weakness, anorexia, nausea, vomiting, upper abdominal pain, and jaundice. Rarely the tumor ruptures and produces hemoperitoneum. Bud-Chiari syndrome and portal hypertension are also uncommon clinical presentations [109].

Ultrasonography, computed tomography, magnetic resonance imaging, and arteriography are useful diagnostic procedures, but a definitive diagnosis requires a biopsy.

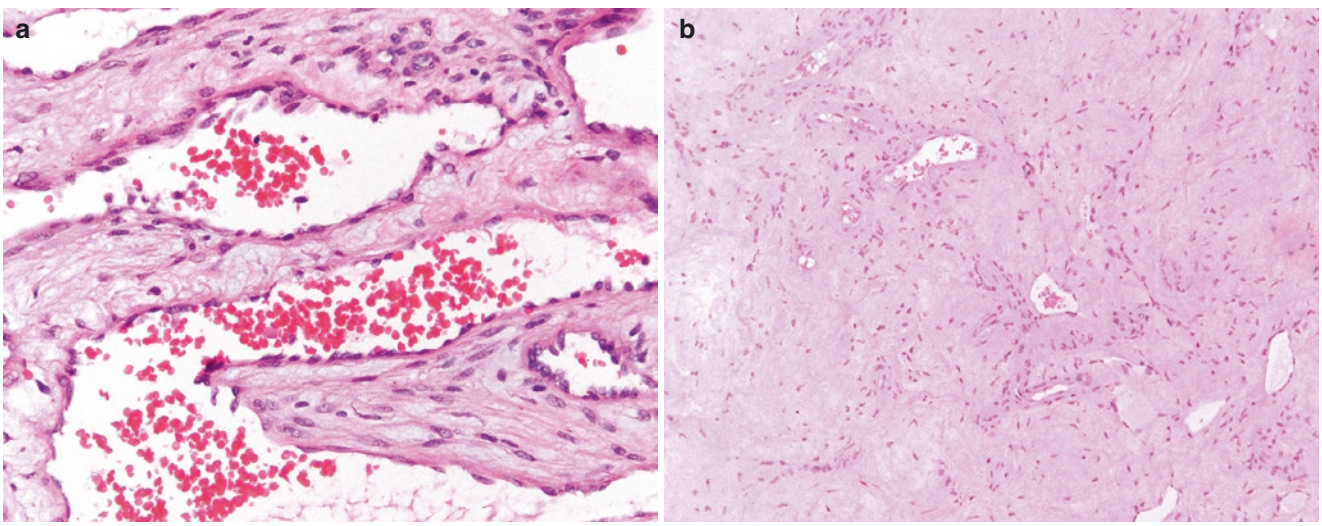

Fig. 13.57 (**a**) Cavernous hemangioma. Blood vessels containing erythrocytes are lined by flat endothelial cells. (**b**) Cavernous hemangioma. The hemangioma is extensively hyalinized

Gross Features

Epithelioid hemangioendothelioma is usually a multifocal neoplastic disease. It consists of multiple nodules of different sizes that often involve both hepatic lobes. The nodules vary from a few millimeters to several centimeters and are well demarcated, gray-white, and firm (Fig. 13.58a, b). When the nodules coalesce, they form a large diffuse mass. In most cases the liver parenchyma adjacent to the tumor is normal.

Microscopic Features

The histologic features of epithelioid hemangioendothelioma are quite characteristic (Figs. 13.58, 13.59, 13.60, 13.61, 13.62, and 13.63). At the periphery of the neoplastic nodules, the tumor infiltrates the sinusoids, terminal hepatic venules, and portal vein branches preserving the acinar architecture. The neoplastic cells that grow within sinusoids are usually epithelioid and may form small nests or papillary structures (Fig. 13.60a). Small tubules may simulate neoplastic glands (Fig. 13.60b). The stroma is abundant, myxoid, or hyalinized and contains neoplastic spindle-shaped or dendritic cells with multiple interdigitating processes (Figs. 13.62 and 13.63). Many neoplastic cells show cytoplasmic vacuoles, which are vascular lumina that may contain erythrocytes. These vacuoles may displace the nuclei toward the periphery mimicking signet ring cells. Multinucleated giant cells may occasionally be seen.

Immunohistochemistry

The tumor cells express the endothelial markers CD31 and CD34 (Fig. 13.63). Rarely some tumor cells may be cytokeratin positive.

Ultrastructural Features

The ultrastructural features of cells of epithelioid hemangioendothelioma are similar to those of normal endothelial cells. They show pinocytotic vesicles and Weibel-Palade bodies. The cytoplasmic vacuoles represent intravascular lumina, and the cytoplasm contains abundant intermediate filaments.

Angiosarcoma

Angiosarcoma is a highly malignant vasoformative neoplasm that has been reported in the skin, breast, soft tissues, and visceral organs, including the liver. It is the most common malignant mesenchymal neoplasm of the liver accounting for one third of primary hepatic sarcomas and 1.8% of all hepatic malignant tumors [110, 111]. Worldwide over 200 cases are diagnosed annually [112]. It has been estimated that 10–20 cases occur per year in the USA [113]. Angiosarcoma has been associated with a variety of risk factors including chronic exposure to vinyl chloride, inorganic arsenic compounds, and anabolic steroids [112]. Angiosarcoma has been induced in experimental animals exposed to vinyl chloride further strengthening the association [114]. Angiosarcomas may develop after injection of thorotrast, a radioactive substance that was used as a radiographic contrast medium that accumulates in the liver. However, thorotrast-induced angiosarcomas of the liver have declined considerably during the last two decades.

Clinical Features

Hepatic angiosarcoma is a tumor of older individuals with a median age of 63 years and a male-female ratio of 3:1 [115]. Signs and symptoms are nonspecific and included hepato-

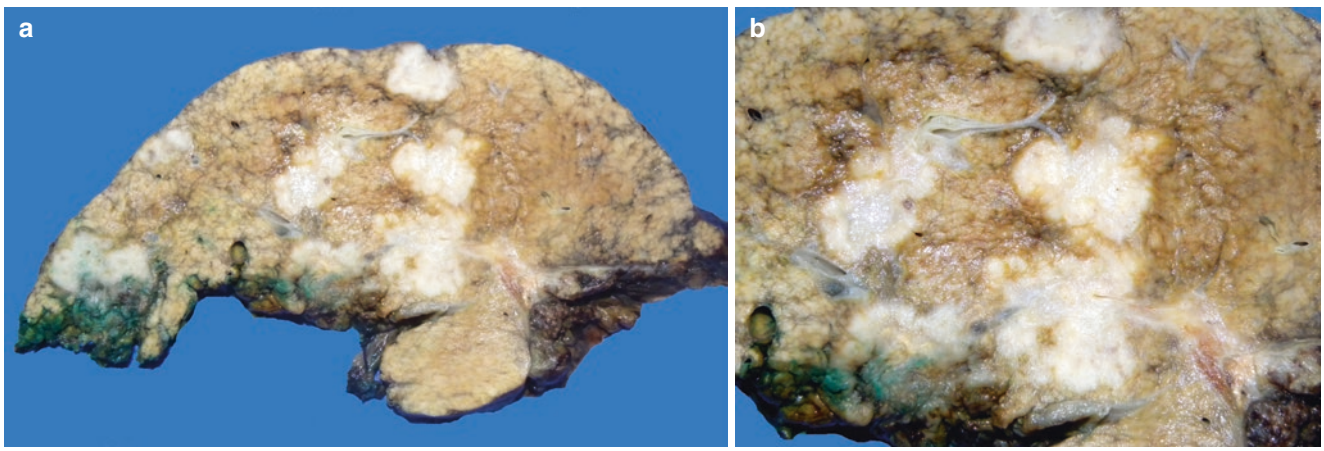

Fig. 13.58 (**a**) Epithelioid hemangioendothelioma. Multiple well-demarcated nodules are seen in the liver. (**b**) Epithelioid hemangioendothelioma. Higher magnification of tumor nodules shown in Fig. 13.58a

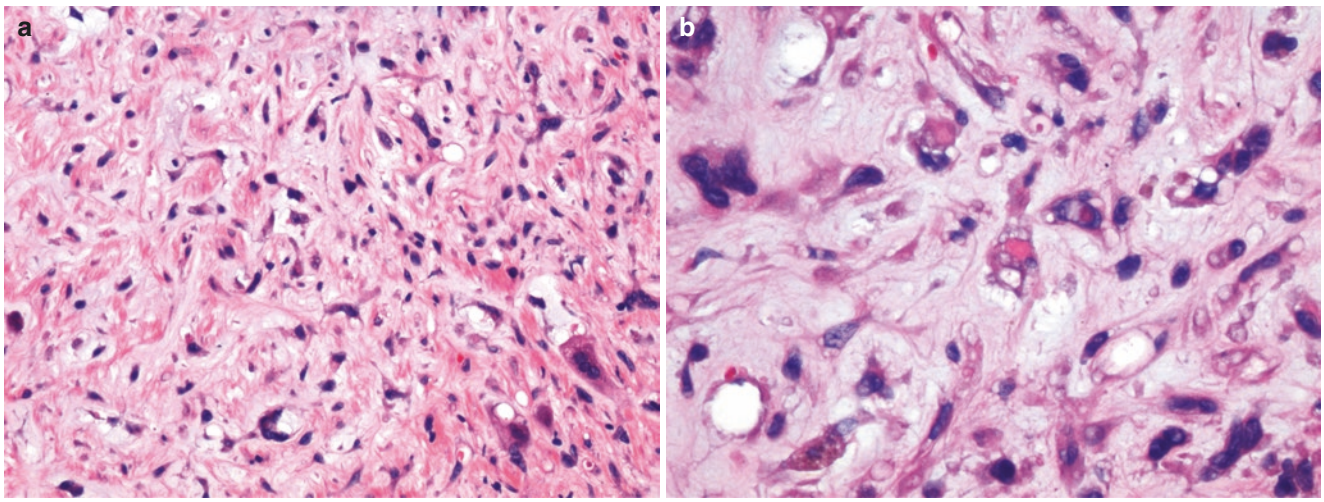

Fig. 13.59 (**a**) Epithelioid hemangioendothelioma. The tumor cells are dendritic and spindle. Some large cells contain cytoplasmic vacuoles. (**b**) Epithelioid hemangioendothelioma. Higher magnification of tumor shown in Fig. 13.59a. Many neoplastic cells contain cytoplasmic vacuoles

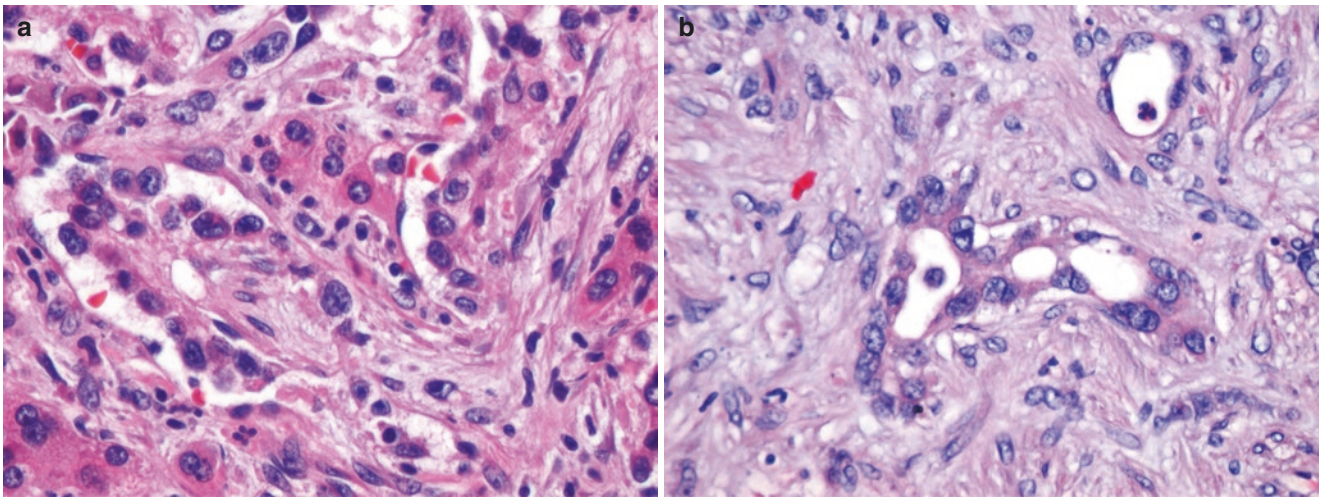

Fig. 13.60 (**a**) Epithelioid hemangioendothelioma. The tumor extends into the sinusoids and displays a papillary pattern. (**b**) Epithelioid hemangioendothelioma. Tubular structures mimicking neoplastic bile ducts are shown

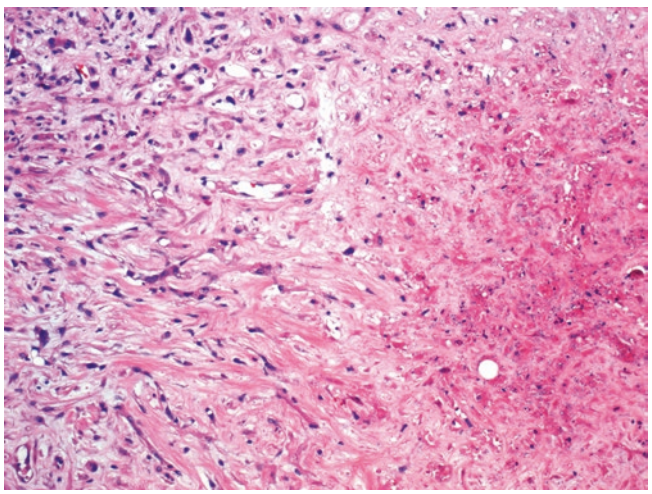

Fig. 13.61 Epithelioid hemangioendothelioma. A focus of necrosis is present

megaly, ascites, abdominal pain, nausea, anorexia, vomiting, weight loss, and fever. Hemoperitoneum due to rupture of the tumor occurs in some cases. Splenomegaly with or without pancytopenia is uncommon. Liver function tests are abnormal in two thirds of the patients [116].

Radiologic Features

Chest X-rays usually show elevation of the diaphragm. CT scan and magnetic resonance imaging are useful diagnostic procedures. Angiographic studies may show an abnormal vascular pattern with a peripheral tumor stain and a central radiolucent area thought to be highly suggestive of angiosarcoma.

Gross Features

The vast majority of angiosarcomas are solid nodular and multicentric (Fig. 13.64). Only one cystic angiosarcoma has been reported in the liver [116]. Angiosarcoma usually

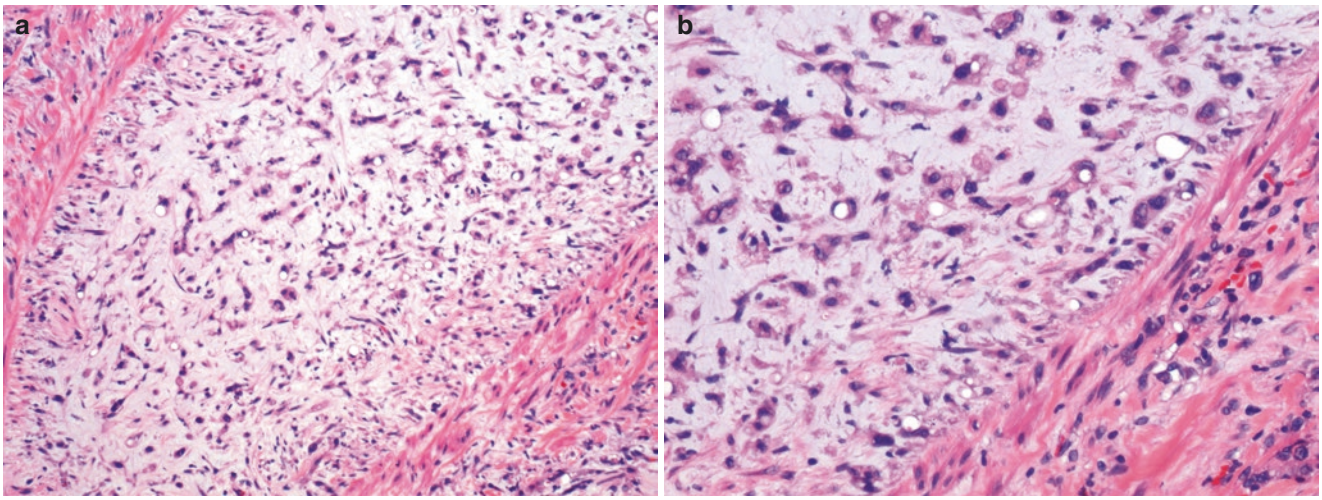

Fig. 13.62 (**a**) Epithelioid hemangioendothelioma. A tumor thrombus occludes a medium-sized vein. The tumor cells lie in a myxoid stroma and are spindle shaped or dendritic. (**b**) Epithelioid hemangioendothelioma. Higher magnification of tumor shown in Fig. 13.62a. The tumor cells which contain cytoplasmic vacuoles are dendritic or spindle shaped and lie in a myxoid stroma

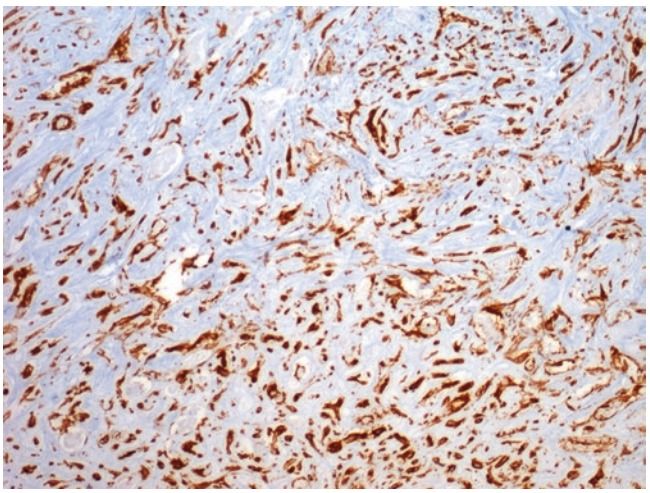

Fig. 13.63 Epithelioid hemangioendothelioma. The vast majority of tumor cells are immunoreactive for CD34

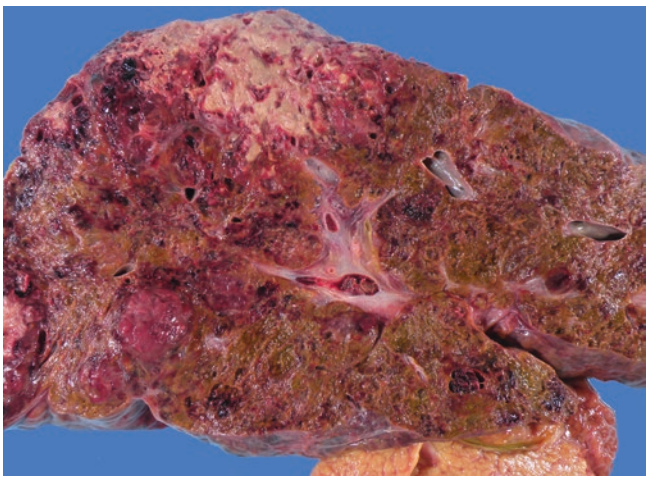

Fig. 13.64 Hepatic angiosarcoma. The dark-red-brown tumor shows irregular areas of necrosis (top)

involves both hepatic lobes and may reach up to 20 cm in greatest dimension. The tumor nodules vary in size from a few millimeters to 7 or 8 centimeters in greatest dimension. Rarely angiosarcoma consists of a single nodule. On sectioning the nodules appear red, black, brown, or hemorrhagic.

Precursor Lesion of Angiosarcoma

A precursor lesion of hepatic angiosarcoma is characterized by isolated cells with large irregular hyperchromatic nuclei that line sinusoids (Fig. 13.65a).

Microscopic Features

The tumor is composed for freely anastomosing vascular channels lined by spindle-shaped or epithelioid cells that are CD31 and CD34 positive (Fig. 13.65b–e). Few cells contain cytoplasmic vacuoles that represent vascular lumens. The nuclei are hyperchromatic or vesicular and contain prominent nucleoli. A variable number of mitotic figures are identified. Multinucleated giant cells are occasionally present. Some of the epithelioid angiosarcomas show anaplastic features having numerous multinucleated giant cells and some fascicles of spindle shape cells (Fig. 13.66a, b).

The neoplastic cells usually grow along sinusoids, terminal hepatic venules, and portal vein branches. They may also grow in nests or solid sheets. Angiosarcomas composed exclusively of epithelioid cells may be confused with carcinoma, and immunostains for CD31 and CD34 may be needed to clarify the diagnosis. When spindle cells grow in fascicles or solid sheets, the tumor may mimic fibrosarcoma. Extensive stromal sclerosis was described in the only example of cystic angiosarcoma reported (Fig. 13.67a, b) [116]. Foci of extramedullary hematopoiesis are relatively common. The few angiosarcomas

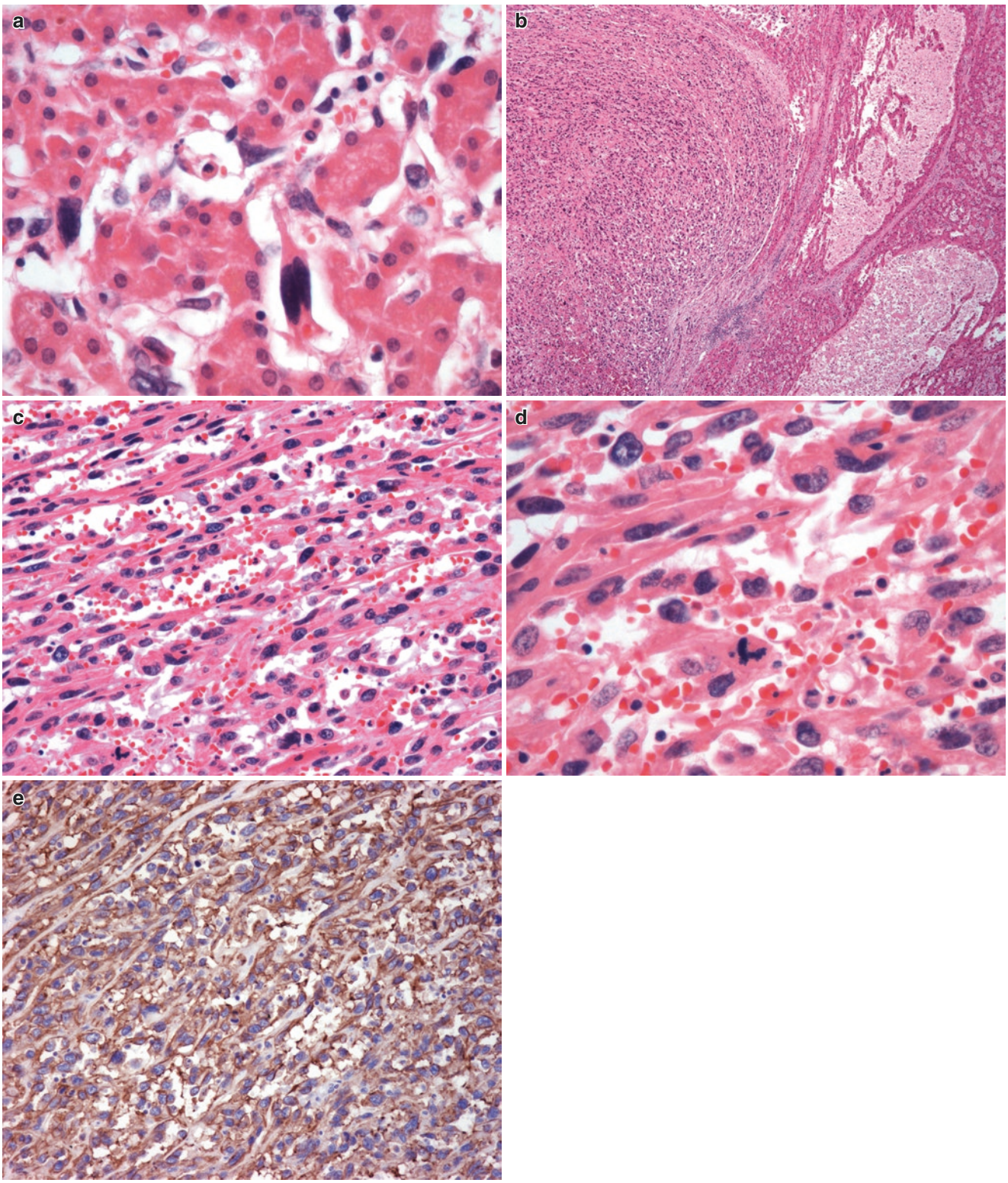

Fig. 13.65 (**a**) Hepatic angiosarcoma. Isolated sinusoidal lining cells have enlarged hyperchromatic nuclei presumably the precursor of angiosarcoma. (**b**) Hepatic angiosarcoma. Low-power view of angiosarcoma showing a nodular pattern. The adjacent hepatic parenchyma is compressed and shows marked sinusoidal dilatation. (**c**) Hepatic angiosarcoma. Anastomosing vascular-like spaces are lined by cells with large hyperchromatic nuclei. (**d**) Hepatic angiosarcoma. An abnormal mitotic figure is seen. (**e**) Hepatic angiosarcoma. Immunoreactivity for CD34 is seen in most tumor cells

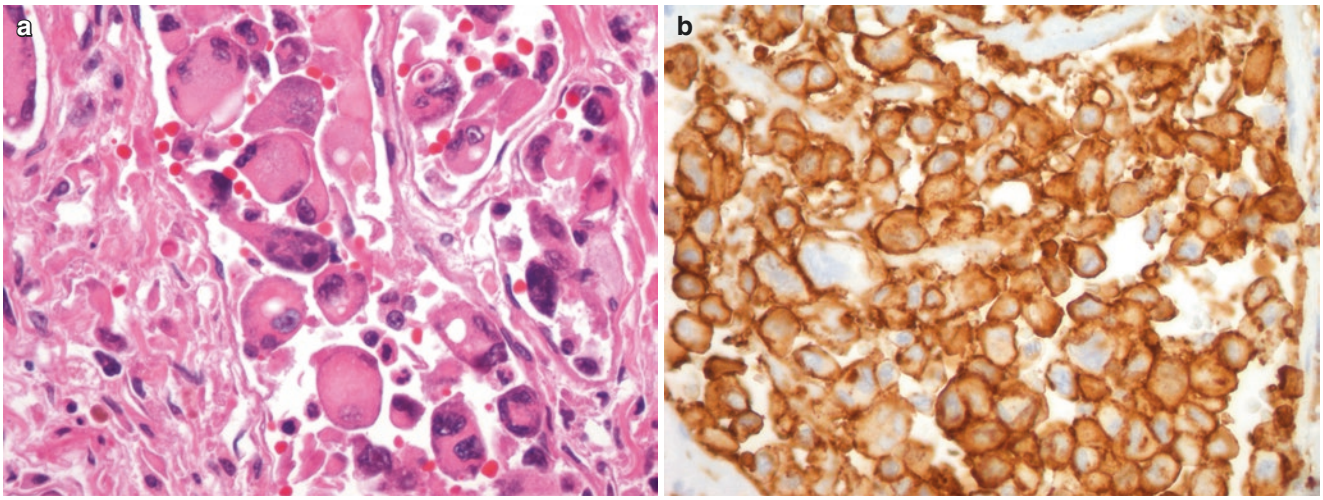

Fig. 13.66 (**a**) Anaplastic angiosarcoma. The tumor is composed of anaplastic mononuclear and multinucleated giant cells, some with cytoplasmic vacuoles. (**b**) Anaplastic angiosarcoma. The neoplastic cells expressed CD34

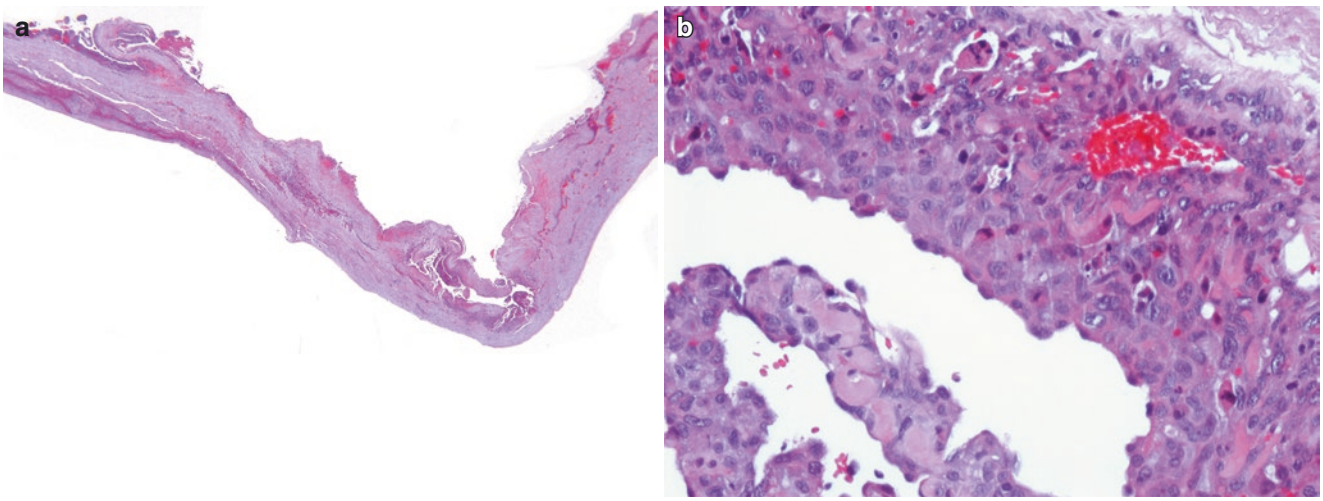

Fig. 13.67 (**a**) Hepatic cystic angiosarcoma. The cystic wall of variable thickness is shown. (**b**) Hepatic cystic angiosarcoma. Higher magnification of the cyst wall showing neoplastic epithelioid cells

reported in children usually have kaposiform areas resembling Kaposi sarcoma, but this tumor occurs only in patients with the acquired immunodeficiency syndrome (AIDS) [104, 117].

Prognosis

The majority of patients with angiosarcoma of the liver die 1 or 2 years after diagnosis because of liver failure, abdominal bleeding, or metastases. The best chance of long-term survival is in patients in which angiosarcoma consists of a single nodule that can be completely resected.

Kaposi Sarcoma

Our experience with Kaposi sarcoma of the liver includes six cases that were incidental autopsy findings in adult patients with AIDS. Rarely Kaposi sarcoma has been reported in immunosuppressed individuals from others causes such as liver transplantation [118]. Two of our AIDS patients had also lesions in the gallbladder, extrahepatic bile ducts, and gastrointestinal tract.

Gross Features

The lesions of Kaposi sarcoma in the liver appear as multiple small irregular red-brown poorly demarcated nodules measuring from a few millimeters to 1.8 cm.

Microscopic Features

The Kaposi sarcoma lesions are confined to the expanded portal spaces. However, the tumor may infiltrate focally the adjacent hepatic parenchyma. Kaposi sarcoma consists of short fascicles of spindle cells and vascular slits (Figs. 13.68, 13.69, and 13.70). Some tumors contain extra- and intracel-

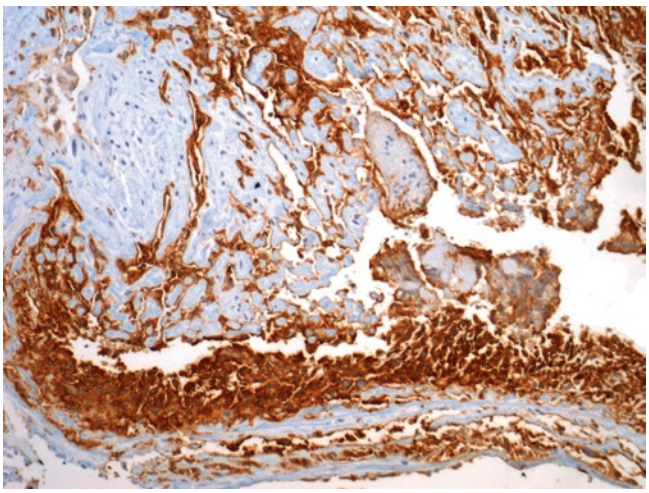

Fig. 13.68 Hepatic cystic angiosarcoma. Many neoplastic cells express CD34

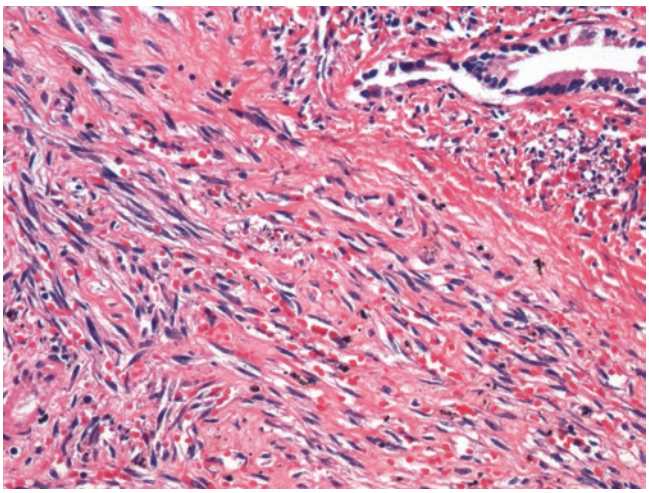

Fig. 13.69 Kaposi sarcoma. Slit-like vascular spaces are present. The endothelial cells are spindle. Part of the intrahepatic bile duct is seen

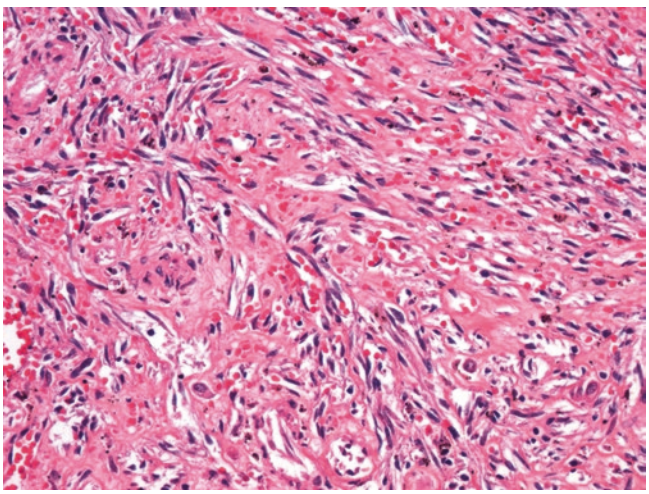

Fig. 13.70 Kaposi sarcoma. Slit-like vascular spaces separated by fibrous tissue. The endothelial cells are spindle shaped

lular hyaline globules, which can be highlighted with the PAS and Masson's trichrome stains. Most likely these globules represent erythrocyte breakdown products. The neoplastic cells express CD31 and CD34. Immunohistochemical and molecular analysis have shown that most Kaposi sarcomas are positive for human herpesvirus 8 [118], which probably plays a role in the development of the tumor.

Other Benign Tumors

Mesenchymal Hamartoma

Mesenchymal hamartoma is a benign tumor-like proliferation composed of variable sized cysts, loose mesenchymal tissue containing small bile ducts and cords of hepatocytes. It occurs predominantly in children under 2 years of age. More than 90% of mesenchymal hamartomas are detected in children under 5 years of age. Because chromosomal abnormalities have been reported in mesenchymal hamartoma, some authors believe that it is a true neoplasm, an opinion we do not share. A small proportion of mesenchymal hamartomas has been reported in adolescents and older adults. There is a slight male predominance.

Clinical Features

Most patients present with an enlarging abdominal mass that may increase in size rapidly. Unusual clinical presentations include jaundice, pyrexia, and disseminated intravascular coagulation [119]. Rarely, congenital anomalies are found in association with mesenchymal hamartoma such as villous hyperplasia of the placenta [120], adrenal cytomegaly, endocardial fibroelastosis, and diffuse endocrinopathy [121].

Radiological Features

Ultrasound has been used in the diagnosis of mesenchymal hamartoma in utero, as well as in children and adults [122]. Computed tomography can demonstrate the solid and cystic nature of mesenchymal hamartoma. Likewise magnetic resonance imaging has been helpful in the diagnosis of mesenchymal hamartoma.

Gross Features

Mesenchymal hamartomas are more common in the right hepatic lobe (75% of cases) than in the left. Approximately 20% of the cases are pedunculated. They vary in size from a few centimeters to 30 cm or more and weigh up to 4 kg. The vast majority of mesenchymal hamartomas contain multiple cysts of varying size from a few millimeters to 15 cm. The cysts are filled with clear to yellow fluid or gelatinous material (Fig. 13.71a). The lining of the cysts is smooth and gray-white [104].

Microscopic Features

Most cysts lack an epithelial lining; a few are lined by a cuboidal biliary-type epithelium. The mesenchyme is disorganized and consists of spindle-shaped or stellate cells lying in a myxoid stroma, which may undergo cystic degeneration (Fig. 13.71b). Surrounding the mesenchyme are abnormal bile ducts and cords of hepatocytes. Extramedullary hematopoiesis and a lymphoplasmacytic infiltrate are often present.

Prognosis

If mesenchymal hamartoma is completely resected, it does not recur. Progression to embryonal sarcoma has been reported in one case.

Angiomyolipoma

Classical angiomyolipomas consist of a mixture of three different mature tissue types (adipose tissue, smooth muscle, and abnormal vessels). They are more common in the kidney than the liver, and the vast majority follows a benign clinical course. However, a malignant variant has been documented [123, 124]. In addition epithelioid and atypical angiomyolipomas have been characterized [125].

Clinical Features

Angiomyolipomas appear to be slightly more common in women. The age ranged is from 10 to 72 years (mean 50 years). They are rare tumors in children and few are associated with tuberous sclerosis. Ultrasonography, computed tomography, and magnetic resonance imaging have been useful tools in diagnosis [124, 125].

Gross Features

In the liver, more angiomyolipomas are located in the right lobe (60%) than in the left. Their size varies considerably from a few centimeters to 35 centimeters. The vast majority of angiomyolipomas are solitary, very few are multiple. Most tumors are well-demarcated. Their color and consistency is related to the proportion of fat and smooth muscle present in the tumor. When fat predominates they are yellow, mottled yellow, or tan and soft. When smooth muscle predominates, they are gray-white and firm. Foci of hemorrhage and necrosis are present in some tumors.

Microscopic Features

When the three components of angiomyolipoma are present in the tumor (adipose tissue, smooth muscle, and abnormal vessels), the diagnosis is simple (Fig. 13.72a–g). However, in tumors composed of large amoeboid cells, multinucleated giant cells, few spindle-shaped and epithelioid cells, scant abnormal blood vessels, and no fat, the diagnosis is problematic and usually requires immunohistochemical stains for HMB45 and melan-A [125–128]. Likewise tumors composed predominantly of smooth muscle cells can be confused with leiomyomas or leiomyosarcoma. Epithelioid smooth muscle cells may have a clear cytoplasm. When the tumor shows a trabecular pattern, it can be confused with

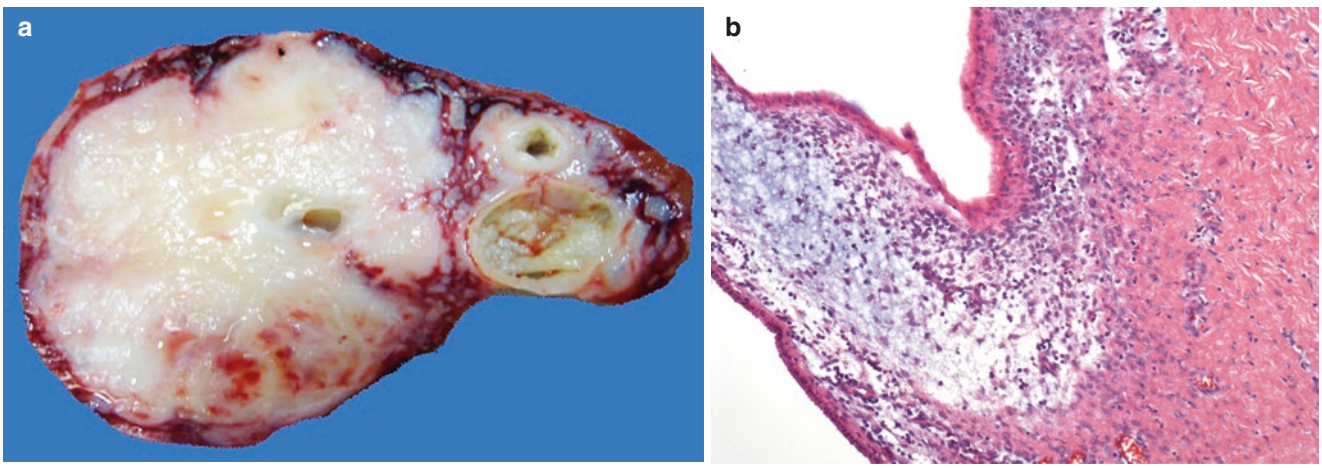

Fig. 13.71 (**a**) Mesenchymal hamartoma. A well-demarcated solid and cystic tumor. The solid component is white. (**b**) Mesenchymal hamartoma. Polypoid myxoid area containing spindle and stellate cells. Overlying normal-appearing biliary epithelium and a band of fibrous tissue are seen (bottom)

hepatocellular carcinoma. However, these areas are Hep par-1 negative. A component of T-cell lymphocytes mixed with the neoplastic cells has been documented [123, 124]. Foci of extramedullary hematopoiesis are found in some tumors, which may lead to the erroneous diagnosis of myelolipoma.

Immunohistochemistry

The spindle-shaped and epithelioid cells including those with clear cytoplasm show immunoreactivity for smooth muscle actin; less frequently these cells are immunoreactive for desmin. Spindle and epithelioid smooth muscle cells as well as the amoeboid cell and multinucleated giant cells express HMB45 and melan-A (Fig. 13.72h, i).

Leiomyoma

Leiomyomas are exceedingly rare primary tumors of the liver that can be sporadic or associated to immunosuppression. The latter are usually smaller (<1 cm) than the former and usually coexist with leiomyomas in the colon, gallbladder, pancreas, spleen, lymph node, and lung [129–131]. The mean age of presentation is 43 years with a slight female predilection (55.6%) [132]. Grossly both types of leiomyomas appear as well-demarcated gray-white firm nodules. The sporadic leiomyoma may reach a size up to 12 cm in greatest dimension. There are two histologic types of hepatic leiomyomas: [1] the conventional type is composed of fascicles of spindle smooth muscle fibers with no cytologic atypia and mitotic activity and [2] the epithelioid type which consists predominantly of epithelioid clear cells as well as fascicles of spindle smooth muscle cells (Figs. 13.73 and 13.74). Both the clear and the spindle cells express HMB45 and melan-A (Figs. 13.75 and 13.76). This variant is referred by some authors as clear cell myomelanocytic tumor [133]. The spindle and epithelioid cells also label with desmin, smooth muscle actin, and H-caldesmon.

Cystic Mesotheliomas

Several examples of benign hepatic cystic mesotheliomas have been reported. Most patients were adult women, and the majority of tumors were incidental autopsy findings [104, 134]. However, 11 cases of malignant hepatic mesotheliomas have been reported, including a recent giant primary malignant mesothelioma [134]. Grossly the benign mesotheliomas were well-circumscribed yellow-tan nodules measuring from 0.5 to 2 cm in greatest dimension, while the malignant ones were larger measuring from 4.4 to 15 cm with a mean size of 11.2 cm. Microscopically, the benign mesotheliomas were composed of multiple cystically dilated spaces lined by cuboidal or flat calretinin-positive mesothelial cells. Occasional papillary projections were also identified. The malignant mesotheliomas were epithelioid (63.6%), biphasic (27.3%), and sarcomatoid (9.1%). Metastatic deposits occur in over 50% of the patients.

Nerve Sheath Tumors

Both benign and malignant nerve sheath tumors have been described in the liver in patients with or without neurofibromatosis. The schwannomas and neurofibromas can be of conventional type or plexiform, while the malignant nerve sheath tumors may be mixed with angiosarcoma [104].

Inflammatory Myofibroblastic Tumor

Inflammatory myofibroblastic tumors have been reported in many anatomic sites including the liver [135, 136]. They are more common in adult men (mean age 56 years). Their size varies from 1 to 20 cm. Inflammatory myofibroblastic tumor of the liver has been confused with an abscess because of their abundant acute inflammatory infiltrate and central necrosis (Fig. 13.77). Local recurrence has been reported in 25% of the cases and metastasis in <5%. Some inflammatory myofibroblastic tumors have been associated with autoimmune pancreatitis and primary sclerosing cholangitis [137]. In a few reports, inflammatory myofibroblastic tumors have also been documented in association with Epstein-Barr virus infection. Microscopically the tumor is composed of spindle myofibroblastic arranged in fascicles (Figs. 13.78, 13.79, and 13.80). The neoplastic cells are mixed with numerous leukocytes, lymphocytes, and plasma cells. The central portion of the tumor shows necrosis with numerous foamy macrophages. Cytologic atypia is minimal and mitotic activity is absent. The myofibroblasts express smooth muscle actin (Fig. 13.81).

Solitary Fibrous Tumor

Solitary fibrous tumor is a rare liver neoplasm similar to those that have been described in the pleura and many other anatomic sites. It usually follows a benign clinical course, but malignant transformation has been documented [138–143].

Clinical Features

Solitary fibrous tumor has been reported exclusively in adults with an age range between 32 and 83 years (mean age 57 years). It appears to be more common in women. Signs and symptoms include upper abdominal mass, abdominal

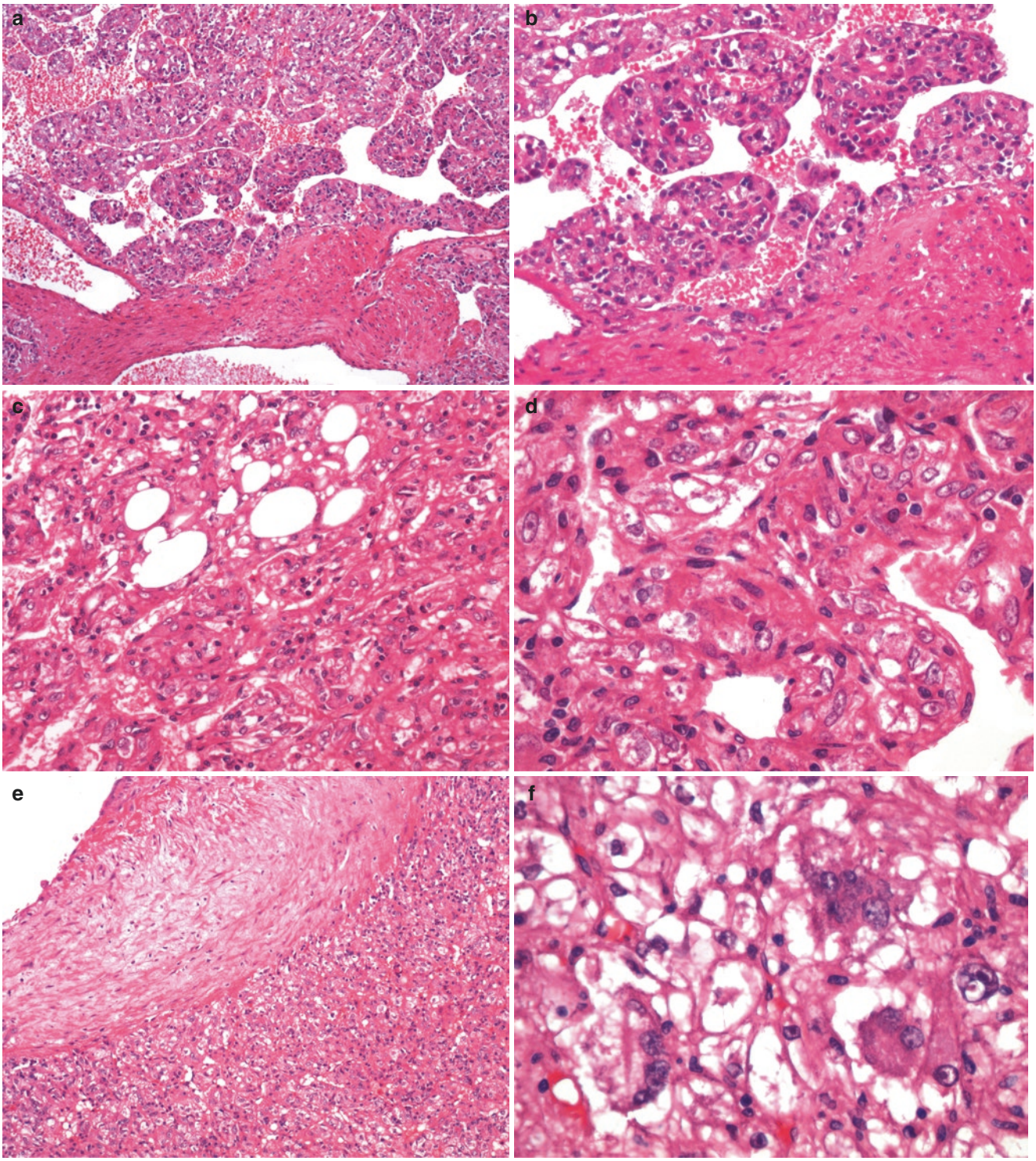

Fig. 13.72 (**a**) Angiomyolipoma. A trabecular pattern that is often confused with hepatocellular carcinoma is illustrated. An abnormal blood vessel is also present. (**b**) Angiomyolipoma. Higher magnification shown in Fig. 13.83a showing sinusoidal and trabecular pattern of the tumor. (**c**) Angiomyolipoma. A microscopic focus of normal-appearing adipose tissue is illustrated. (**d**) Angiomyolipoma. High magnification showing spindle-shaped smooth muscle cells and small vessels. (**e**) Angiomyolipoma. An abnormal vessel from which angiomyolipoma seem to arise. (**f**) Angiomyolipoma. Multinucleated giant cells and epithelioid smooth muscle cells with clear cytoplasms

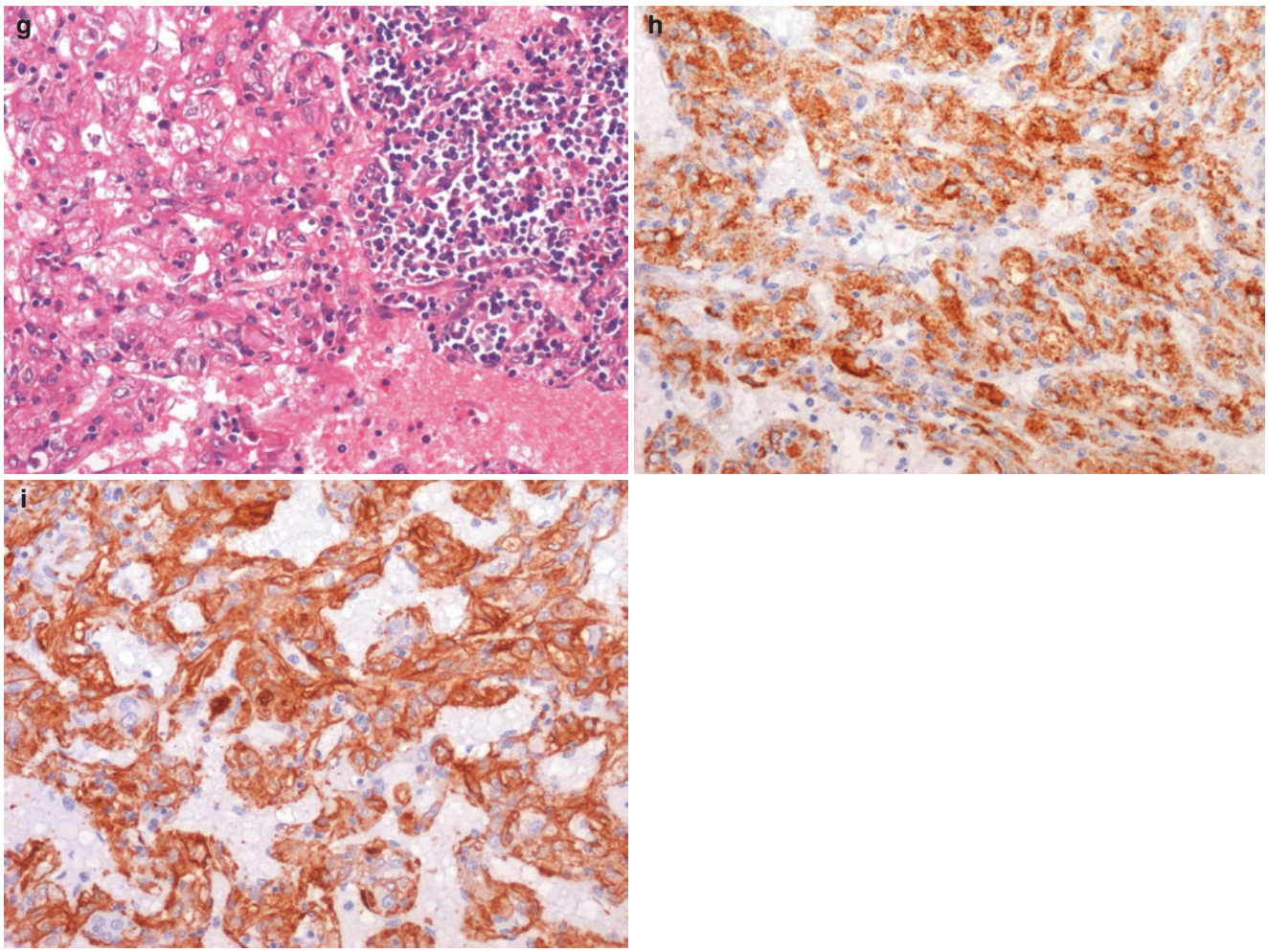

Fig. 13.72 (continued) (**g**) Angiomyolipoma. A collection of T-cell lymphocytes adjacent to epithelioid smooth muscle cells with eosinophilic and clear cytoplasms is illustrated. (**h**) Angiomyolipoma. Diffuse granular reactivity for HMB45. (**i**) Angiomyolipoma. Diffuse smooth muscle actin reactivity

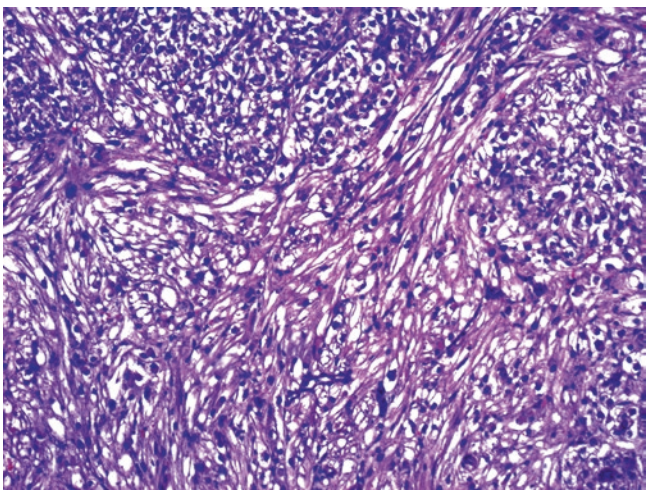

Fig. 13.73 Epithelioid clear cell leiomyoma. Fascicles of spindle-shaped cells and nodules of epithelioid smooth muscle cells are illustrated

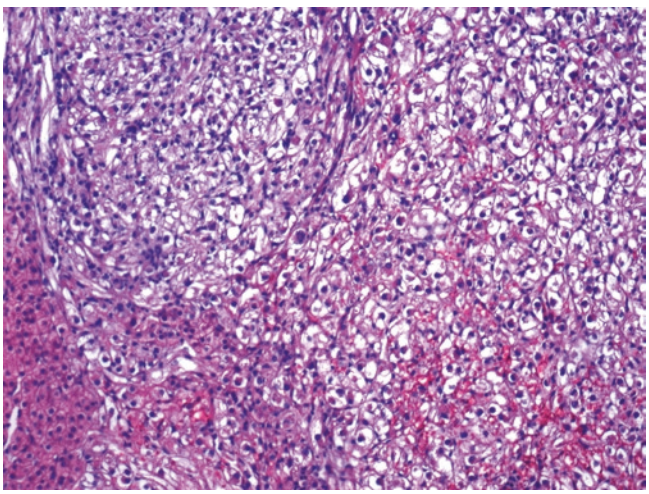

Fig. 13.74 Epithelioid clear cell leiomyoma. The predominant component of epithelioid smooth muscle cells with clear cytoplasm is shown

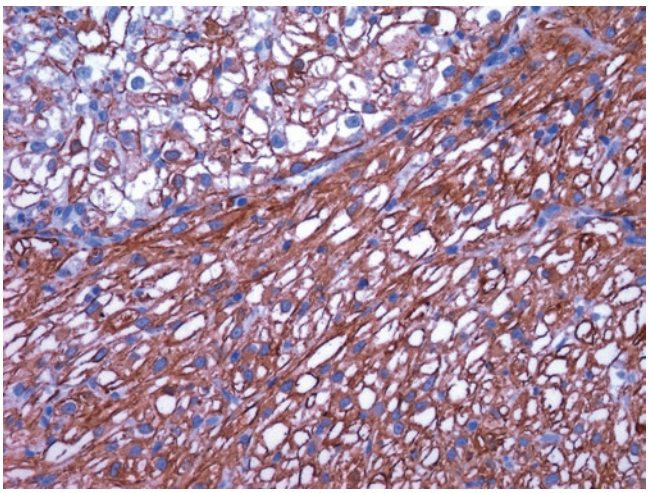

Fig. 13.75 Epithelioid clear cell leiomyoma. Smooth muscle actin reactivity is stronger in the conventional spindle-shaped cells than in the epithelioid clear smooth muscle cells

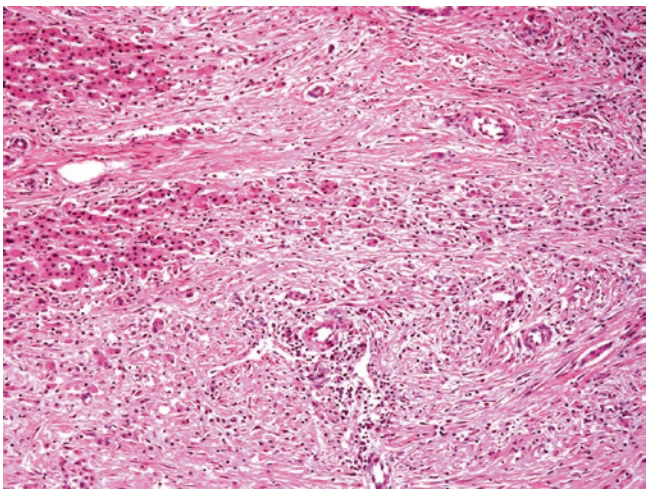

Fig. 13.78 Inflammatory myofibroblastic tumor. The tumor was composed of spindle myofibroblastic cells arranged in fascicles that extend into the liver parenchyma

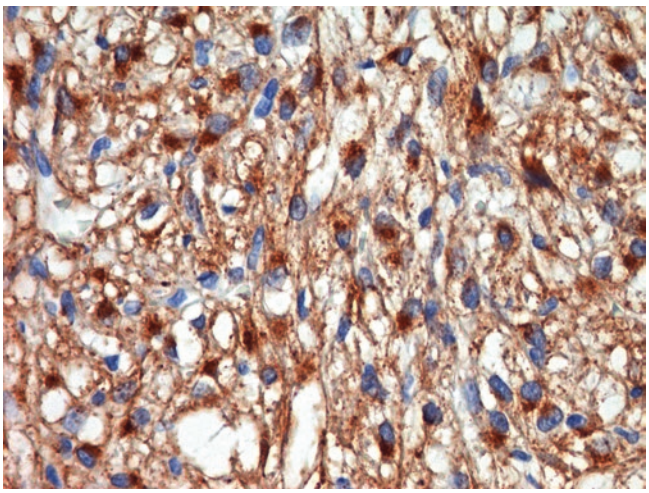

Fig. 13.76 Epithelioid clear cell leiomyoma. Diffuse granular reactivity for HMB45 in the epithelioid component of the tumor

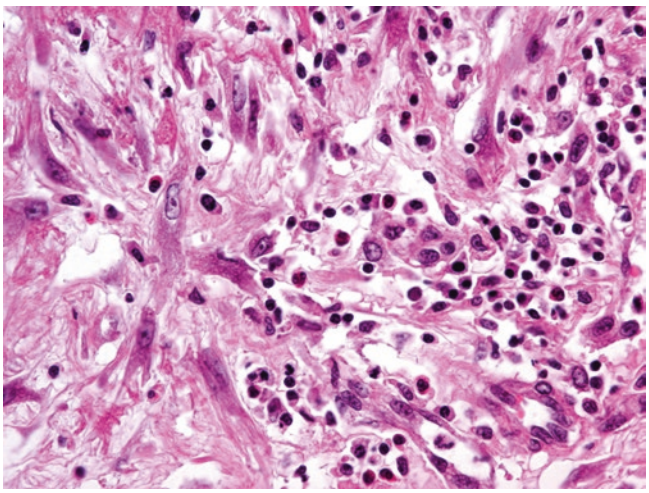

Fig. 13.79 Inflammatory myofibroblastic tumor. The tumor cells were mixed with numerous leukocytes, lymphocytes, and plasma cells

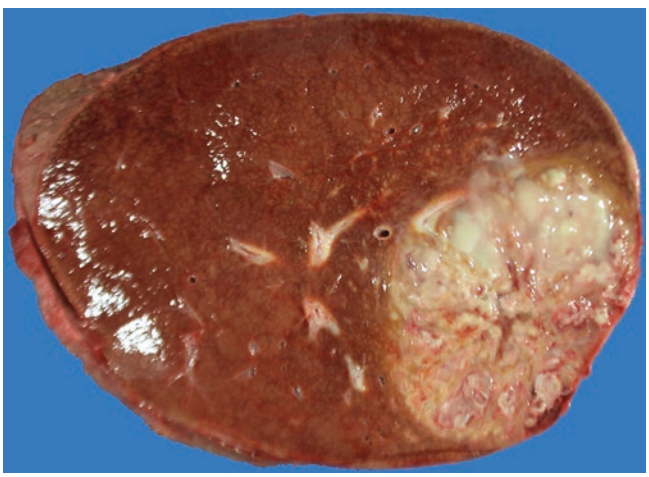

Fig. 13.77 Inflammatory myofibroblastic tumor. A non-encapsulated but well-demarcated hepatic tumor with central necrosis of 11 cm in greatest dimension was seen

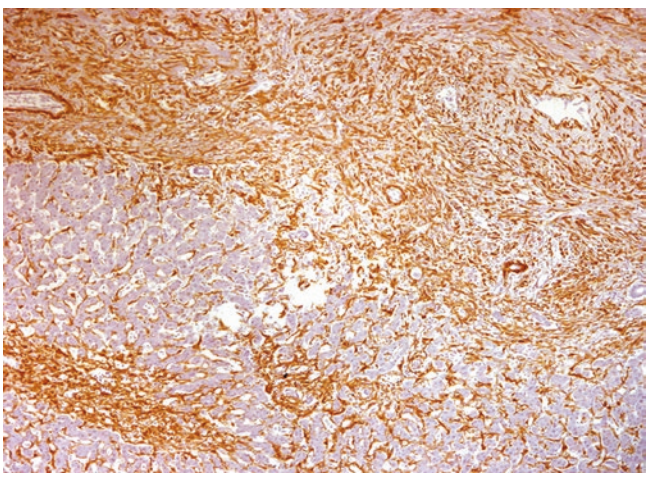

Fig. 13.80 Inflammatory myofibroblastic tumor. The myofibroblastic cells were strong and diffusely positive for smooth muscle actin

discomfort, or pain. Some patients are asymptomatic, while few others develop hypoglycemia [139] as a result of the production of an insulin-like growth factor.

Gross Features

The size of the tumors varies considerably from 2 to 20 cm and may weight over 3000 gr. They are well-demarcated, firm, and rarely pedunculated. The external surface is smooth, whereas the cut surface is gray-white with a whorled texture.

Microscopic Features

Characteristically the tumor shows hypo- and hypercellular areas and a fibrous stroma containing numerous blood vessels producing a hemangiopericytic pattern. The predominant cells are spindled-shaped arranged in short fascicles. Storiform and herringbone pattern are relatively common.

Malignant solitary fibrous tumor show greater cellularity, cytologic atypia, and mitotic activity. Benign solitary fibrous tumor nearly always expresses CD34 and Bcl-2; malignant ones often do not express these markers [139, 142].

Other Malignant Tumors

Leiomyosarcoma

There are two types of primary leiomyosarcoma of the liver. The most common related to immunosuppression may occur in children or adults following human immunodeficiency virus infection or liver transplantation and usually arise in the wall of the vena cava [144–148]. The sporadic type of hepatic leiomyosarcoma is a tumor of adults and occurs equally in men and women and probably arises in the wall of small vessels such as hepatic veins. The mean age at presentation in the sporadic type is 52 years. Symptoms and signs include upper abdominal mass, abdominal pain, and weight loss. A Budd-Chiari syndrome has been reported in patients with leiomyosarcomas arising in the hepatic veins or inferior vena cava [146–149].

Gross Features

Primary leiomyosarcomas of the liver are usually solitary and can attain a large size. They are nodular, firm, and rubbery. On cut surface they are gray-white with foci of necrosis and hemorrhage.

Microscopic and Immunohistochemical Features

The tumors are composed of short fascicles of spindles-shaped cells (Fig. 13.81a, b). Nuclei are hyperchromatic and elongated and have blunt ends. Mitotic activity is variable. Most tumors cells express muscle-specific actin, and less frequently they are positive for desmin and H-caldesmon. Immunoreactivity for cytokeratin and EMA has been detected in some tumors (Fig. 13.82). Epstein-Barr virus has been detected in cells of leiomyosarcoma from AIDS patients.

Ultrastructure

The neoplastic cells of leiomyosarcoma have thin myofilaments, dense bodies, and pinocytotic vesicles.

Embryonal Sarcoma

Embryonal sarcoma is a rare but distinctive malignant primary tumor of the liver that occurs predominantly in children

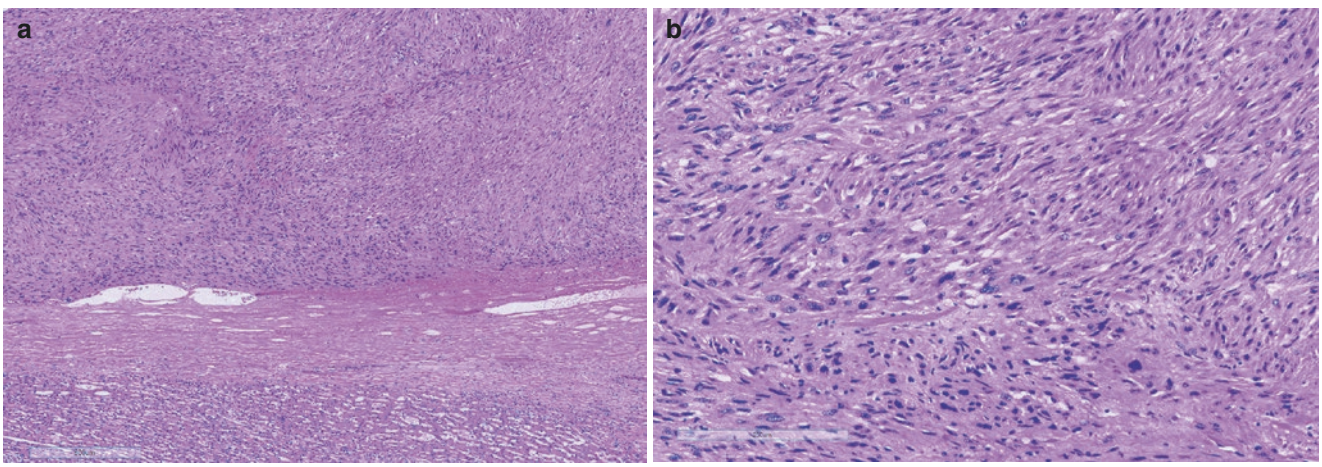

Fig. 13.81 (**a**) Moderately differentiated hepatic leiomyosarcoma. A well-demarcated tumor nodule is compressing the liver parenchyma. (**b**) Moderately differentiated hepatic leiomyosarcoma. Higher magnification of the tumor shown in Fig. 13.81a in which fascicles of smooth muscle cells, some with considerable nuclear pleomorphism, are present

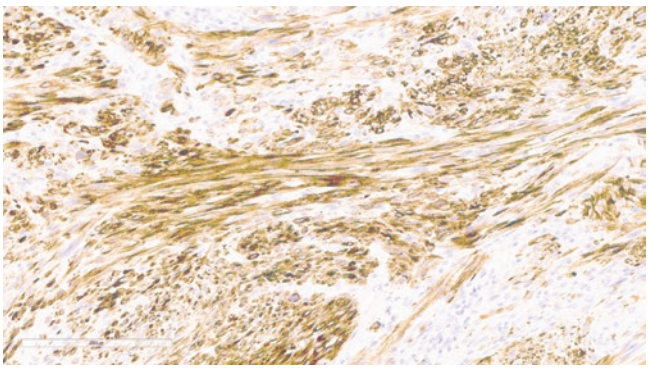

Fig. 13.82 Moderately differentiated hepatic leiomyosarcoma. Diffuse reactivity for desmin

and adolescents and less frequently in young adults and older individuals. It accounts for 15% of all primary hepatic neoplasms in patients under 20 years of age [150, 151].

Clinical Features

More than half the patients are between 5 and 10 years of age. Signs and symptoms include a rapidly growing palpable abdominal mass, pain, and weight loss. Sonography and CT scan show a solid and cystic mass. Arteriography reveals a hypervascular mass.

Gross Features

Embryonal sarcomas are usually large measuring between 10 and 20 cm in greatest dimension with an average weight of 1300 g. The majority of tumors are located in the right hepatic lobe and are well demarcated and sometimes partially encapsulated. The cut surface is variegated with solid, glistening gray-white tumor tissue alternating with cystic gelatinous areas and hemorrhagic and necrotic foci of variable extent.

Microscopic Features

The tumor cells are stellate or spindle shaped and with poorly defined outlines (Fig. 13.83a–c). Numerous bizarre multinucleated giant cells with large hyperchromatic nuclei are mixed with the mononuclear cells. Some of these giant cells contain multiple hyaline globules of different sizes (Fig. 13.83d). These globules are diastase resistant and PAS-positive and appear to be giant lysosomes. Abundant mitotic figures are identified. The stroma is myxoid and rich in acid mucopolysaccharides or fibrous. Entrapped cystically dilated bile ducts are present in most tumors. Extensive tumor necrosis is common.

Immunohistochemistry

The vast majority of embryonal sarcomas express vimentin and alpha-1-anti-chemotripsin, but only a few are cytokeratin positive. The hyaline eosinophilic globules are alpha-fetoprotein negative. The immunoprofile lacks specificity.

Prognosis and Treatment

In recent years the prognosis of embryonal sarcoma has improved considerably with the use of chemotherapy and surgical treatment.

Embryonal Rhabdomyosarcoma

Primary embryonal rhabdomyosarcoma of the liver usually arises in the intrahepatic bile ducts. It is less common than embryonal rhabdomyosarcoma of the extrahepatic bile ducts, which is the most common neoplasm of the biliary tree in children [104, 152].

Clinical Features

Most patients are children under 5 years of age, but occasional tumors have been reported in adults [152]. Common presenting symptoms include obstructive intermittent jaundice often with fever and hepatosplenomegaly. Ultrasonography, computed tomography, and magnetic resonance imaging demonstrate the mass.

Gross and Microscopic Features

The tumor may be multinodular, gelatinous, polypoid, or grape-like. The grape-like structures may project into the lumen of the bile ducts (sarcoma botryoides) whose walls are thickened.

Microscopically, the polypoid structures are covered by normal biliary epithelium, which may be focally ulcerated. A dense concentration of neoplastic cells is identified immediately beneath the biliary epithelium (cambium layer). The cells may be round, spindled, strap-shaped, or racquet-shaped. Nuclei are hyperchromatic and elongated. Numerous mitotic figures are present. Cross-striations may be seen in some tumor cells. The stroma is myxoid and rich in acid mucopolysaccharides. A few collagen fibers may be seen between tumor cells. Ultrastructural studies reveal both thick and thin myofilaments with occasional Z bands in some cells [104, 152].

Immunohistochemical Features

In our experience desmin and Myo-D1 are the most sensitive immunohistochemical markers for the diagnosis of embryonal rhabdomyosarcoma from all anatomic sites, including the liver [104, 152]. Tumor cells also express myosin, myoglobin, and muscle-specific actin.

Prognosis and Treatment

Initial surgical treatment should be follow by multidrug chemotherapy and radiotherapy. With this form of treatment, the prognosis of embryonal rhabdomyosarcoma has improved considerably.

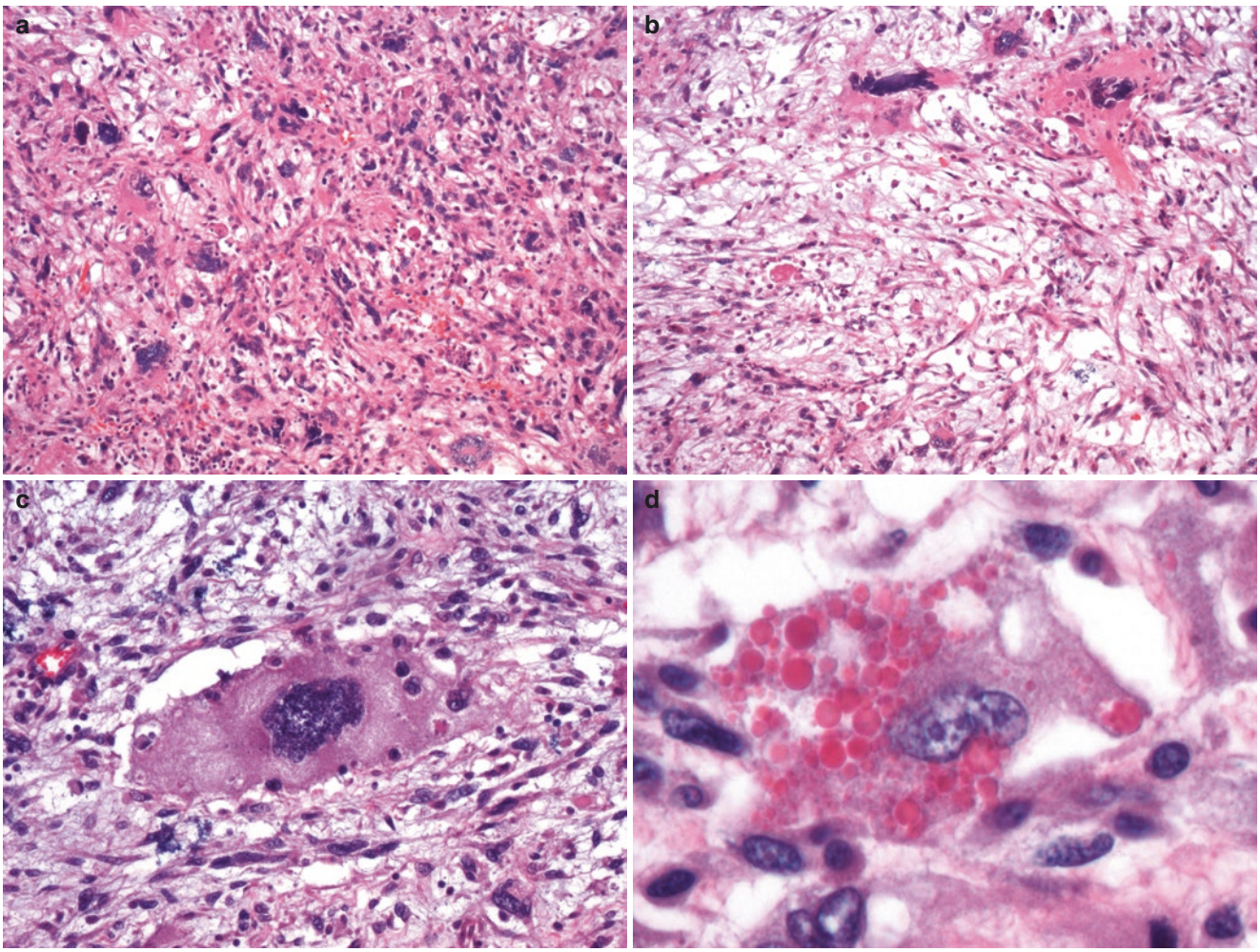

Fig. 13.83 (**a**) Embryonal sarcoma. Multinucleated giant cells and spindle-shaped cells with hyperchromatic nuclei are present. (**b**) Embryonal sarcoma. Spindle-shaped cells lying in a myxoid area as well as multinucleated giant cells (top) with large hyperchromatic nuclei are present. (**c**) Embryonal sarcoma. A large multinucleated giant cell with hyperchromatic nuclei and phagocytized lymphocytes is surrounded by neoplastic spindle-shaped cells. (**d**) Embryonal sarcoma. Hyaline cytoplasmic globules with marked variation in size are seen in a large binucleated cell

Yolk Sac Tumor

First described in the testes and ovaries, yolk sac tumors have subsequently been reported in extragonadal site such as the liver, gallbladder, mediastinum, etc. [104, 153]. In the liver yolk sac tumors can be pure or be a component of hepatocellular carcinoma and hepatoblastoma.

Clinical Features

Patients have ranged in age from 8 months to 62 years. The most common clinical presentation is a rapidly growing palpable hepatic mass and abdominal pain.

Gross and Microscopic Features

The cut surface of the tumors has been described as variegated. Microscopically yolk sac tumors of the liver are similar to the most common gonadal tumors. Reticular, pseudopapillary, and sheet-like patterns are the most common. Characteristic structures are the Schiller-Duval bodies which consist of a central thin-walled blood vessel surrounded by primitive columnar cells, which in turn are surrounded by a space lined by hobnail-shaped cells. Most tumors express alpha-fetoprotein.

Leukemias and Lymphomas

Primary Hepatosplenic T-Cell Lymphoma (HSTL)

Systemic malignant lymphomas often involve the liver [154]. Primary T-cell hepatosplenic lymphoma on the other hand is an exceedingly rare lymphoid neoplasm composed of cytotoxic T cells usually of g/d T-cell receptor type [155–157].

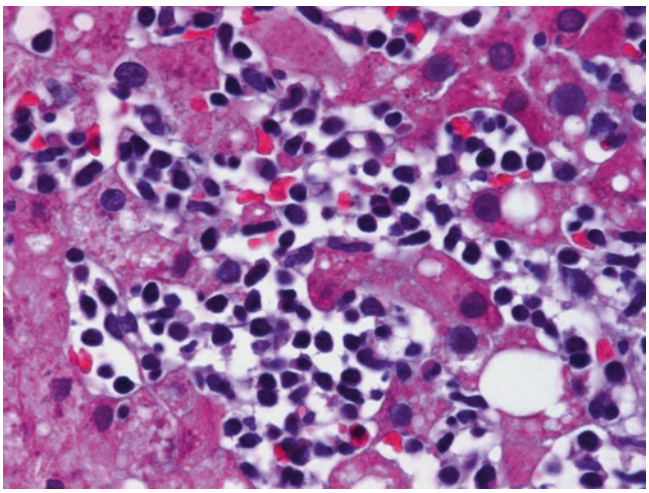

Fig. 13.84 Hepatosplenic lymphoma. The neoplastic T-cell lymphocytes infiltrate the sinusoids of the liver

HSTL is associated with the presence of isochromosome 7q [153]. The neoplastic lymphoid cells are small or medium sized that display a prominent sinusoidal infiltration of the liver, spleen, and bone marrow. HSTL represents <1% of all non-Hodgkin lymphomas. It is more common in males. Peak incidence occurs in adolescents and young adults with a medium age of 35 years.

Pathogenesis

Close to 20% of HSTL arise in the setting of chronic immunosuppression due to therapy for solid organ transplantation or prolonged antigenic stimulation. HSTL has also been described in patients, especially children treated with azathioprine and infliximab for Crohn's disease.

Clinical Features

Patients present with hepatomegaly and splenomegaly but without peripheral lymphadenopathy. The bone marrow is nearly always involved. Systemic symptoms are usually present. Anemia, leukopenia, and thrombocytopenia are common.

Gross and Microscopic Features

Although the liver and spleen are enlarged, there are no discernible gross lesions.

Microscopic Features

The neoplastic lymphoid cells show a prominent sinusoidal infiltration in the liver and spleen (Fig. 13.84). The cords and sinusoids of the splenic pulp are packed with neoplastic lymphoid cells, which lead to atrophy of the white pulp. A predominant intrasinusoidal infiltration of tumor cells is also seen in the bone marrow. The cells display round or ovoid nuclei with inconspicuous nucleoli and pale cytoplasm. Occasional large blastic cells may be identified especially with disease progression.

Immunophenotype

The neoplastic lymphoid cells express CD3 and usually TCRb1. They are usually negative for CD4, CD8, and CD5.

Prognosis

Prognosis is poor. The median survival is <2 years.

Serous Cystadenoma

Serous cystadenomas similar to those more commonly described in the pancreas and occasionally associated with von Hippel-Lindau syndrome are exceedingly rare in the liver [104]. They are composed of small cystic structures lined by a single layer of cuboidal clear cells rich in glycogen. The cells usually express CK7, CK8, CK19, and alpha-inhibin. The tumors usually follow a benign clinical course.

Metastatic Tumors

Metastases are the most common malignant neoplasms in the non-cirrhotic liver but are extremely uncommon in the cirrhotic liver [86, 104]. Although countless malignant epithelial and mesenchymal neoplasms can metastasize to the liver, the most common are carcinomas of the lung, colon, breast, pancreas, and stomach. Metastases are often detected in patients with known primary tumors that are being evaluated for stage of disease. Metastases that are symptomatic are usually far advanced at the time of presentation. Clinical signs and symptoms include hepatomegaly, anorexia, weight loss, and right upper quadrant abdominal pain. Approximately 10% of patients with liver metastases have a palpable mass. Metastatic functioning endocrine tumors from the gastrointestinal tract or pancreas may lead to different systemic manifestations such as the carcinoid syndrome, insulinoma, glucagonoma, somatostatinoma, gastrinoma, and VIPoma [104]. Metastatic pheochromocytoma may give rise to hypertension.

References

1. Rappaport AM. The structural and functional unit in the human liver (liver acinus). Anat Rec. 1958;130(4):673–89.
2. Rappaport AM. Hepatic blood flow: morphologic aspects and physiology regulation. Int Rev Physiol. 1980;21:1–63.
3. Peng H, Wisse E, Tian Z. Liver natural killer cells: subsets and roles in liver immunity. Cell Mol Immunol. 2016;13(3):328–36.
4. Davidoff S, Kim S, Friedman B. von Meyenburg complexes (bile duct hamartomas). Clin Gastroenterol Hepatol. 2006;4:A26.

5. Redston MS, Wanless IR. The hepatic von Meyenburg complex: prevalence and association with hepatic and renal cysts among 2843 autopsies. Mod Pathol. 1996;9:233–7.
6. Sinakos E, Papalavrentios L, Chourmouzi D, et al. The clinical presentation of Von Meyenburg complexes. Hippokratia. 2011;15(2):170–3.
7. Jain D, Ahrens W, Finkelstein S. Molecular evidence for the neoplastic potential of hepatic Von-Meyenburg complexes. Appl Immunohistochem Mol Morphol. 2010;18:166–71.
8. Rogers TN, Woodley H, Ramsden W, et al. Solitary liver cysts in children: not always so simple. J Pediatr Surg. 2007;42(2):333–9.
9. Bhathal PS, Hughes NR, Goodman ZD. The so-called bile duct adenoma is a peribiliary gland hamartoma. Am J Surg Pathol. 1996;20(7):858–64.
10. Allaire GS, Rabin L, Ishak KG, Sesterhenn IA. Bile duct adenoma. A study of 152 cases. Am J Surg Pathol. 1988;12:708–15.
11. Wei J, Zhang D, Yang J, Xu C. Intrahepatic bile duct adenoma (peribiliary gland hamartoma): a case report and review of literature. Int J Clin Exp Pathol. 2015;8(5):5908–13.
12. Hughes NR, Goodman ZD, Bhathal PS. An immunohistochemical profile of the so-called bile duct adenoma: clues to pathogenesis. Am J Surg Pathol. 2010;34:1312–8.
13. Albores-Saavedra J, Hoang MP, Murakata LA, et al. Atypical bile duct adenoma, clear cell type. Am J Surg Pathol. 2001;25: 956–60.
14. Wu WW, Gu M, Lu D. Cytopathologic, histopathologic, and immunohistochemical features of intrahepatic clear cell bile duct adenoma: a case report and review of the literature. Case Rep Pathol. 2014;2014:874826.
15. Roncalli M, Sciarra A, Tommaso LD. Benign hepatocellular nodules of healthy liver: focal nodular hyperplasia and hepatocellular adenoma. Clin Mol Hepatol. 2016;22(2):199–211.
16. Chang CY, Hernandez-Prera JC, Roayaie S, Schwartz M, Thung SN. Changing epidemiology of hepatocellular adenoma in the United States: review of the literature. Int J Hepatol. 2013;2013:604860.
17. Sasaki M, Nakanuma Y. Overview of hepatocellular adenoma in Japan. Int J Hepatol. 2012;2012:648131.
18. Bühler H, Pirovino M, Akobiantz A, Altorfer J, Weitzel M, Maranta E, et al. Regression of liver cell adenoma. A follow-up study of three consecutive patients after discontinuation of oral contraceptive use. Gastroenterology. 1982;82:775–82.
19. Lerut JP, Ciccarelli O, Sempoux C, Danse E, deFlandre J, Horsmans Y, et al. Glycogenosis storage type I diseases and evolutive adenomatosis: an indication for liver transplantation. Transpl Int. 2003;16:879–84.
20. Huurman VA, Schaapherder AF. Management of ruptured hepatocellular adenoma. Dig Surg. 2010;27:56–60.
21. van Aalten SM, de Man RA, IJzermans JN, Terkivatan T. Systematic review of haemorrhage and rupture of hepatocellular adenomas. Br J Surg. 2012;99:911–6.
22. Erdogan D, Busch OR, van Delden OM, Ten Kate FJ, Gouma DJ, van Gulik TM. Management of spontaneous haemorrhage and rupture of hepatocellular adenomas. A single centre experience. Liver Int. 2006;26:433–8.
23. Noels JE, van Aalten SM, van der Windt DJ, Kok NF, de Man RA, Terkivatan T, et al. Management of hepatocellular adenoma during pregnancy. J Hepatol. 2011;54:553–8.
24. Stoot JH, van Roosmalen J, Terpstra OT, Schaapherder AF. Life-threatening hemorrhage from adenomas in the liver during pregnancy. Dig Surg. 2006;23:155.
25. Mathieu D, Vilgrain V, Mahfouz AE, Anglade MC, Vullierme MP, Denys A. Benign liver tumors. Magn Reson Imaging Clin N Am. 1997;5:255–88.
26. Deneve JL, Pawlik TM, Cunningham S, Clary B, Reddy S, Scoggins CR, et al. Liver cell adenoma: a multicenter analysis of risk factors for rupture and malignancy. Ann Surg Oncol. 2009;16:640–8.
27. Witjes CD, Ten Kate FJ, van Aalten SM, Dwarkasing RS, Willemssen FE, Verhoef C, et al. Hepatocellular adenoma as a risk factor for hepatocellular carcinoma in a non-cirrhotic liver: a plea against. Gut. 2012;61:1645–6.
28. Dhingra S, Fiel MI. Update on the new classification of hepatic adenomas: clinical, molecular, and pathologic characteristics. Arch Pathol Lab Med. 2014;138(8):1090–7.
29. Nault JC, Bioulac-Sage P, Zucman-Rossi J. Hepatocellular benign tumors-from molecular classification to personalized clinical care. Gastroenterology. 2013;144:888–902.
30. Bellamy CO, Maxwell RS, Prost S, Azodo IA, Powell JJ, Manning JR. The value of immunophenotyping hepatocellular adenomas: consecutive resections at one UK centre. Histopathology. 2013;62:431–45.
31. Lagana SM, Salomao M, Bao F, Moreira RK, Lefkowitch JH, Remotti HE. Utility of an immunohistochemical panel consisting of glypican-3, heat shock protein-70, and glutamine synthetase in the distinction of low-grade hepatocellular carcinoma from hepatocellular adenoma. Appl Immunohistochem Mol Morphol. 2013;21:170–6.
32. Nault JC, Zucman-Rossi J. TERT promoter mutations in primary liver tumors. Clin Res Hepatol Gastroenterol. 2016;40:9–14.
33. Ronot M, Bahrami S, Calderaro J, Valla DC, Bedossa P, Belghiti J, et al. Hepatocellular adenomas: accuracy of magnetic resonance imaging and liver biopsy in subtype classification. Hepatology. 2011;53:1182–91.
34. Sempoux C, Paradis V, Komuta M, Wee A, Calderaro J, Balabaud C, et al. Hepatocellular nodules expressing markers of hepatocellular adenomas in Budd-Chiari syndrome and other rare hepatic vascular disorders. J Hepatol. 2015;63:1173–80.
35. Chiche L, Dao T, Salamé E, Galais MP, Bouvard N, Schmutz G, et al. Liver adenomatosis: reappraisal, diagnosis, and surgical management: eight new cases and review of the literature. Ann Surg. 2000;231:74–81.
36. Whelan TJ, Baugh JH, Chandor S. Focal nodular hyperplasia of the liver. Ann Surg. 1973;177:150–8.
37. Mathieu D, Kobeiter H, Maison P, Rahmouni A, Cherqui D, Zafrani ES, et al. Oral contraceptive use and focal nodular hyperplasia of the liver. Gastroenterology. 2000;118:560–4.
38. Bioulac-Sage P. Angiopoietines play a physiopathological role in focal nodular hyperplasia. Gastroenterol Clin Biol. 2004;28:200–1.
39. Wanless IR, Albrecht S, Bilbao J, et al. Multiple focal nodular hyperplasia of the liver associated with vascular malformations of various organs and neoplasia of the brain: a new syndrome. Mod Pathol. 1989;2(5):456–62.
40. Scardapane A, Ficco M, Sabbà C, et al. Hepatic nodular regenerative lesions in patients with hereditary haemorrhagic telangiectasia: computed tomography and magnetic resonance findings. Radiol Med. 2013;118(1):1–13.
41. Maetani Y, Itoh K, Egawa H, et al. Benign hepatic nodules in Budd-Chiari syndrome: radiologic-pathologic correlation with emphasis on the central scar. Am J Roentgenol (AJR). 2002;178(4):869–75.
42. Paradis V, Laurent A, Flejou JF, Vidaud M, Bedossa P. Evidence for the polyclonal nature of focal nodular hyperplasia of the liver by the study of X-chromosome inactivation. Hepatology. 1997;26:891–5.
43. Wanless I, Sapp H, Guindi M. The pathogenesis of focal nodular hyperplasia: an hypothesis based on histologic review of 20 lesions including 3 occurring in early biliary cirrhosis. Hepatology. 2006;44:491A.
44. Rebouissou S, Couchy G, Libbrecht L, Balabaud C, Imbeaud S, Auffray C, et al. The beta-catenin pathway is activated in focal

nodular hyperplasia but not in cirrhotic FNH-like nodules. J Hepatol. 2008;49:61–71.
45. Rebouissou S, Bioulac-Sage P, Zucman-Rossi J. Molecular pathogenesis of focal nodular hyperplasia and hepatocellular adenoma. J Hepatol. 2008;48:163–70.
46. Bosch FX, Ribes J, Cléries R, Díaz M. Epidemiology of hepatocellular carcinoma. Clin Liver Dis. 2005;9(2):191–211.
47. Darbari A, Sabin KM, Shapiro CN, Schwarz KB. Epidemiology of primary hepatic malignancies in U.S. children. Hepatology. 2003;38(3):560–6.
48. Tsukuma H, Hiyama T, Tanaka S, et al. Risk factors for hepatocellular carcinoma among patients with chronic liver disease. N Engl J Med. 1993;328(25):1797–801.
49. Fitzmorris P, Singal AK. Surveillance and diagnosis of hepatocellular carcinoma. Gastroenterol Hepatol (N Y). 2015;11(1):38–46.
50. Trojan J, Zangos S, Schnitzbauer AA. Diagnostics and treatment of hepatocellular carcinoma in 2016: standards and developments. Visc Med. 2016;32(2):116–20.
51. Thorgeirsson SS, Grisham JW. Molecular pathogenesis of human hepatocellular carcinoma. Nat Genet. 2002;31(4):339–46.
52. Terracciano L, Tornillo L. Cytogenetic alterations in liver cell tumors as detected by comparative genomic hybridization. Pathologica. 2003;95(2):71–82.
53. Tornillo L, Carafa V, Richter J, et al. Marked genetic similarities between hepatitis B virus-positive and hepatitis C virus-positive hepatocellular carcinomas. J Pathol. 2000;192(3):307–12.
54. Lee JS, Thorgeirsson SS. Genetic profiling of human hepatocellular carcinoma. Semin Liver Dis. 2005;25(2):125–32.
55. Laurent-Puig P, Legoix P, Bluteau O, Belghiti J, Franco D, Binot F, Monges G, Thomas G, Bioulac-Sage P, Zucman-Rossi J. Genetic alterations associated with hepatocellular carcinomas define distinct pathways of hepatocarcinogenesis. Gastroenterology. 2001;120(7):1763–73.
56. Zondervan PE, Wink J, Alers JC, et al. Molecular cytogenetic evaluation of virus-associated and non-viral hepatocellular carcinoma: analysis of 26 carcinomas and 12 concurrent dysplasias. J Pathol. 2000;192(2):207–15.
57. Niketeghad F, Decker HJ, Caselmann WH, et al. Frequent genomic imbalances suggest commonly altered tumour genes in human hepatocarcinogenesis. Br J Cancer. 2001;85(5):697–704.
58. Tornillo L, Carafa V, Sauter G, et al. Chromosomal alterations in hepatocellular nodules by comparative genomic hybridization: high-grade dysplastic nodules represent early stages of hepatocellular carcinoma. Lab Investig. 2002;82(5):547–53.
59. Wong N, Lai P, Lee SW, et al. Assessment of genetic changes in hepatocellular carcinoma by comparative genomic hybridization analysis: relationship to disease stage, tumor size, and cirrhosis. Am J Pathol. 1999;154(1):37–43.
60. Boige V, Laurent-Puig P, Fouchet P, et al. Concerted nonsyntenic allelic losses in hyperploid hepatocellular carcinoma as determined by a high-resolution allelotype. Cancer Res. 1997;57(10):1986–90.
61. Kusano N, Shiraishi K, Kubo K, et al. Genetic aberrations detected by comparative genomic hybridization in hepatocellular carcinomas: their relationship to clinicopathological features. Hepatology. 1999;29(6):1858–62.
62. Lerebours F, Olschwang S, Thuille B, et al. Fine deletion mapping of chromosome 8p in non-small-cell lung carcinoma. Int J Cancer. 1999;81(6):854–8.
63. Nishida N, Nishimura T, Ito T, et al. Chromosomal instability and human hepatocarcinogenesis. Histol Histopathol. 2003;18(3):897–909.
64. Chang MH, Chen CJ, Lai MS, et al. Universal hepatitis B vaccination in Taiwan and the incidence of hepatocellular carcinoma in children. Taiwan Childhood Hepatoma Study Group. N Engl J Med. 1997;336(26):1855–9.
65. Chang MH, Shau WY, Chen CJ, et al. Hepatitis B vaccination and hepatocellular carcinoma rates in boys and girls. JAMA. 2000;284(23):3040–2.
66. Yamashita S, Vauthey JN, Kaseb AO, et al. Prognosis of fibrolamellar carcinoma compared to non-cirrhotic conventional hepatocellular carcinoma. J Gastrointest Surg. 2016;20(10):1725–31.
67. Riggle KM, Turnham R, Scott JD, et al. Fibrolamellar hepatocellular carcinoma: mechanistic distinction from adult hepatocellular carcinoma. Pediatr Blood Cancer. 2016;63(7):1163–7.
68. Sergi CM. Hepatocellular carcinoma, fibrolamellar variant: diagnostic pathologic criteria and molecular pathology update. A primer. Diagnostics (Basel). 2016;6(1):3–12
69. Honeyman JN, Simon EP, Robine N, et al. Detection of a recurrent DNAJB1-PRKACA chimeric transcript in fibrolamellar hepatocellular carcinoma. Science. 2014;343:1010–4.
70. Atienza LG, Berger J, Mei X, et al. Liver transplantation for fibrolamellar hepatocellular carcinoma: a national perspective. J Surg Oncol. 2016;115:319. https://doi.org/10.1002/jso.24515.
71. Kassahun WT. Contemporary management of fibrolamellar hepatocellular carcinoma: diagnosis, treatment, outcome, prognostic factors, and recent developments. World J Surg Oncol. 2016;14(1):151.
72. Aronson DC, Meyers RL. Malignant tumors of the liver in children. Semin Pediatr Surg. 2016;25(5):265–75.
73. Giardiello FM, Offerhaus GJ, Krush AJ, et al. Risk of hepatoblastoma in familial adenomatous polyposis. J Pediatr. 1991;119(5):766–8.
74. Hamada Y, Takada K, Fukunaga S, Hioki K. Hepatoblastoma associated with Beckwith-Wiedemann syndrome and hemihypertrophy. Pediatr Surg Int. 2003;19(1–2):112–4.
75. Krush AJ, Traboulsi EI, Offerhaus JA, et al. Hepatoblastoma, pigmented ocular fundus lesions and jaw lesions in Gardner syndrome. Am J Med Genet. 1988;29(2):323–32.
76. Mussa A, Ferrero GB. Screening hepatoblastoma in Beckwith-Wiedemann syndrome: a complex issue. J Pediatr Hematol Oncol. 2015;37(8):627.
77. Ozawa MG, Cooney T, Rangaswami A, Hazard FK. Synchronous hepatoblastoma, neuroblastoma, and cutaneous capillary hemangiomas: a case report. Pediatr Dev Pathol. 2016;19(1):74–9.
78. Sumazin P, Chen Y, Treviño LR, et al. Genomic analysis of hepatoblastoma identifies distinct molecular and prognostic subgroups. Hepatology. 2016;65:104. https://doi.org/10.1002/hep.28888.
79. Buendia MA. Genetic alterations in hepatoblastoma and hepatocellular carcinoma: common and distinctive aspects. Med Pediatr Oncol. 2002;39(5):530–5.
80. Curia MC, Zuckermann M, De Lellis L, et al. Sporadic childhood hepatoblastomas show activation of beta-catenin, mismatch repair defects and p53 mutations. Mod Pathol. 2008;21(1):7–14.
81. Czauderna P, Haeberle B, Hiyama E, et al. The Children's Hepatic Tumors International Collaboration (CHIC): novel global rare tumor database yields new prognostic factors in hepatoblastoma and becomes a research model. Eur J Cancer. 2016;52:92–101.
82. Chablé-Montero F, Shah BSA, Montante-Montes de Oca D, Angeles-Ángeles A, Henson DE, Albores-Saavedra J. Thyroid-like cholangiocarcinoma of the liver: an unusual morphologic variant with follicular, trabecular and insular patterns. Ann Hepatol. 2012;11(6):961–5.
83. Shaib Y, El-Serag HB. The epidemiology of cholangiocarcinoma. Semin Liver Dis. 2004;24(2):115–25.
84. Khan SA, Emadossadaty S, Ladep NG, Thomas HC, Elliott P, Taylor-Robinson SD, Toledano MB. Rising trends in cholangiocarcinoma: is the ICD classification system misleading us? J Hepatol. 2012;56(4):848–54.

85. Patel T. Worldwide trends in mortality from biliary tract malignancies. BMC Cancer. 2002;2:10.
86. Goodman ZD. Neoplasms of the liver. Mod Pathol. 2007;20(Suppl 1):S49–60.
87. Albores-Saavedra J, Henson DE, Klimstra DS. Tumors of the gallbladder, extrahepatic bile ducts and Vaterian system. Atlas of tumor pathology. Washington DC: Armed Forces Institute of Pathology. Fascicle 23; 2015.
88. Hall C, Mamlok V, Al-Khalil I. A sporadic case of advanced metastatic cholangiocarcinoma in a child: a case report and review of literature. J Pediatr Hematol Oncol. 2015;37(5):e333–5.
89. Guglielmi A, Ruzzenente A, Campagnaro T, Nicoli P, Cappellani A, Malfermoni G, Iacono C. Intrahepatic cholangiocarcinoma: prognostic factors after surgical resection. World J Surg. 2009;33(6):1247–54.
90. Lee SJ, Kwon W, Kang MJ, Jang JY, Chang YR, Jung W, Kim SW. Clinical features and survival outcome of locally advanced extrahepatic cholangiocarcinoma. Korean J Hepatobiliary Pancreat Surg. 2014;18(1):1–8.
91. Yeh CN, Wang SY, Chen YY, Chen MH, Chiang KC, Cheng CT, Tsai CY, Wang CC, Yeh TS, Chen TC. A prognostic nomogram for overall survival of patients after hepatectomy for intrahepatic cholangiocarcinoma. Anticancer Res. 2016;36(8):4249–58.
92. Tan Y, Milikowski C, Toribio Y, et al. Intraductal papillary neoplasm of the bile ducts: a case report and literature review. World J Gastroenterol. 2015;21(43):12498–504.
93. Chu C, Felbel W, Chu F. Intrahepatic biliary intraductal oncocytic papillary neoplasm/carcinoma: first reported case in Australia and Literature Review. Radiol Case Rep. 2015;2(3):95.
94. Martin RC, Klimstra DS, Schwartz L, et al. Hepatic intraductal oncocytic papillary carcinoma. Cancer. 2002;95(10):2180–7.
95. Sudo Y, Harada K, Tsuneyama K, Katayanagi K, Zen Y, Nakanuma Y. Oncocytic biliary cystadenocarcinoma is a form of intraductal oncocytic papillary neoplasm of the liver. Mod Pathol. 2001;14:1304–9.
96. Wolf HK, Garcia JA, Bossen EH. Oncocytic differentiation in intrahepatic biliary cystadenocarcinoma. Mod Pathol. 1992;5:665–8.
97. Albores-Saavedra J, Córdova-Ramón JC, Chablé-Montero F, Dorantes-Heredia R, Henson DE. Cystadenomas of the liver and extrahepatic bile ducts. Morphologic and immunohistochemical characterization of the biliary and intestinal variants. Ann Diagn Pathol. 2015;19(3):124–9.
98. Albores-Saavedra J, Henson DE, Klimstra DS. Tumors of the gallbladder, extrahepatic bile ducts and Vaterian system. In: Atlas of tumor pathology. 4th series, fascicle. Washington DC: American Registry of Pathology; 2015. p. 23.
99. Huang L, Li J, Zhou F, et al. Giant cystic lymphangioma of the liver. Hepatol Int. 2010;4(4):784–7.
100. Haratake J, Koide O, Takeshita H. Hepatic lymphangiomatosis: report of two cases, with an immunohistochemical study. Am J Gastroenterol. 1992;87(7):906–9.
101. Van Steenbergen W, Joosten E, Marchal G, et al. Hepatic lymphangiomatosis. Report of a case and review of the literature. Gastroenterology. 1985;88(6):1968–72.
102. Okano H, Shiraki K, Inoue H, et al. Natural course of cavernous hepatic hemangioma. Oncol Rep. 2001;8(2):411–4.
103. Lanne JS, Dumortier J, Hervieu V, et al. Polycythemia and elevated serum erythropoietin associated with a liver haemangioma. Gastroenterol Clin Biol. 2010;34(11):629–32.
104. Ishak KG, Goodman ZD, Stocker JT. Tumors of the liver and intrahepatic bile ducts. Atlas of tumor pathology. 3rd series. Fascicle 31. Washington, D.C.: Armed Forces Institute of Pathology; 1999.
105. Mocchegiani F, Vincenzi P, Coletta M, et al. Prevalence and clinical outcome of hepatic haemangioma with specific reference to the risk of rupture: a large retrospective cross-sectional study. Dig Liver Dis. 2016;48(3):309–14.
106. Dail DH, Liebow AA. Intravascular bronchioloalveolar tumor. Am J Pathol. 1975;78:6a–7a.
107. Sardaro A, Bardoscia L, Petruzzelli MF, Portaluri M. Epithelioid hemangioendothelioma: an overview and update on a rare vascular tumor. Oncol Rev. 2014;8(2):259.
108. Hayashi Y, Inagaki K, Hirota S, et al. Epithelioid hemangioendothelioma with marked liver deformity and secondary Budd-Chiari syndrome: pathological and radiological correlation. Pathol Int. 1999;49(6):547–52.
109. Mani H, Van Thiel DH. Mesenchymal tumors of the liver. Clin Liver Dis. 2001;5:219–57. viii
110. Chaudhary P, Bhadana U, Singh RA, Ahuja A. Primary hepatic angiosarcoma. Eur J Surg Oncol. 2015;41(9):1137–43.
111. Zhu YP, Chen YM, Matro E, et al. Primary hepatic angiosarcoma: a report of two cases and literature review. World J Gastroenterol. 2015;21(19):6088–96.
112. Falk H, Herbert J, Crowley S, Ishak KG, Thomas LB, Popper H, Caldwell GG. Epidemiology of hepatic angiosarcoma in the United States: 1964–1974. Environ Health Perspect. 1981;41:107–13.
113. Block JB. Angiosarcoma of the liver following vinyl chloride exposure. JAMA. 1974;229:53–4.
114. Bioulac-Sage P, Laumonier H, Laurent C, Blanc JF, Balabaud C. Benign and malignant vascular tumors of the liver in adults. Semin Liver Dis. 2008;28:302–14.
115. Molina E, Hernandez A. Clinical manifestations of primary hepatic angiosarcoma. Dig Dis Sci. 2003;48:677–82.
116. Cano-García F, Athie-Athie Ade J, García-Gómez JI, et al. Cystic angiosarcoma of the liver. A previously undescribed neoplasm. Ann Hepatol. 2016;15(2):283–6.
117. Rubinstein PG, Aboulafia DM, Zloza A. Malignancies in HIV/AIDS: from epidemiology to therapeutic challenges. AIDS. 2014;28(4):453–65.
118. Dittmer DP, Damania B. Kaposi sarcoma-associated herpesvirus: immunobiology, oncogenesis, and therapy. J Clin Invest. 2016;126(9):3165–75.
119. Rao SP, Bhagavath S, Chen CK, Tolete-Velcek F. Mesenchymal hamartoma of the liver in an older child: association with disseminated intravascular coagulation. Med Pediatr Oncol. 1984;12(2):112–5.
120. Mack-Detlefsen B, Boemers TM, Groneck P, Bald R. Multiple hepatic mesenchymal hamartomas in a premature associated with placental mesenchymal dysplasia. J Pediatr Surg. 2011;46(8):e23–5.
121. Cook JR, Pfeifer JD, Dehner LP. Mesenchymal hamartoma of the liver in the adult: association with distinct clinical features and histological changes. Hum Pathol. 2002;33(9):893–8.
122. Qureshi SS, Bhagat M, Kembhavi S, et al. Benign liver tumors in children: outcomes after resection. Pediatr Surg Int. 2015;31(12):1145–9.
123. Goodman ZD, Ishak KG. Angiomyolipoma of the liver. Am J Surg Pathol. 1984;8:745–50.
124. Nonomura A, Enomoto Y, Takeda M, et al. Angiomyolipoma of the liver: a reappraisal of morphological features and delineation of new characteristic histological features from the clinicopathological findings of 55 tumours in 47 patients. Histopathology. 2012;61(5):863–80.
125. Delgado R, de Leon Bojorge B, Albores-Saavedra J. Atypical angiomyolipoma of the kidney: a distinct morphologic variant that is easily confused with a variety of malignant neoplasms. Cancer. 1998;83(8):1581–92.
126. Tsui WMS, Colombari C, Portmann BC, et al. Hepatic angiomyolipoma; a clinicopatholgic study of 30 cases and delineation of unusual morphologic variants. Am Surg Pathol. 1999;23:34–8.
127. Ashfaq R, Weinberg AG, Albores-Saavedra J. Renal angiomyolipomas and HMB-45 reactivity. Cancer. 1993;71(10):3091–7.

128. Tsui WMS, Yuen AKT, Ma KF, Tse CCH. Hepatic angiomyolipoma with a deceptive trabecular pattern and HMB-45 reactivity. Histopathology. 1992;21:569–73.
129. Monforte-Muñoz H, Kapoor N, Albores-Saavedra J. Epstein-Barr virus-associated leiomyomatosis and posttransplant lymphoproliferative disorder in a child with severe combined immunodeficiency: case report and review of the literature. Pediatr Dev Pathol. 2003;6(5):449–57.
130. Vyas S, Psica A, Watkins J, Yu D, Davidson B. Primary hepatic leiomyoma: unusual cause of an intrahepatic mass. Ann Transl Med. 2015;3(5):73.
131. Luo XZ, Ming CS, Chen XP, Gong NQ. Epstein-Barr virus negative primary hepatic leiomyoma: case report and literature review. World J Gastroenterol. 2013;19(25):4094–8.
132. Omiyale AO. Primary leiomyoma of the liver: a review of a rare tumour. HPB Surg. 2014;2014:959202.
133. Wang ZS, Xu L, Ma L, et al. Hepatic falciform ligament clear cell myomelanocytic tumor: a case report and a comprehensive review of the literature on perivascular epithelioid cell tumors. BMC Cancer. 2015;15:1004.
134. Haji Ali R, Khalife M, El Nounou G, et al. Giant primary malignant mesothelioma of the liver: a case report. Int J Surg Case Rep. 2016;30:58–61.
135. Chablé-Montero F, Angeles-Ángeles A, Albores-Saavedra J. Inflammatory myofibroblastic tumor of the liver. Ann Hepatol. 2012;11(5):708–9.
136. Schnelldorfer T, Chavin KD, Lin A, Lewin DN, Baliga PK. Inflammatory myofibroblastic tumor of the liver. J Hepato-Biliary-Pancreat Surg. 2007;14(4):421–3.
137. Zen Y, Fujii T, Sato Y, Masuda S, Nakanuma Y. Pathological classification of hepatic inflammatory pseudotumor with respect to IgG4-related disease. Mod Pathol. 2007;20(8):884–94.
138. Dey B, Gochhait D, Kaushal G, et al. Solitary fibrous tumor of the liver: a rare tumor in a rarer location. Rare Tumors. 2016;8(3):6403.
139. Thway K, Ng W, Noujaim J, et al. The current status of solitary fibrous tumor: diagnostic features, variants, and genetics. Int J Surg Pathol. 2016;24(4):281–92.
140. Silvanto A, Karanjia ND, Bagwan IN. Primary hepatic solitary fibrous tumor with histologically benign and malignant areas. Hepatobiliary Pancreat Dis Int. 2015;14(6):665–8.
141. Beltrán MA. Solitary fibrous tumor of the liver: a review of the current knowledge and report of a new case. J Gastrointest Cancer. 2015;46(4):333–42.
142. Teixeira F Jr, de Freitas Perina AL, de Oliveira Mendes G, et al. Fibrous solitary tumour of the liver. J Gastrointest Cancer. 2014;45(Suppl 1):216–7.
143. Feng LH, Dong H, Zhu YY, Cong WM. An update on primary hepatic solitary fibrous tumor: an examination of the clinical and pathological features of four case studies and a literature review. Pathol Res Pract. 2015;211(12):911–7.
144. Chi M, Dudek AZ, Wind KP. Primary hepatic leiomyosarcoma in adults: analysis of prognostic factors. Onkologie. 2012;35(4):210–4.
145. Hasheminasab Zavareh R, Riahi Beni H, Iranpour A, et al. Leiomyosarcoma of inferior vena cava and right atrium with ascites and jaundice: a case report. Int J Hematol Oncol Stem Cell Res. 2016;10:232–5.
146. Ravaioli M, Serenari M, Cescon M, et al. Liver and Vena Cava En Bloc resection for an invasive Leiomyosarcoma causing Budd-Chiari syndrome, under Veno-Venous bypass and liver hypothermic perfusion : liver hypothermic perfusion and Veno-Venous bypass for inferior Vena Cava Leiomyosarcoma. Ann Surg Oncol. 2017;24(2):556–7.
147. Jadhav SA, Atluri VS, Prajapati R, Satoskar RR. Leiomyosarcoma of inferior vena cava. J Postgrad Med. 2011;57(4):332–4.
148. Shivathirthan N, Kita J, Iso Y, et al. Primary hepatic leiomyosarcoma: case report and literature review. World J Gastrointest Oncol. 2011;3(10):148–52.
149. Thapar PM, Mathur SK, Saksena DS, Shah HK. Leiomyosarcoma of inferior vein cava presenting as acute Budd-Chiari syndrome. Indian J Gastroenterol. 2001;20(1):33–5.
150. Putra J, Ornvold K. Undifferentiated embryonal sarcoma of the liver: a concise review. Arch Pathol Lab Med. 2015;139(2):269–73.
151. Sánchez-Aguilar AC, Díaz-Flores O, Albores-Saavedra J. Embryonal sarcoma of the liver in a young. Ann Hepatol. 2009;8(1):63.
152. Schoofs G, Braeye L, Vanheste R, et al. Hepatic rhabdomyosarcoma in an adult: a rare primary malignant liver tumor. Case report and literature review. Acta Gastroenterol Belg. 2011;74(4):576–81.
153. Reznichenko AA, Klingbeil LR, Shah SA. Giant primary yolk sac tumor of the liver. J Gastrointest Surg. 2016;20(9):1669–70.
154. Jaffe ES, Nicolae A, Pittaluga S. Peripheral T-cell and NK-cell lymphomas in the WHO classification: pearls and pitfalls. Mod Pathol. 2013;26(Suppl 1):S71–87.
155. Shi Y, Wang E. Hepatosplenic T-cell lymphoma: a clinicopathologic review with an emphasis on diagnostic differentiation from other T-cell/natural killer-cell neoplasms. Arch Pathol Lab Med. 2015;139(9):1173–80.
156. Calvaruso M, Gulino A, Buffa S, et al. Challenges and new prospects in hepatosplenic γδ T-cell lymphoma. Leuk Lymphoma. 2014;55(11):2457–65.
157. Visnyei K, Grossbard ML, Shapira I. Hepatosplenic γδ T-cell lymphoma: an overview. Clin Lymphoma Myeloma Leuk. 2013;13(4):360–9.